abc amsterdam brain & cognition

June 2018 | Issue 7

Journal

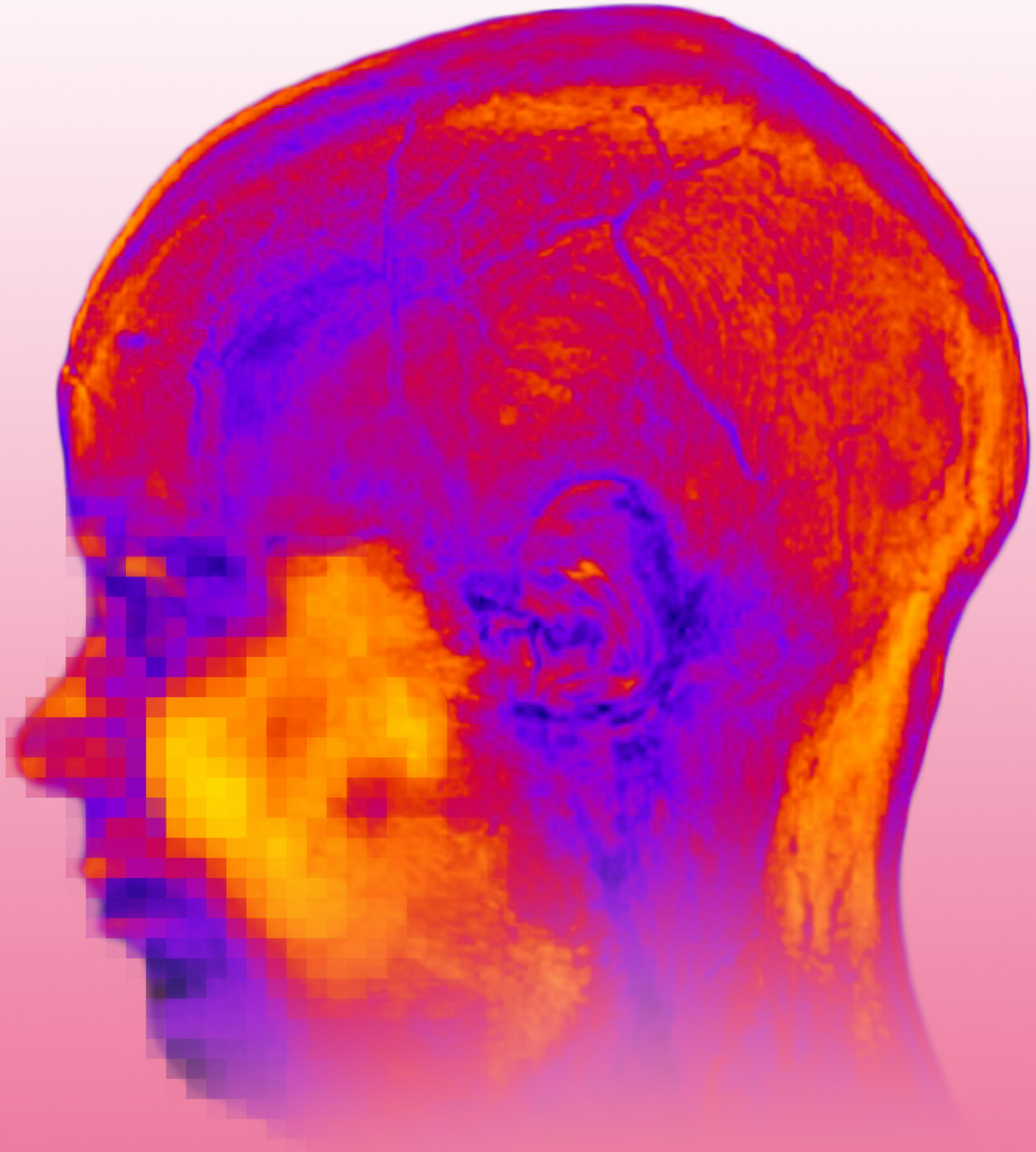

The Ethics of Scientific Journalism

Ethics of Animal Testing

Neuroethics: Interview with Pim Haselager

Editorial Board of the ABC Journal

ABOUT THE COVER IMAGE:

The cover image was generated by rendering a standard 3D anatomical image acquired using MRI. The voxels in the non-brain regions are spatially smoothed to diminish the detailed facial features of the subject. It is becoming a standard practice to "deface" the images before storing and sharing MRI data, for the purpose of anonymizing subject's' identity. The image was acquired as a standard acquisition for an fMRI study assessing the performance of multi-slice acquisition for detecting BOLD signal. Multi-slice acquisition is thought to increase statistical power by allowing higher sampling rate while acquiring BOLD images.

Ritu Bhandari, Social Brain Lab, Netherlands Institute for Neuroscience, Amsterdam

Table of Contents

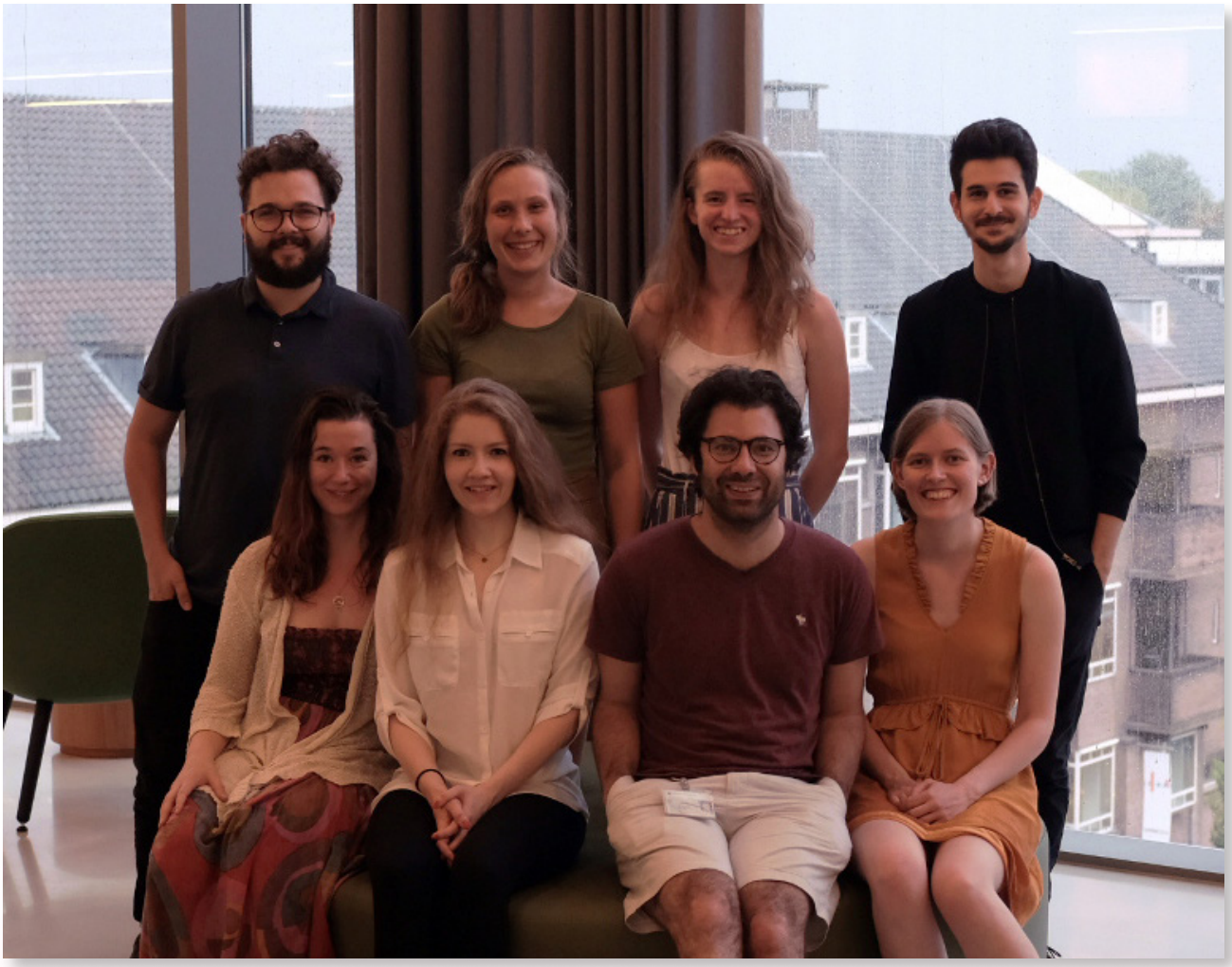

The ABC Journal committee.

Steven Voges, Amber Brands, Sammy Millard, Nikos Kolonis, Laura Stolp, Vanessa Utz, Ilja Sligte, Maite van der Miesen
(Not pictured: Janna Cousijn, Vincent Tijms)

LETTER FROM THE EDITORS

Dear ABC Journal readers,

We are very excited to present to you the 7th issue of the ABC Journal, which is all about ethics in Brain and Cognitive Science. Our decision to make ethics the main focus was influenced by our discussions with fellow students, who felt ethics were infrequently discussed within the master's, as well as by the timely nature of the topic. It was a little more than a year ago that the Dutch government took the innovative decision to gradually phase out animal testing, with the ultimate goal of eliminating animal use for safety research on chemicals, food ingredients, pesticides, and medicines. Apart from that, we feel that with the rapid advancements being made within neuroscientific research, such as research in AI, neurocognitive and pharmacological enhancement, and even neuromarketing, it is important to take a step back and assume an ethical perspective. Following our decision to explore ethics, the Cambridge Analytica scandal hit the headlines and came as a confirmation to this decision, raising further questions regarding what is and isn't ethical in research.

This issue features many original articles, touching upon several issues surounding ethics, such as scientific journalism, animal testing, ethics education, and the future of AI. Additionally, we have conducted an enlightening interview with philosopher and cognitive scientist Pim Haselager, delving deeper into the topics of ethics education, communicating neuroscience to society and AI.

As always, this issue serves as a showcase for the best research reports from students of the Brain and Cognitive Sciences master's programme. We received many high quality and diverse submissions, so it has been really hard to pick out the best ones. We decided on three fantastic reports from Antonia Kaiser, Yasmin Mzayek and Iris Marchal, that can be found within the pages of this issue. Antonia Kaiser's report on the effects of cardiovascular fitness on hippocampal volume and vasculature in young adults was selected as the chief editor's choice and we conducted an interview with her to get an insight into her internship experience and current work.

A special thank you to Ilja Sligte and Vincent Tijms for their support in making this issue a reality and to all our editors for their hard work on it. We would also like to thank Vanessa, for expanding our social media presence, and Steven, for joining our team later in the year. With this issue, we also bid farewell to three of our journal members, our second-year members, Amber and Maite, and Canada bound Vanessa. Best of luck with your next endeavours!

Best regards on behalf of the editorial team,

Nikos Kolonis and Sammy Millard

GDPR and the University

by Vincent Tijms

The GDRP is not only changing the way that research groups deal with sensitive data, but also has implications for the educational side of the university. After all, when you apply to a programme like MBCS you have to turn in your resume, grade transcripts and other information that might prove sensitive. While you study, you receive grades, you create drafts, you get feedback, you maybe build up a personal history at the study advisor's office. In the whole process from application to graduation, both the programme and the students create a data trail that brings its own ethical challenges.

We have always been aware that parts of that data trail contain sensitive information -- such as medical information shared with the study advisor or the performance history of students -- but sometimes those handling parts of that information have taken an overly optimistic view. Take for example the grade lists handed out to students. Why are they often single files, 'anonymized' by just listing student number and grade? The reason is that teaching staff is partial to assuming that nobody is going to deanonymize such a file, even if it is trivial to do so. That reasoning will not work under the GDRP anymore. From May 25 onwards, such grade lists are a thing of the past: your results have to be shared with you and you alone.

The same goes for internal information sharing at our programme. Central information systems like Datanose offer a fine-grained control over data access and we have been hard at work to determine roles for everyone at the IIS that comply with the GDRP. The data access that any single person has must always be justifiable. If we take courses grades as an example again, it will be possible for the study advisor to see your individual results, but the Board of Examiners will only access aggregate information, as they do not deal with individual student but evaluate the efficacy of courses.

Overall I am happy with how much awareness the new legislation has created. The first step to ethical behavior is professional integrity, but that is no longer enough when dealing with sensitive data. In our current reality, even ostensibly harmless information, such as that one column about food allergies in the study trip registration form, can theoretically be fed into a data mining algorithm and obtain a new meaning for, say, an insurance company. This is why ethics now comes down to both professional integrity and the clear data policy that GDRP tries to offer. The only thing I find a pity is that the MBCS graduation tradition, in which I cite from people's application letters and the crowd has to guess who wrote what, is probably not GDRP-compliant.

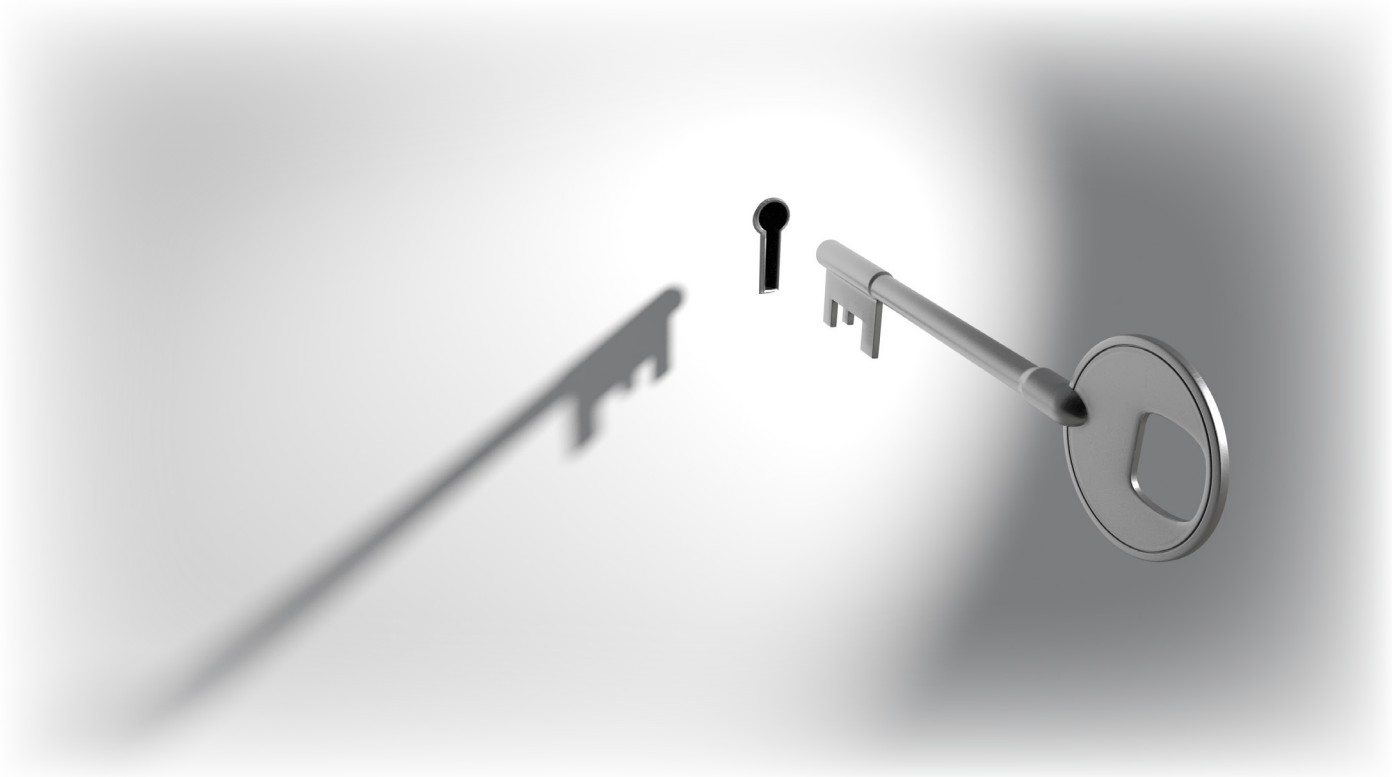

Abstracts

The hyperarousal theory of insomnia: Assessing GABA and glutamate levels in thalamus and sensorimotor cortex

Laura Bavelaar | Cognitive Neuroscience track
Supervisor: Jessica Foster-Dingley
Netherlands Institute for Neuroscience, Sleep and Cognition Lab

Though many are suffering from the often chronic and debilitating sleep problems and their associated daytime consequences that make up insomnia, an efficient treatment has not been discovered yet. The mechanism underlying insomnia still calls for clarification. One of the current theories is the hyperarousal theory, stating that sleep problems arise from increased somatic, cognitive and cortical activity. The question remains whether this hyperarousal arises from disturbed de-arousal or increased arousal. This study delineates these two processes by assessing γ-aminobutyric acid (GABA) and Glx (glutamate + glutamine) levels in the thalamus and sensorimotor cortex of insomniacs and good sleepers using 3 T magnetic resonance spectroscopy (MRS). GABA is the primary inhibitory neurotransmitter of the brain and thus functions as a measure of de-arousal, glutamate is the main excitatory neurotransmitter and reflects hyperarousal. GABA and Glx levels did not differ between insomniacs and good sleepers. However, a relation between thalamic GABA and Glx and wake time after sleep onset (WASO) was found, a sleep-parameter that is increased for insomniacs. Additionally, a mediation model was validated in which the relation between insomnia and neurobiological hyperarousal is mediated by psychological and neurophysiological hyperarousal. No mediation effects were found. The results might be accounted for by the heterogeneous insomnia population consisting of distinct insomnia subtypes and the subjective nature of the disorder.

Software for automated quantification of flexible behaviour

Erik de Keijzer | Behavioural Neuroscience track
Supervisor: Francesco Battaglia
Donders Institute Nijmegen

The medial prefrontal cortex (mPFC) plays an important role in social decision making and is implicated in multiple poorly understood mental disorders like schizophrenia and autism. Deficits in local synchrony within the mPFC as well as long-range connectivity between mPFC and hippocampus have been implicated in schizophrenia, whereas prefrontal expression of nicotinic receptors is critical in an animal model of autism. A better understanding of prefrontal functioning during social interaction could provide insight into these debilitating diseases characterized by abnormal or impaired social behaviour.

The prelimbic area of the mPFC is thought to be involved in decision making and switching between rules, strategies or attentional sets, which are considered important processes during social interaction. After social deprivation, mice are motivated to interact with a novel conspecific. In a novel environment, this motivation will compete with the motivation to explore the environment.

The interplay between competing motivations can evoke flexible behaviour which would likely be represented in the activity in the prelimbic cortex.

During this project, a beginning was made to construct a set-up for the simultaneous recording of camera images and electrophysiology data in freely moving mice. Microdrives for implantation were constructed to record electrophysiology data according to an open-source approach. During the course of the internship, preliminary electrophysiological data was collected in a befriended laboratory using these microdrives. As this data has not yet been analysed, this report will focus on the analysis of behaviour.

To analyse behaviour a top-view camera recorded two mice. These recordings could subsequently be analysed using semi-automated tracking software. Flexible behaviour was evoked using a social interaction task. The recording and automated analysis of behaviour, also known as computational ethology, can provide a powerful tool for deciphering different behavioural states and transitions between them. Especially in combination with the simultaneous recording of electrophysiology data this could provide a wealth of information about activity in the mPFC during behavioural epochs.

To investigate prefrontal functioning during social interaction it will be necessary to record and analyse flexible social behaviour automatically. Can we record flexible behaviour and analyse this behaviour automatically?

An Investigation of Localist and Distributed Representation Models using the Neuronal Coherence of Concept Cell Activity with the Human Medial Temporal Lobe

Suzanne Martens | Cognitive Neuroscience track
Supervisor: Conrado Bosman (Daily Supervisor: Tom Sikkens)
Cognitive and Systems Neuroscience group, University of Amsterdam

Introduction

Since the discovery of concept cells in the human hippocampus, scientists have debated whether their existence supports localist (LM) or distributed representation models(DRM). LM view concept cells as the last step in the hierarchy of visual processing, while DRM think of concept cells as parts of high-level memory networks. Implicitly, LM assume that concept cells primarily communicate with low-level downstream neurons while DRM assume that they primarily communicate with (relatively) nearby members of the network they belong to. Using the ING/PING model of communication within neuronal ensembles, this study investigates whether concept cells behave like they are part of neuronal ensembles (supporting DRM) or not (supporting LM).

Methods

Data was collected from 16 patients suffering from pharmacologically intractable epilepsy. Patients were implanted with chronic depth electrodes with micro-wires at their tips for 10 – 14 days. During this time, patients were asked to perform a computerized task designed for finding concept cells that consisted of viewing pictures of celebrities, famous places and personally relevant people or locations.

Results

A total of 13 concept cells was found and analyzed. Local LFP signals of tissue directly surrounding the cells showed a sharp increase of power in the low gamma band and weaker increases in all other frequencies 0.2-0.6s after presenting a preferred stimulus. None of these effects were observed when other pictures were presented. Local LFP signals slightly further removed from the cells showed an increase in coherence in the low gamma band 0.1-0.7s after presenting other pictures as well as a short decrease in high gamma (0-0.2s)and a late onset increase in theta (0.5-0.7s). None of these effects were observed when preferred pictures were presented. Finally, an increase in spike-LFP coherence in the low and high gamma band was observed between spikes of the concept cells and the LFPs when preferred stimuli were presented compared to when other stimuli were presented, as well as a decrease in the alpha band.

Conclusions

The results from the WPLI and spike-LFP coherence analyses are in line with ING/PING models and support the idea that concept cells behave like they are part of neuronal ensembles. Therefore, this study supports DRM over LM. These findings need to be confirmed in a study using larger sample sizes per picture and a larger population of concept cells.

Naturally occurring auditory-visual synesthesia experience under dark adaptation

Anupama Nair | Cognitive Neuroscience track
Supervisor: David Brang
University of Michigan

Synesthesia is a perceptual phenomenon in which stimulation of one sensory modality evokes additional experiences in an unrelated modality (e.g., sounds evoking colors). This condition is thought to arise from increased connectivity between associated sensory areas. However, non-synesthetes can experience these sensations via hallucinogens or as a result of brain damage, raising the possibility that synesthesia exists as a latent feature in all individuals, manifesting only when the balance of activity across the senses has been altered. Indeed, multisensory connections are present in all individuals that support the processing of dynamic auditory, visual, and tactile information present in the environment, but it is thought that inhibition of these pathways and the presence of dominant bottom-up information prevents normal multisensory interactions from evoking the subjective experience of synesthesia. The present research explores the conditions necessary to evoke auditory-visual synesthetic experiences in non-synesthetes. First, subjects performed a visual-imagery task in a visually deprived environment while simultaneously being presented with startling sounds from two spatial locations at random, infrequent intervals. The visual imagery task served to increase top-down feedback to early visual areas and from previously conducted pilot studies, startling sounds were found to be more effective in over-stimulating the multisensory network present in all individuals. Visual synesthetic percepts, evoked by startling sounds, were observed in ~60% of our non synesthetic subjects across several behavioural experiments. To identify the neural correlates of this phenomenon, we conducted an EEG study to explore differences in early visual areas for trials in which the participants experienced hallucinatory percepts vs. when they reported no such experiences. The EEG signals reflected a difference in average ERP activity for the two conditions within 100 ms of sound exposure implying differential visual cortex activation for the presence of hallucinatory experiences

versus its absence. Across all experiments, subjects reported seeing visual images (vivid colors and Klüver's form-constants) localized to the position of the speaker. These results indicate a higher prevalence of synesthetic experiences in the general population and a link to normal multisensory processes.

When is visual awareness continuous and when is it all-or-none?

Rafał Szymanek | Cognitive Neuroscience track
Supervisor: Prof. John-Dylan Haynes
Bernstein Center for Computational Neuroscience, Berlin

In an influential paper, Sergent and Dehane (2004) claimed that visual awareness is all-or-none. This finding has recently been confirmed by Asplund and colleagues (2014) who showed that responses in a colour-detection task can be modelled as a mixture of guesses and correct trials of fixed precision. However, several theoretical approaches (Kanwisher, 2001), as well as empirical data (Ramsøy & Overgaard, 2004; Christensen, Ramsøy, Lund, Madsen, & Rowe, 2006; Sandberg, Bibby, Timmermans, Cleeremans, & Overgaard, 2011) suggest that awareness is a continuum. Here, we attempt to reconcile these differences by proposing that visual awareness depends on two processes. The bottom-up process depends on stimulus quality and has continuous characteristics, while the top-down process is contingent on attention and is dichotomous. We propose that differences in findings stem from using different paradigms: experiments employing the attentional blink are actually studying the top-down process, whereas research on backward masking is tapping into the bottom-up process. Therefore, findings from either of the paradigms cannot be generalized onto awareness as a whole. In the present study, we embedded the methodology of Asplund and colleagues (2014) in a backward masking paradigm. Unlike the original authors, who studied the attentional blink, we find that our findings cannot be explained by mere increase in the guess rate and that response precision is affected. The experiment provides support for our two-process model.

Reputation Concern versus In-group Identification as Underlying Mechanisms of Parochial Cooperation in relation with Social Value Orientation

Thanaphat Thongpaibool | Cognitvie Science track
Supervisor: Hillie Aaldering
Work and Organizational Psychology group, University of Amsterdam

In intergroup settings where cooperation is possible between two or more groups, parochial cooperation—making self-costly contributions to one's in-group—is pervasive and generally preferred over universal cooperation which benefits all groups. In two experiments, using the Collective Incentive game, which allows for cooperation on the in-group and/or the collective level, we investigated the potential drivers of parochial cooperation by manipulating in-group identification and reputation concern based on Social Identity Theory (SIT) and the Theory of Bounded Generalized Reciprocity (BGR). We also examined the moderating role of social value orientation on parochial cooperation. Experiment 1 tested whether low in-group identification and/or low reputation concern decreased parochial cooperation, compared to a control condition (N = 204). Experiment 2 compared the differences between high vs. low in-group identification and high vs. low reputation concern on parochial cooperation (N = 374). Results showed tentative support for SIT only in Experiment 2, and no firm conclusion can be reached regarding the drivers of parochial cooperation. Parochial cooperation consistently prevailed over universal cooperation and was motivated by a preference to favor the in-group. When parochial cooperation harms the out-group, universal cooperation was preferred (Experiment 1 and 2). A pro-social inclination was positively associated with universal cooperation (Experiment 1 and 2), but with parochial cooperation only in Experiment 2. Pro-sociality, however, did not affect how in-group identification and reputation concern impact parochial cooperation (Experiment 1 and 2). We discuss implications for both theories and another possible determinant driving parochial cooperation, namely outcome dependence.

Effects of cardiovascular fitness on hippocampal volume and vasculature in young adults

Antonia Kaiser
Supervisor: Anouk Schrantee
Amsterdam Medical Center - Radiology Department

ABSTRACT

Physical exercise is well known to benefit both physical and mental health. An increase in brain volume, especially in the hippocampus, has been shown after exercise intervention. It has recently become clear that non-neuronal elements can exhibit a similar capacity for plastic changes (angiogenesis) induced by physical exercise. Neuronal changes are accompanied by substantial increases in glia and capillary volume. For example, changes in cerebral blood flow (CBF) and cerebral blood volume (CBV) have been associated with sensory, motor, and cognitive task performance. The aim of this study was to assess the influence of high- (HI) versus low-intensity (LI) training on the healthy young hippocampus and shed light on which mechanism can explain the exercise-induced changes in brain structure. The effects on hippocampal volume, CBV and CBF and VO2-max as a measurement of aerobic fitness were analyzed and compared between groups. We show a general trend towards our hypothesis, that high intensity training has a positive influence on hippocampal volume, CBV and CBF based on an increase of aerobic fitness (VO2-max). Only females showed a significantly higher increase in VO2-max in the HI group than in the LI group. Hippocampal and gray matter CBF was found to be significantly more increased in females with an increase in VO2-max compared to those with a decrease in VO2-max. Since the results of this study were not entirely in line with the stated hypothesis, further research has to be done to fully understand the influence of high- and low-intensity training on the young, healthy hippocampus.

KEYWORDS

angiogenesis, MRI, exercise, hippocampus, plasticity, VO2-max, CBF, CBV

INTRODUCTION

Physical exercise is well known to benefit both physical and mental health. Consistent exercise effectively enhances the maximal rate of oxygen consumption (VO2-max) by increasing cardiac output, and peripherally by widening the arterial-venous oxygen difference (Seals et al., 1984). VO2-max is a measurement of milliliters of oxygen consumed per kilogram of body weight per minute (ml/kg/min). An increase in VO2-max correlates strongly with an increase in aerobic fitness, and with a reduced risk of chronic disease and a longer lifespan (Sawada et al., 2012). In addition to enhancing the function of the cardio-vascular system, exercise has been shown to increase bone density, improve muscle quality, and protect against metabolic dysfunction (Brooks et al., 1996). Especially high-intensity sports training is known to be beneficial for improving VO2-max (Mi-lanovic et al., 2015; Gormley et al., 2008).

Exercise also improves brain function (cognition) and influences brain structure. An increase in brain volume, especially in the hippocampus has been shown after exercise intervention (Erickson et al., 2010). The hippocampus is a highly plastic brain region, which can generate new neurons in the adult brain, a process called adult neurogenesis (van Praag et al., 1999). Van der Borght et al. (2009) found that the cell proliferation in the dentate gyrus of rodents is regulated by physical activity. Furthermore, an exercise induced increase in vascular volume has been shown in monkeys (Rhyu et al., 2010). Exercise in older adults plays an important role in maintaining healthy brain function and neurogenesis.

An increase in neurogenesis can affect the hippocampus in a

number of different ways, by means of neuron proliferation, differentiation, an increase in survival rates of new neurons or the effect of the maturation and integration of new neurons. Nerve growth factors, brain derived neurotrophic factors (BDNF) and glial cell line-derived trophic factors (GDNF) play a key role in the process of neurogenesis.

Nevertheless, not all studies have found a positive relationship between hippocampal structure and high intensity exercise. For example Wagner et al. (2015) found a negative correlation of high-intensity training and hippocampal volume, suggesting an inflammatory response after exercise, whereas others suggest mild instead of intensive exercise is beneficial for hippocampal neurogenesis (Inoue et al., 2015). The frequency and the duration of exercise training that is needed to stimulate plasticity remains vague. Additionally, it is not known whether an increase in VO2-max (as indicator for fitness) is needed to change the brain morphology.

It has recently become clear that non-neuronal elements can exhibit a similar capacity for plastic changes (angiogenesis). Neuronal changes are accompanied by substantial increases in glia and capillary volume. For example, changes in cerebral blood flow (CBF, ml blood per 100ml brain per minute) and cerebral blood volume (CBV, ml blood per 100ml/g brain) have been associated with sensory, motor, and cognitive task performance (Ogawa et al., 1990). Exercise has been shown to have an influence on the formation of new blood vessels in the rodent hippocampus (Pereira et al., 2006). In humans, angiogenesis allows a higher supply of oxygen and trophic factors to reach the brain and has a positive effect on cardiopulmonary and cognitive function (Pereira et al., 2006). It is a splitting process (intussusception) of new branches from capillaries that merge onto one another, regulated by neuroectodermal derived growth factors that bind to tyrosine kinase receptors expressed on endothelial cells. The vascular endothelial growth factor (VEGF) plays a pivotal role in this process. Angiogenesis is part of growth and development, but also of transition of tumors. It causes changes that increase nutrient delivery and efficiency. Angiogenesis and neurogenesis are tightly linked and lead to improvement in neurological function.

Isaacs et al. (1992) showed an influence of voluntary exercise in rodents on the density of capillaries and Pereira et al. (2007) found an increase in CBV in the dentate gyrus of rodents. In humans a positive effect of physical activity on the vertebral vasculature has been found (Bullitt et al., 2009). Guiney et al. (2015) point to cerebral blood flow (CBF) as a mechanism that drives physical activity-related cognitive benefits.

The precise adjustment mechanisms in the hippocampus to sport and physical exercise are not thoroughly researched yet. Especially the difference between high-intensity and low-intensity training and the relationship to neuronal processes in the hippocampus are still to be investigated. To our knowledge there have not been any studies conducted that explore the underlying cellular mechanisms of the influence of physical activity on the hippocampus of healthy young participants.

The aim of this study was to assess the influence of high- versus low-intensity training on the healthy young hippocampus and shed light on which mechanism can explain the exercise-induced changes in brain structure. This will help to provide a better training to increase cardiorespiratory fitness and brain function, but also use physical activity as a protection and treatment for neurodegenerative and neuropsychiatric disorders. The effects on hippocampal volume, CBV and CBF and VO2-max as a measurement of fitness were analyzed and compared between groups. Based on previous literature we expect that hippocampal volume, CBV and CBF increase after 12 weeks of high-intensity training but not low-intensity training, based on an increase in VO2-max.

MATERIALS AND METHODS

Participants

We enrolled 52 young healthy sedentary volunteers (table 1) from Amsterdam and surrounding areas via flyers, posters and social media.

Inclusion criteria were age between 18-30 years, BMI 30 kg/m2, VO2-max 55 ml/kg/min (males), VO2-max 45 ml/kg/min (females), use of oral contraceptive or intrauterine device (females) and a stable exercise history 3 months prior to study inclusion. Participants were excluded from participation if they met any of the following criteria: General contraindications for MRI, history of chronic renal insu ciency, allergy to Gadolinium-containing compounds, history of psychiatric disorders, excessive smoking (>pack/day), excessive alcohol consumption (>21 units/week), or other regular drug use.

Participants that already engaged in intensive sports prior to the study intervention (>3 times/week) were also excluded. A compensation after completion of the study was payed.

Ethics

This study was approved by the Medical Ethical Committee of Amsterdam according to the standard of the National Committee of Health Research Ethics. All experiments were conducted along with the Helsinki Declaration of 2012 and written informed consent was obtained from all participants included in the study.

Design and Intervention

Participants were encompassed into a double-blind, randomized controlled trial of two intervention groups: high-intensity aerobic exercise (high intensity; HI) or stretching and toning exercise (low intensity; LI). Before and after the intervention several MRI mea-

Table 1. Demographics and mean values (standard deviation) - Exercise Groups

	Low-intensity (n = 22)	High-intensity (n = 23)	p-value
Gender (number of females)	11	13	0.78
Age (years)	24.05 (3.28)	22.87 (2.34)	0.17
BMI	23.75 (3.15)	22.75 (2.43)	0.24
VO2-max$_{PRE}$	37.06 (5.80)	37.35 (7.42)	0.88
VO2-max$_{POST}$	38.00 (7.71)	39.63 (7.05)	0.46
Hours of sport$_{self reported}$	29.46 (12.09)	31.72 (14.67)	0.58
Hours of sport$_{POLAR}$	20.91 (9.35)	18.80 (9.98)	0.47
Sport over heart rate of 75% (h)	2.73 (1.80)	8.24 (4.41)	<0.01 **
Sport over heart rate of 75% (%)	12.36 (6.47)	47.81 (16.46)	<0.01 **
Hippocampal volume$_{PRE}$	3709.76 (312.91)	3845.87 (423.60)	0.23
Hippocampal volume$_{POST}$	3708.09 (326.82)	3842.57 (401.51)	0.23
CBV$_{PRE}$	2.86 (0.84)	2.85 (0.92)	0.97
CBV$_{POST}$	2.51 (0.86)	2.88 (1.18)	0.25
CBF$_{hippocampus,PRE}$	37.18 (5.54)	34.79 (6.58)	0.20
CBF$_{hippocampus,POST}$	35.92 (5.87)	35.17 (4.33)	0.63
CBF$_{graymatter,PRE}$	51.73 (7.13)	47.98 (9.73)	0.15
CBF$_{graymatter,POST}$	49.80 (8.09)	49.43 (6.85)	0.87

surements, VO2-max sports tests, blood samples, neuropsychological tests and questionnaires were conducted. Participants received a three months membership at the Science Park University Sport Centrum (USC) and a list of suggestions for sport classes fitting their training group. Both exercise groups engaged in 45 minutes of exercise three times a week additionally to the number of trainings they were doing prior to the study. High-intensity sports training was defined by training at a minimum of 75% of maximal heart rate. Heart rate was controlled by a heart rate monitor (POLAR) that had to be worn during all exercise trainings. A weekly questionnaire was send to participants to control the duration, number and kind of exercises they did. Additionally, participants gym visits were tracked and controlled (table 1). For motivational purposes every participant trained with one of the experimenters once and was contacted frequently.

VO2-max measurement

VO2-max tests before and after the 12-week intervention were performed at the USC Amsterdam. Fitness was assessed using a cycle ergometer and a graded exercise test where intensity was increased gradually while measuring participants oxygen consumption with an oxygen mask. The exercise test continued until maximal effort or exhaustion was achieved. For exercise tests to be considered maximal, participants had to reach both a plateau in VO2-max with increasing workload and a respiratory exchange ratio >1.1. The highest VO2 attained during the test was recorded as VO2-max. The exercise test was conducted at least 24 hours before or after the MRI scan.

MRI acquisition

High-resolution T1 anatomical scans were obtained on a 7T Philips whole body MR-scanner (Philips Healthcare, Best, The Netherlands) running under software release 3.2.1 or higher with a 32-channel receive channels head coil (Nova medi-cal). Whole brain T1-weighted images were obtained using a 3D TFE sequence with the following parameters: resolution=0.9mm isotropic; FOV=218.51x240x180; TR/TE=4.115/1.847ms, FA=7°.

Perfusion and blood volume measurements were performed on a 3T whole body MR scanner (Philips Healthcare, Ingenia, The Netherlands) running under software release 5.1.8 or higher using a 32 receive channel head coil. It has been shown that CBV is a surrogate marker for the in vivo quantification of angio-genesis. CBV and CBF (as a quantification of angiogenesis) in the in vivo brain can be measured with T1 weighted data of contrast-enhanced MRI (Maass et al., 2016). To obtain hip-pocampal CBV, T1 values for tissue and blood were determined before and after gadolinium contrast administration. For T1 tis-sue, T1 mapping was performed using a 3D Look-Locker se-quence (Look and Locker, 1970). Parameters providing signal data from 16 time points after an adiabatic inversion pulse with 200ms time intervals, a TE=3.99ms, TR=10ms, FA=5° and 26 slices with a slice thickness of 3mm were used (Lindgren et al., 2014). A partial scan was obtained, so that the field of interest, the hippocampus, was inside the scanned area.

Additionally, the T1 blood scan was planned perpendicular to the posterior sagittal sinus and comprised a multi time-point inversion recovery experiment with TE=15.97ms, TR=110ms, FA=95°. A global inversion pulse followed by a 95° section-selective readout pulse, which saturated the tissue surrounding the sinus. Gadolinium (CA, Gadovist, Bayer B.V., Mijdrecht, The Netherlands) was administered using automatic bolus injection (Mallinckrodt Optistar, Liebel-Flarsheim, Cincinnati, OH, USA) with a speed of 1-2 mL/s followed by 20 mL saline (0.9% NaCl). Injection duration was approximately 1s with a dose of 0.1 ml/kg of bodyweight. To obtain hippocampal and graymatter (GM) CBF a gradient-echo single shot EPI pCASL sequence was used to obtain perfusion-weighted images with 22 slices, using TE=16.173ms, TR=4091ms, FA=90°, label duration=1,650ms, post-label delay=1,525ms and label gap=20 mm. Background suppression was used. A separate sequence for reference measurement of M0 was applied using the same parameters as in the pCASL sequence, except for TR=2000ms and without background suppression. An image of the labeling plane from the first investigation was used as a guide for positioning of the labeling plane at the second investigation.

MRI post-processing

CBV

T1 images were acquired at multiple time points on the recovery curve, and pixel-wise curve fitting was performed to estimate the relaxation time parameter to produce a pixel-map of T1. The measured values were fit to the 3-parameter model to estimate A, B, and T1* which were used to approximate T1 T1 (B/A - 1). The derivation for the so-called Look-Locker correction factor B/A - 1 is based on a continuous readout using Fast Low Angle Shot (FLASH) (Deichmann and Haase, 1992) These images were processed with in-house MATLAB scripts, according to Deichmann & Haases (1992) method for T1 maps (figure 1). Individual hippocampus masks were produced with automatic FreeSurfer (surfer.nmr.mgh.harvard.edu/) segmentation using 7T anatomical scans. Segmentation of the subcortical white matter and greymatter volumetric structures (including the hippocampus) was performed. The corresponding hippocampus masks were thresholded and eroded with FSL. FSL was also used for registration (FLIRT Jenkinson et al., 2002) and value extraction. Outliers were removed with the smooth function in MATLAB. CBV was calculated using equations by Lindgren et al. (2014) by first cal-

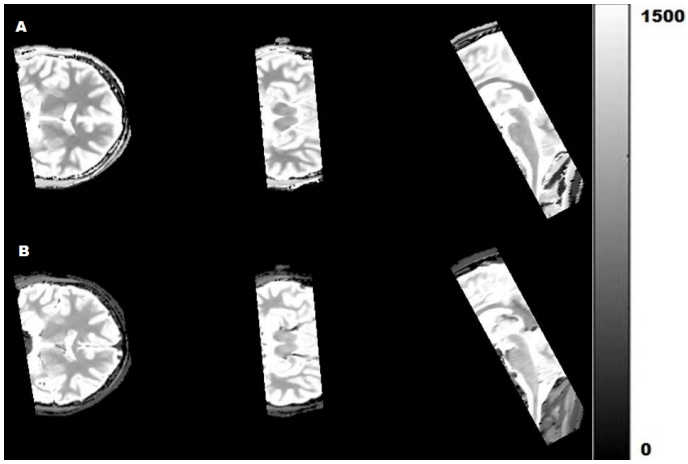

Figure 1. T1maps of one representative participant A pre bolus injection B post bolus injection

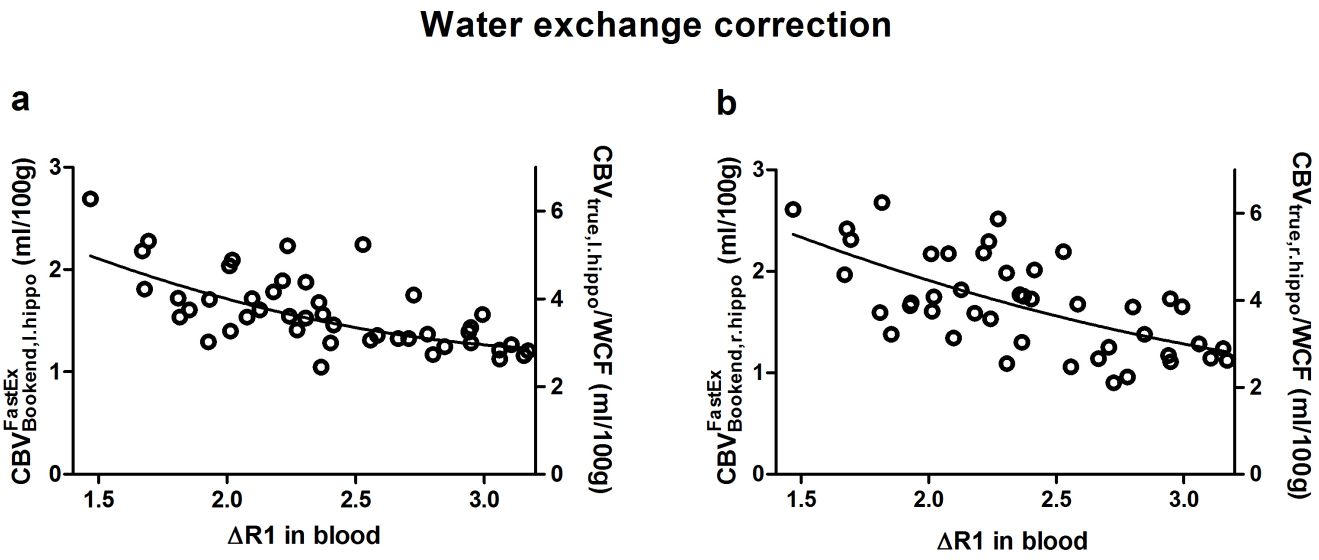

Figure 2. Extraction of the water correction factor (WCF) established with a second-order polynomial fit to CBV_{true}=CBV_{FastEx}. Cicular markers: CBV_{FastEx} (scale: left y-axis) in a left hippocampus and b right hippocampus. Solid lines: CBV_{true}=WCF fit (scale: right y-axis).

culating the mean value of T1 pre-CA and T1 post-CA in the hippocampus using p=1.04 g/ml, HctLV =0.45 and HctS V =0.25. Median hippocampal T1 was calculated per participant (right and left).

T1 blood values were then calculated with in-house MATLAB scripts. The five pixels showing the highest signal of the last 10 slices in the sagittal sinus were selected to represent blood. These values were used to calculate the CBVfastex values per participant for pre intervention and post intervention (equation 1). WCF correction factors were established fitting a second-order polynomial to the CBVfastex values using 4R1 (equation 3) in MATLAB to correct for expected deviations from the fast-water exchange limit (figure 2; Shin et al., 2006). These were multiplied with the CBVfastex values to get the true CBV values per participant (equation 2).

Freesurfer was used for automatic hippocampus segmentation and FSL for registration (FLIRT Jenkinson et al., 2002) and value extraction.

CBF

ASL post-processing was performed with an in-house developed

$$CBV^{FastEx}_{Bookend,tissue} = 100 \times \frac{1}{p} \times \frac{1 - Hct_{LV}}{1 - Hct_{SV}} \times \frac{(\frac{1}{T1_{post}} - \frac{1}{T1_{pre}})_{tissue}}{(\frac{1}{T1_{post}} - \frac{1}{T1_{pre}})_{blood}} \quad (1)$$

$$CBV_{Bookend,tissue} = WCF(\triangle R1) \times CBV^{FastEx}_{Bookend,tissue} \quad (2)$$

$$\triangle R_1 = \frac{1}{T1^{blood}_{post}} - \frac{1}{T1^{blood}_{pre}} \quad (3)$$

toolbox based on SPM (Statistical Parametric Mapping, Wellcome Trust Centre for Neuroimaging, London, UK) (ExploreASL toolbox; Mutsaerts et al., 2016). T1 images were registered to the MNI template and segmented into GM and white matter (WM) probability maps. Motion estimation was used for the ASL series to detect large motion artifacts. Any motion spike frames with a spike exclusion threshold over the mean + 3 standard deviations (SD) were deleted. Accurate motion estimation was run with a cleaned dataset (participants with a mean frame-wise displacement vector >2mm were removed). Subsequently, the ASL perfusion-weighted images were registered to the GM tissue probability maps of each participant using 6 parameter rigid body registration. Then, the label and control images were pairwise subtracted (4M), corrected for slice gradients and averaged. CBF was calculated using methods of Alsop et al. (2014), using a separate M0 image. After, voxel-based outlier rejection and quantification was applied and the CBF images were averaged. Transformation fields were applied to CBF maps and the GM tissue probability maps were normalized using the Diffeomorphic Anatomical Registration analysis using Exponentiated Lie algebra (DARTEL) algorithm (Ashburner, 2007). CBF values of the hippocampus were corrected with signal-to-noise ratio (SNR) masks (threshold=1.5), created with FSL. The SNR masks were substracted from the CBF maps, assuming they represent blood vessels. An example of a CBF map can be found in figure 3. The hippocampal mask was extracted from the Harvard-Oxford Subcortical Structural Atlas and eroded with a threshold of 10. Gray matter CBF was extracted with individual gray matter masks made from rcT1 scans and thresholded with 15% of the highest values using FSL. Median hippocampal CBF values were calculated per participant (left/right).

Statistics

Hippocampal volume (HV), CBV and CBF values were av-eraged for each hemisphere of each participant (left HV, right HV, left CBV, right CBV, left CBF and right CBF).

No a priori hypothesis was made about hemispheric lateraliza-tion, therefore we tested for hemisphere effects with a repeated-measures analysis of variance (ANOVA) with hemisphere as a within-subject factor and group as a between-subject factor. No

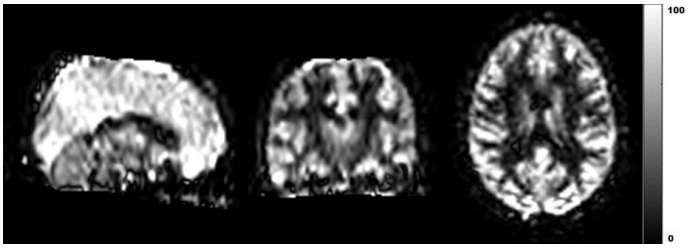

Figure 3. CBF map of one representative participant

significant interactions could be found for pre- and post-intervention: volume (F(1)=0.11, p=0.74, F(1)=0.95, p=0.76, respectively), CBV (F(1)=0.27,p=0.36, F(1)=0.60, p=0.44, re-spectively) and CBF (F(1)=0.09,p=0.77, F(1)=0.04 , p=0.84 , respectively). Therefore, all parameters (HV, CBV, CBF) were collapsed across hemispheres (averaged left/right).

For each subject, the total exercise time (TET), total number of training (TNT) and total number of weeks exercised (TWE) were calculated using the weekly questionnaires. POLAR heart rate data was used to calculate how much time of the total ex-ercise time was spent above 75% of the maximal heart rate. This variable was included to compare the intensity of sports-training between groups, using a t-test.

Change in VO2-max was calculated using absolute scores expressed in milliliters of oxygen per kilogram of body mass per minute (ml/(kg min)).Change variables were calculated subtracting the absolute pre intervention values from the post in-tervention values per participant. The mean was used for group comparison. T-tests were used to compare volume, CBV and CBF between groups. Repeated measures ANOVA with exercise group (LI/HI) or VO2-max change (increase or decrease) and gender as between-subject factors and time (pre and post exercise) as a within-subject factor were used to test the change over time.

Statistical analyses were performed using The Statistical Package for Social Sciences software (SPSS version 20, IBM Cor-poration, Armonk, NY: http://www.spss.com).

RESULTS

We excluded 7 participants during the study, one because of injury, five because they did not participate in the sports training or did not show up for the post measurement and one because of a too high BMI. A total of 45 participants were analyzed.

Comparing the two groups of high and low training intensity, we found a significant difference between the groups in the time spent with a heart rate over 75% of their maximal heart rate (t(29.4)=5.53, p<0.01), but both groups did not differ in average training duration (HI; M=31.72, STD=14.67; LI; M=29.46, STD=12.09; t(43)=-0.57, p=0.58). No significant difference in VO2-max change was found (HI; M=2.28, STD=5.22; LI; M=0.94, STD=5.36; t(43)=-0.85, p=0.40) (figure 4).

As we defined VO2-max as an indicator of fitness we decided to divide our analysis in two parts. The comparison between exercise groups, taking gender and time into account and the comparison between participants that increased their VO2-max (IVO2) and decreased their VO2-max (DVO2). The high exer-cise group contained 13 females and 10 males, the low exercise group contained 11 females and 11 males (table 1). The IVO2 group enclosed 14 females and 12 males, the DVO2 group had 10 females and 9 males (table 2).

Exercise Groups

A repeated measures ANOVA with time as within-subject factor and exercise group and gender as within-subject factors was performed for every variable. Hippocampal volume was not found to have any significant effect (time: F(1)=0.06, r=0.81; time*exercise group: F(1)=0.01, r= 0.93; time*exercise group*gender: F(1)=1.74, p=0.20). There was also no significant results found for CBV (time: F(1)=0.83, p=0.38; time*exercise group: F(1)=1.15, p= 0.29; time*exercise group*gender: F(1)=1.32, p=0.26) , CBFhippo (time: F(1)=0.78, p=0.38; time*exercise group: F(1)=1.51, p= 0.23; time*exercise group*gender: F(1)=0.06, p=0.81) or CBFgm (time: F(1)=0.25, p=0.62; time*exercise group: F(1)=2.54, p= 0.12; time*exercise group*gender: F(1)=0.86, p=0.36).

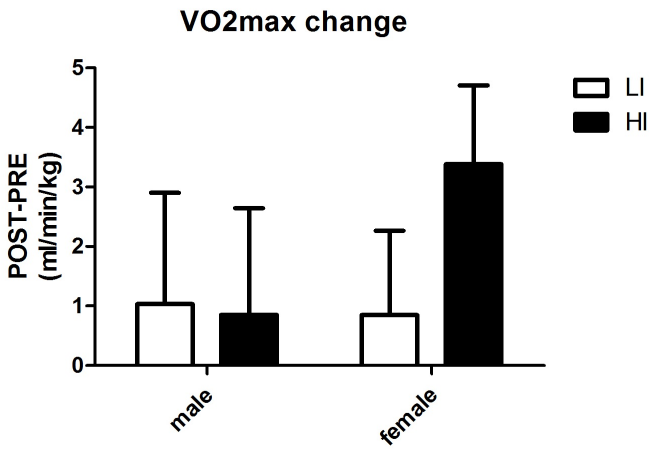

Figure 4. Change (Post-Pre) of VO2-max for both exercise groups

Table 2. Demographics and mean values (standard deviation) - VO2-change Groups

	decreased VO2-max (n = 19)	increased VO2-max (n = 26)	p-value
Gender (number of women)	11	15	
Age (years)	24.32 (2.81)	22.81 (2.8)	0.08
BMI	23.12 (3.49)	23.33 (2.28)	0.81
VO2-max$_{PRE}$	39.00 (7.09)	35.89 (6.02)	0.12
VO2-max$_{POST}$	35.78 (7.97)	41.06 (6.07)	0.02 **
Hours of sport$_{self reported}$	30.14 (7.33)	36.79 (5.81)	0.61
Hours of sport$_{POLAR}$	18.30 (8.86)	20.95 (10.17)	0.37
Sport over heart rate of 75% (h)	4.19 (3.08)	6.54 (4.93)	0.07
Sport over heart rate of 75% (%)	23.23 (18.36)	35.78 (22.95)	0.06
Hippocampal volume$_{PRE}$	3818.90 (363.3)	3746.59 (387.08)	0.53
Hippocampal volume$_{POST}$	3820.89 (376.11)	3740.71 (365.81)	0.48
CBV$_{PRE}$	2.72 (0.88)	2.96 (0.87)	0.37
CBV$_{POST}$	2.67 (1.35)	2.71 (0.75)	0.88
CBF$_{hippocampus,PRE}$	38.00 (6.39)	34.45 (5.62)	0.05
CBF$_{hippocampus,POST}$	35.42 (5.50)	35.61 (4.85)	0.91
CBF$_{graymatter,PRE}$	52.80 (7.83)	47.63 (8.75)	0.05
CBF$_{graymatter,POST}$	50.20 (8.61)	49.15 (6.45)	0.65

Independent samples t-tests were performed with exercise as grouping variable and gender as splitting variable. No significant differences were found. Interestingly, females had the opposite change in hippocampal CBV in the HI group than males, meaning females had a decreased CBV after sport intervention in both groups, whereas males had a decrease in the LI group and an increase in the HI group. This effect was opposite for hippocampal CBF, where males had a slight decrease over time in both groups, whereas females showed a decrease in the LI group and increase in the HI group, which can also be seen in gray matter CBF (figure 5).

Performing an independent t-test with exercise group as grouping variable and gender as splitting variable on the change from pre to post of every variable revealed no additional significant results.

VO2-max-change Groups

First, a repeated measures ANOVA with time as within-subject factor and VO2 change (increase/decrease) and gender as within-subject factor was performed for all variables. No significant ef-

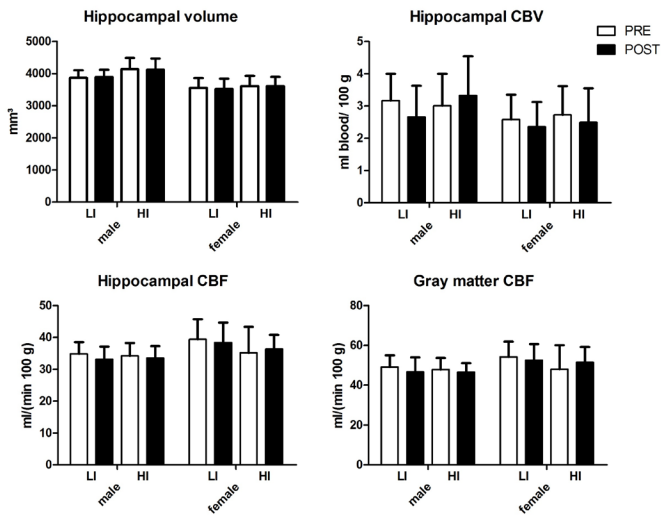

Figure 5. Values of all four variables (volume, CBV, CBFhippocampus, CBFgraymatter for both exercise groups (females/males) before and after the exercise intervention.

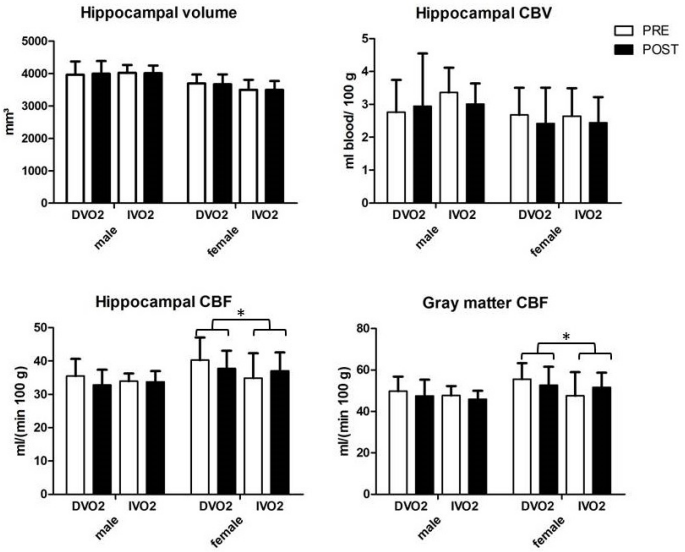

Figure 6. Values of all four variables (volume, CBV, CBFhippocampus, CBFgraymatter for both VO2groups (females/males) before and after the exercise intervention.

fects were found for hippocampal volume (time: F(1)= 0.01, p=0.91; time*VO2group: F(1)=0.19, p= 0.67; time*VO2group*gender: F(1)=2.31, p=0.14) and CBV(time: F(1)=0.67, p=0.42; time*VO-2group: F(1)=0.37, p= 0.54; time*VO2group*gender: F(1)=0.54, p=0.47). In hippocampal CBF a significant interaction effect of time and VO2group was found (F(1)=5.00, p=0.02). In gray matter CBF the interaction effect of time and VO2group shows a trend of F(1)=3.33, p=0.07.

Independent samples t-tests were also performed with VO2group as grouping variable and gender as splitting variable. No significant differences were found. Hippocampal CBV in males showed a trend towards an increase in CBV for participants with a decrease in VO2 and a decrease in CBV when they had an increase in VO2. This e ect cannot be seen in females. Both groups slightly decreased after the intervention. An interesting trend can be seen in hippocampal CBF for both females and males. Participants with a decrease in VO2 showed a decrease in CBF in both genders and females showed an in-crease in CBF when they had an increase in VO2, males did not change in this category. A general decrease of gray matter CBF was found in three of the categories, only females with an increase in VO2 showed an increase in gray matter CBF (figure 6). Performing an independent t-test with VO2-change as grouping variable and gender as splitting variable on the change from pre to post of every variable revealed a trend towards a significant difference between groups in hippocampal CBF for males and a significant differences for females (m: F(18)=0.11, p=0.07; f: F(18.36)=4.78, p=0.04).

The gray matter CBF change was also significantly different between groups for females (F(22)=1.59, p=0.05).

DISCUSSION

In this study we investigated the effects of high- and low-intensity sports training on hippocampal volume and vascula-ture of young healthy adults.

We found a large difference in VO2-max change comparing the LI and HI group in females, but not in males. Both hippocampal and gray matter CBF changed more in the IVO2 group of the females than in the DVO2 group. A general trend towards our hypothesis is visible.

In this study a high-intensity sports training was compared to a low-intensity sports training. Interestingly, we only found a high change in VO2-max in the HI group of the females but not the males. Several studies have found individual differences between the responsiveness to certain exercise training and in-tensities. The effect of training depends on many factors, such as level of fitness before the intervention, age, gender, genetic settings, stress responsiveness and more (Heijnen et al., 2016). We quantified the effect of training with a VO2-max test.

Both gender groups started with a relatively low VO2-max for their age. Wilmore et al. (2015) found an average VO2-max of 33-42 for females and of 43-52 for males in an age group of 20 to 29. The average of our females was in the lower bound of that range, the males were even a little lower than the general average. This shows that we recruited young volunteers with a low fitness level as we intended, because a low VO2-max value has been shown to be easier to improve. Estrogen, the primary female sex hormone, may protect muscles from exercise-induced damage and has an influence on how much glycogen is burned during prolonged training (Rooney et al., 1993). This might explain the change in cardiorespiratory fitness in females but not in males. Another explanation could be, that females seemed to be more motivated and dedicated in our study. They trained more regularly and were more responsive in questionnaires and tests.

In this study we included a high-intensity group, which was set to a training intensity of 75% of maximal heart rate. The intensity level was personalized and the maximal heart rate was determined by a sport test. This level might have been too high for some participants, causing for example demotivation or over-training. Angeli et al. (2004) point out that exercise induced stress exceeds the capacity of neuroendocrine adaptation and therefore causes physical and psychological disturbances. Additionally, we asked the participants to train three more times on top of the number of days of training they were doing before. This could have also led to a high level of stress, which can lead to a negative effect on neuro- and angiogenesis. Stress has been shown to have an influence on serotonin levels, which decreases BDNF levels in the hippocampus, which in turn is

responsible for neurogenesis (Vaidya et al., 1999).

We included a low-intensity exercise group and not a sedentary control group. LI training (toning and stretching) has not been found to increase VO2-max before (Maass et al., 2016) and was chosen as a control intervention to hold variables like social interactions, schedule, stress and motivation as similar as possible to the training group whilst not affecting cardiovascular fitness. This might have led to smaller differences between our groups. Furthermore, participants had the freedom to do a high range of different sport-training. They were preselected and tested, but participants could also do their own individual training. The POLAR heart rate monitor was used to control their heart rate and questionnaires were used to track the duration and kind of exercise. There was a significantly higher heart rate for the HI group, which indicates a successful division in training groups, according to indications by heart rate. The duration of exercises did not differ significantly between groups.

Hippocampal volume has been shown to be influenced by physical exercise (Erickson et al., 2010). In this study no significant changes could be found, whereas other variables changed from pre to post intervention. This points towards a different relationship of hippocampal volume and angiogenesis than hypothesized. In this study no connection could be shown.

Changes in CBV were minimal and non-significant in this participant group. Because we used young healthy participants we could have reached a ceiling effect. Rhyu et al. (2010) found in a study with macaques, that 5 months of treadmill training increased the vascular volume and perfusion in the motor cortex in older animals, but not in middle-aged animals.

Hippocampal and gray matter CBF in females increased more in the IVO2 group than in the DVO2 group. These results show an influence of sport training on VO2-max depending on gender. The changes in VO2-max are in line with the changes in gray matter and hippocampal CBF. This points towards VO2-max as a good predictor for perfusion and changes in vascular fitness.

Given that both gray matter and hippocampus CBF increased significantly we cannot say anything about the regional specificity of CBF to the hippocampus. Further analysis has to be done to conclude a specificity to the hippocampus as hypothesized.

The level of capillary density in the hippocampus has previously been found to have a rapid time course. Van der Borght et al. (2009) have found that it occurs three days after onset of training and already shows a decline after 24h of sedentary behavior. The consistency and regularity of training, differing between participants, could have had an influence on the perfusion and blood volume values.

Because of time constraints some of the post-processing steps can still be improved. CBV was calculated using the T1tissue and T1blood and a fitted water correction factor. The regis-tration of the T1 tissue maps to the individuals brain caused high standard deviations in values, especially for T1 post contrast measurements. Additionally, an improvement of T1blood fitting was not yet performed. Fit errors between participants varied, different fitting algorithms and methods could improve T1 blood values and thus CBV quantification.

Literature points towards a change in perfusion and blood volume (CBV and CBF) in explicitly the dentate gyrus, but not the whole hippocampus after exercise interventions (Maass et al., 2016, Pereira et al., 2006). In this study only the whole hippocampus was analyzed. A separation in substructures could shed light on the regional selectivity of exercise targeting the hippocampus. The resolution of the structural scan and the CBV maps is high enough to segment subfields of the hip-pocampus. To calculate hippocampal CBF, ASL scans were used. The signal to noise ratio in these scans is relatively low. Analyzing subfields of the hippocampus with this method might be too speculative, and therefore other scanning methods should be considered.

Conclusion

In sum, we show a general trend towards our hypothesis, that high intensity training has a positive influence on hippocampal volume, CBV and CBF based on an increase of VO2-max. Only females showed a significantly higher increase in VO2-max in the HI group than in the LI group. Hippocampal and gray matter CBF was found to be significantly more increased in females with an increase in VO2-max compared to those with a decrease in VO2-max.

Since the results of this study were not entirely in line with the stated hypothesis, further research has to be done to fully understand the influence of high and low intensity training on the young, healthy hippocampus. Eventually, this knowledge will allow us to provide better training programs to increase cardiorespiratory health and brain function as well as to maximize cognitive potential in development and lessen the influence of cognitive decline in the aging population.

REFERENCES

Alsop, D. C., Detre, J. A., Golay, X., Günther, M., Hendrikse, J., Hernandez-Garcia, L., Lu, H., MacIntosh, B. J., Parkes, L. M., Smits, M., van Osch, M. J. P., Wang, D. J. J., Wong, E. C., and Zaharchuk, G. (2015). Recom-mended implementation of arterial spin-labeled perfusion MRI for clinical applications: A consensus of the ISMRM perfusion study group and the Eu-ropean consortium for ASL in dementia. Magnetic Resonance in Medicine, 73(1):102–116.

Ashburner, J. (2007). A fast di eomorphic image registration algorithm. Neu-roImage, 38(1):95–113.

Brooks, G. A. G. A., Fahey, T. D. T. D., and White, T. P. (1996). Exercise physiology: human bioenergetics and its applications. Mayfield Pub. Co.

Bullitt, E., Rahman, F. N., Smith, J. K., Kim, E., Zeng, D., Katz, L. M., and Marks, B. L. (2009). The e ect of exercise on the cerebral vasculature of healthy aged subjects as visualized by MR angiography. American Journal of Neuroradiology, 30:1857–1863.

Deichmann, R. and Haase, a. (1992). Quantification of T 1 values by SNAPSHOT-FLASH NMR imaging. Journal of Magnetic Resonance (1969), 612:608–612.

Erickson, K. I., Voss, M. W., Prakash, R. S., Basak, C., Szabo, A., Chaddock, L., Kim, J. S., Heo, S., Alves, H., White, S. M., Wojcicki, T. R., Mailey, E., Vieira, V. J., Martin, S. A., Pence, B. D., Woods, J. A., Mcauley, E., and Kramer, A. F. (2010). Exercise training increases size of hippocampus and improves memory. PNAS, 108(7):3017–3022.

Gormley, S. E., Swain, D. P., High, R., Spina, R. J., Dowling, E. A., Kotipalli, U. S., and Gandrakota, R. (2008). E ect of Intensity of Aerobic Training on VO2max. Medicine & Science in Sports & Exercise, 40(7):1336–1343.

Guiney, H., Lucas, S. J., Cotter, J. D., and Machado, L. (2015). Evidence cerebral blood-flow regulation mediates exercisecognition links in healthy young adults. Neuropsychology, 29(1):1–9.

Heijnen, S., Hommel, B., Kibele, A., and Colzato, L. S. (2016). Neuromodula-tion of Aerobic ExerciseA Review. Frontiers in Psychology, 6:1890.

Inoue, K., Okamoto, M., Shibato, J., Lee, M. C., Matsui, T., Rakwal, R., and Soya, H. (2015). Long-Term Mild, rather than Intense, Exercise Enhances Adult Hippocampal Neurogenesis and Greatly Changes the Transcriptomic Profile of the Hippocampus. PLOS ONE, 10(6):e0128720.

Isaacs, K. R., Anderson, J., Alcantara, A. A., Black, J. E., and Greenough, T. (1992). Exercise and the Brain: Angiogenesis in the Adult Rat Cerebel-lum After Vigorous Physical Activity and Motor Skill Learning. Journal of Cerebral Blood Flow and Metabolism, 12:110–119.

Jenkinson, M., Bannister, P., Brady, M., and Smith, S. (2002). Improved opti-mization for the robust and accurate linear registration and motion correction of brain images. NeuroImage, 17(2):825–41.

Kenney, W. L., Wilmore, J., and Costill, D. (2015). Physiology of Sport and Exercise 6th Edition. Human kinetics.

Lindgren, E., Wirestam, R., Markenroth Bloch, K., Ahlgren, A., van Osch, M. J. P., van Westen, D., Surova, Y., Ståhlberg, F., and Knutsson, L. (2014). Absolute quantification of perfusion by dynamic susceptibility contrast MRI using Bookend and VASO steady-state CBV calibration: a comparison with pseudo-continuous ASL. Magma (New York, N.Y.), 27:487–499.

Look, D. C. and Locker, D. R. (1970). Time saving in measurement of NMR and EPR relaxation times. Review of Scientific Instruments, 41(2):250–251.

Maass, A., Duzel, S., Brigadski, T., Goerke, M., Becke, A., Sobieray, U., Neu-mann, K., Lovden, M., Lindenberger, U., Backman, L., Braun-Dullaeus, R., Ahrens, D., Heinze, H.-J.,Muller, N. G., Lessmann, V., Sendtner, M., and Duzel, E. (2016). Relationships of peripheral IGF-1, VEGF and BDNF levels to exercise-related changes in memory, hippocampal perfusion and volumes in older adults. NeuroImage, 131:142–54.

Milanovic, Z., Sporis, G., and Weston, M. (2015). E ectiveness of High-Intensity Interval Training (HIT) and Continuous Endurance Training for VO2max Improvements: A Systematic Review and Meta-Analysis of Con-trolled Trials. Sports Medicine, 45(10):1469–1481.

Mutsaerts, H., Thomas, D., Petr Jan, de Vita, E., Cash, D., Van Osch, M., Groot, P., Van Swieten, J., Laforce Jr, R., Tagliavini, F., Borroni, B., Galimberti, D., Rowe, J., Gra , C., Frisoni, G., Finger, E., Sorbi, S., Mendonca, A., Rossor, M., Rohrer, J., Masellis, M., and MacIntosh, B. (2016). Addressing multi-centre image registration of 3T arterial spin labeling images from the GENetic Frontotemporal dementia Initiative (GENFI). Singapore. ISMRM 2016.

Ogawa, S., Lee, T. M., Kay, A. R., and Tank, D. W. (1990). Brain magnetic resonance imaging with contrast dependent on blood oxygenation. Proceedings of the National Academy of Sciences of the United States of America, 87(24):9868–72.

Pereira, A. C., Huddleston, D. E., Brickman, A. M., Sosunov, A. A., Hen, R., Mckhann, G. M., Sloan, R., Gage, F. H., Brown, T. R., and Small, S. A. (2006). An in vivo correlate of exercise-induced neurogenesis in the adult dentate gyrus. PNAS, 104(13):5638–5643.

Rhyu, I., Bytheway, J., Kohler, S., Lange, H., Lee, K., Boklewski, J., Mc-Cormick, K., Williams, N., Stanton, G., Greenough, W., and Cameron, J. (2010). E ects of aerobic exercise training on cognitive function and corti-cal vascularity in monkeys. Neuroscience, 167(4):1239–1248.

Rooney, T. P., Kendrick, Z. V., Carlson, J., Ellis, G. S., Matakevich, B., Lorusso, S. M., and McCall, J. A. (1993). E ect of estradiol on the temporal pattern of exercise-induced tissue glycogen depletion in male rats. Journal of applied physiology (Bethesda, Md. : 1985), 75(4):1502–6.

Sawada, S., Miyachi, M., Murakami, H., Kawakami, R., Tanaka, S., Ishikawa-Takata, K., Tabata, I., Oida, Y., Oguma, Y., Miyatake, N., Okamoto, T., Tsukamoto, K., Tanaka, H., Lee, I., and Blair, S. (2012). Dose-response re-lationship between cardiorespiratory fitness and morbidity/mortality: a sys-tematic review and meta-analysis. Journal of Science and Medicine in Sport, 15:S25.

Seals, D. R., Hagberg, J. M., Hurley, B. F., Ehsani, A. A., and Holloszy, J. O. (1984). Endurance training in older men and women. I. Cardiovascular re-sponses to exercise. Journal of applied physiology: respiratory, environ-mental and exercise physiology, 57(4):1024–9.

Shin, W., Cashen, T. A., Horowitz, S. W., Sawlani, R., and Carroll, T. J. (2006). Quantitative CBV measurement from static T1 changes in tissue and cor-rection for intravascular water exchange. Magnetic Resonance in Medicine, 56:138–145.

Szuhany, K. L., Bugatti, M., and Otto, M. W. (2015). A meta-analytic review of the e ects of exercise on brain-derived neurotrophic factor. Journal of Psychiatric Research, 60:56–64.

Vaidya, V. A., Terwilliger, R. M., and Duman, R. S. (1999). Role of 5-HT2A re-ceptors in the stress-induced down-regulation of brain-derived neurotrophic factor expression in rat hippocampus. Neuroscience letters, 262(1):1–4.

Van Der Borght, K., Kobor´-Nyakas, D. E., Klauke, K., Eggen, B. J. L., Nyakas, C., Van Der Zee, E. A., and Meerlo, P. (2009). Physical exercise leads to rapid adaptations in hippocampal vasculature: Temporal dynamics and relationship to cell proliferation and neurogenesis. Hippocampus, 19:928– 936.

Van Praag, H., Kempermann, G., and Gage, F. H. (1999). Running increases cell proliferation and neurogenesis in the adult mouse dentate gyrus. Nature America Inc., 2(3).

Wagner, G., Herbsleb, M., de la Cruz, F., Schumann, A., Brunner, F., Schachtzabel, C., Gussew, A., Puta, C., Smesny, S., Gabriel, H. W., Reichenbach, J. R., and Bar, K.-J. (2015). Hippocampal Structure, Metabolism, and In-flammatory Response after a 6-Week Intense Aerobic exercise in Healthy Young Adults: A Controlled Trial. Journal of Cerebral Blood Flow & Metabolism, 35(10):1570–1578.

INTERVIEW Q&A with Antonia Kaiser

by Nikos Kolonis

Antonia Kaiser is currently a PhD student at the Academic Medical Center of Amsterdam. Her research report for the latest project she conducted for her master's was selected for publication in the ABC Journal as the Editor's Choice. We talked with her about her experience working on that project and her current work.

I would like to congratulate you for your research report being selected as the editor's choice in this issue of the ABC Journal. Where would you attribute the success of your project and, consequently, your report?

In general, I think that the project is a very innovative idea. These kinds of studies have only been done in older adults, not young adults, and nobody really knows what the underlying mechanisms of the changes in the hippocampus that are found in older adults after exercise training are. That's why I think this was an innovative idea to come up with, which was definitely not my doing, but my professors'.

Was it a project that your supervisor had started, before you joined and started working on it?

Yes. My current professors and supervisors are the post-doc Anouk Schrantee and the professor Paul Lucassen, who work together with Liesbeth Reneman. It was the three of them that came up with the idea to do this study. They started the whole project and did the first measurement. I visited them at that stage to help and get an idea about the project. I was still writing my literature thesis at the time, so I joined after they had finished with the exercise training to help with the post-measurement.

How was your experience working at the radiology department of the AMC?

Fun fact is that I'm also a PhD student there now. It was a really nice experience. It was really interesting to work in an interdisciplinary team. The department was mostly focused on the development of new sequences for MRI, so it was quite technical. I really loved that I could at the same time learn about the brain, learn how to interpret data that you get from an MRI and also work on technical things, like for example influencing the sequence in order to get to see all these parts of the brain that we actually want to see and tweaking these little values to make the machine do exactly what we want it to.

You said you are doing your PhD in the same lab. What are you currently working on?

I am actually still working on that exercise study. We are trying to publish it soon, so I am now analyzing the last parts of that project to write it up. Other than that, I have two other projects on ADHD and one on stress. These four projects are all part of my PhD.

Is this a career plan that you knew you wanted to follow while doing your master's?

Once I started my master's and got back into the whole studying and learning process, I was one hundred percent sure that I wanted to continue as a PhD student afterwards.

What do you think were the skills you gained during the master's that are useful for you in your current position?

Some of the things I learned were to think critically, to not take everything for granted, to be curious and question things, to be able to solve problems by myself without having to rely on others and to understand things from a different perspective and, therefore, to have a broader view on neuroscience than just the psychological or computational for example. I was able to talk to people from different disciplines and understand their perspective. The programming and technical skills I mostly acquired during my bachelor's.

> "Some of the things I learned were to think critically, to not take everything for granted, to be curious and question things."

What are your plans from now on?

To publish my first paper this year and then finish my PhD in the next three years. After that, I definitely want to stay in the field and I would like to be given the opportunity to teach.

Thank you for your time and I wish you the best of luck with your current and future endeavours.

Disposable Beings

by George Lafferty

Consciousness matters for two reasons: because it is mysterious, and because of its deep relationship with suffering. These factors make for a terrifying combination. How do we know if another (apparent) agent that we are interacting with is conscious? If it is, then what we do to it might cause suffering, and (hopefully) we don't want to cause suffering. Our moral status is at stake in these situations. Our world is rapidly becoming populated with 'entities' that behave increasingly more like conscious agents as their technology advances. This means it is becoming increasingly easy to imagine a near future where it really isn't clear what the conscious state of certain other agents is. How closely does something need to resemble us before it can suffer, or before we should start treating it as if it can? The current debate is dominated by fears about what to do when conscious Artificial Intelligence (AI) starts to emerge, but the problem is already at our doorstep. It is a problem of uncertainty. What do we do when we don't know what it is we're dealing with? We have moved on from established examples of moral quandaries to a strange world, where even our ability to distinguish conscious and unconscious agents is suspicious.

The philosopher Nick Bostrom suggests we are starting to give up our agency to the agents we create as their complexity increases (e.g. Bostrom, 2011) and their inner workings become more of a black box to us. Many discussions about AI ethics focus on the possibility of our accidentally (or deliberately) building AI that can suffer, or their consequences for us. This is reasonable, but we shouldn't ignore the risks that come when AI presents us with simulated ethical problems. Some of these AI will have bodies, others minds, some will physically resemble us, and others functionally. If it is hard to predict the behavior of an agent like this, we shouldn't assume we can predict the effects of interacting with it on our own psyches either.

It could even be argued that these troubling simulated agents are already among us. In a video game, you can act out moral violations towards other characters without consequences for you or your avatar's welfare. Yet playing violent video games, and real-life violent acts, could be separated by years and by a multitude of other sociopsychological factors (APATF, 2015). A recent sophisticated statistical analysis of the causes of violent behaviour saw violent video games 'shrink to insignificance', when considered in the context of a violent person's broader developmental situation (DeCamp, 2015). So, despite intuitive arguments, what we do to these computer-generated interactants is not really enough to dissolve our moral integrity. Perhaps the separation from the action, through controller and screen, makes the difference. Maybe less than 20 years ago, we could settle the matter at this. But this is not where we are going.

Sex robots are a strange recent development we can't afford to ignore. Sex is a situation where moral judgement has the potential to clash with basal instincts. Kathleen Richardson is a philosopher who founded the 'Campaign Against Sex Robots' which argues that the use of these robots doesn't mimic consensual sex, but rape, because the robot is bought with money, and is therefore fundamentally objectified. Of course, a proper treatment of objectification is way beyond the reach of this article, but it does seem to risk a loss of respect for suffering beings, and any consequences that come with that. Her direct opponent in this debate is David Levy, a philosopher who also compares sex robots to human prostitutes...but favourably. He argues that sex robots will reduce the use of human sex workers. This debate doesn't show signs of resolution, and we're back to the same problem again: psychology still lacks the measurement techniques to prove a causal link between this reduction of women to objects through the use of sex robots. Nonetheless, Richardson highlights the risk I'm discussing well, where even seemingly morally-inert situations may have distal consequences for individuals and even lead to the distribution of destructive behavioural norms across groups.

"...psychology still lacks the measurement techniques to prove a causal link between this reduction of women to objects through the use of sex robots."

In the previous examples, we remain mostly situated in everyday reality. However, Virtual Reality (VR) is already changing this today. We will be interacting 'face-to-face' with complex virtual agents who behave like they are able to suffer. Despite that, we will 'know' they are nothing more than lines of code. Our acts, however out of line they are with our normal behaviour, will be consequence-free (e.g. Brey, 1999). The separation of the player and the medium in 'traditional' video games has been broken down. There

is already evidence that VR can become hard to distinguish from reality (Aardema, 2010). Other research shows that virtual stand-ins for the players hands can easily become integrated into their sensorimotor system, leading to a vivid sense of ownership over the hands and an unprecedented sense of immersion into the virtual world (Suzuki et al., 2013). The VR situation is therefore embodied to a level we have never encountered before, and we cannot predict what our actions on that side of the headset will do to us on this side.

I will end with a hypothetical scenario: it's 2070, a new robot moves in with you, equipped with the kind of generalized intelligence necessary to help out with every household task imaginable, and provide you with company too. It really behaves like a living thing. You become attached to it, feeling the same kind of affection you might feel towards a beloved Tamagotchi. The makers assure you that it is unconscious though, and incapable of suffering. Over time, the novelty wears off. Perhaps you get a cat, and being so busy, the right thing to do is obviously to give all your time, love and attention to the feline. It's a living animal, after all. The house robot breaks with wear-and-tear and a new model arrives. You have no attachment to it, and despite its protests (a cute way to signal maintenance requirements) its status is more like that of a dustpan and brush than a being who deserves care and respect. What the company fails to acknowledge though, are minor updates in the AI's cognitive architecture. Whether the designers know it or not, the new system is really approximating something like suffering now. After habituation to generations of pseudo-conscious agents who cannot suffer, we are entering a grey-zone littered with false negatives. Consequently, we should watch the effect this will have on our psyches more closely than ever before.

Echoing philosophers such as Nick Bostrom, I think now is the time to start considering this problem. Our evidence against the consequences of simulating immoral acts has become outdated by technology. New forms of AI will put users in situations where only context can tell them apart from interactions with suffering agents. We should not assume that these users will have the epistemic vigilance to tread carefully through this grey-zone. If we do, even the best of us risk the loss of our moral integrity. Is that a price you want to pay?

References

Aardema, F., O'Connor, K., Côté, S. and Taillon, A. (2010). Virtual Reality Induces Dissociation and Lowers Sense of Presence in Objective Reality. Cyberpsychology, Behavior, and Social Networking, 13(4), pp.429-435.

APA Task Force on Violent Media. (2015). Technical report on the review of the violent video game literature. Retrieved from http://www.apa.org/pi/families/violent-media.aspx. [Accessed 17 Apr. 2017].

Bostrom, N. (2011). The Ethics of Artificial Intelligence. In: W. Ramsey and K. Frankish, ed., Cambridge Handbook of Artificial Intelligence, 1st ed. Cambridge University Press.

Brey, P. (1999). The Ethics of Representation and Action in Virtual Reality. Ethics and Information Technology, 1(1), p5-14.

Gloor, L. and Mannino, A. (2017). The Case for Suffering-Focused Ethics – Foundational Research Institute. [online] Foundational Research Institute. Available at: https://foundational-research.org/the-case-for-suffering-focused-ethics/ [Accessed 17 Apr. 2017].

Richardson, A. (1999). "Subjective Experience: Its Conceptual Status, Method of Investigation, and Psychological Significance". The Journal of Psychology: Interdisciplinary and Applied. Helen Dwight Reid Educational Foundation. 133 (5), p469–485.

Smith, S. and Vela, E. (2001). Environmental context-dependent memory: A review and meta-analysis. Psychonomic Bulletin & Review, 8(2), pp.203-220.

Suzuki, K., Garfinkel, S., Critchley, H. and Seth, A. (2013). Multisensory integration across exteroceptive and interoceptive domains modulates self-experience in the rubber-hand illusion. Neuropsychologia, 51(13), pp.2909-2917.

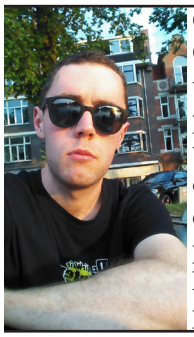

George Britton is a first year student on the Cognitive Science track of the Research Master's Brain and Cognitive Sciences. He completed his BSc in Neuroscience with Cognitive Science at the University of Sussex and is currently an intern in the Brain and Cognition lab, UvA where he is researching emotion perception. George is interested in neurophilosophy and the science of contemplative practices such as mindfulness meditation.

The Ethics of Science Journalism

by Vanessa Utz

Have you ever read an article in the science section of a mass media outlet and thought that the claims seem a bit too good to be true? Even dedicated science journalism platforms sometimes make claims that appear outlandish to those within the scientific community. For instance: in 2016 The Independent published an article titled 'Chocolate makes you cleverer: A 40-year psychological study proves that the sweet treat can boost our grey matter' (Ferdman, 2016b). This fun topic was sure to attract attention, hence why many other media outlets also reported on the findings, including The Washington Post (Ferdman, 2016a) and The Telegraph (Graham, 2016). But is this responsible science journalism? Especially since the original study did not 'prove' that eating chocolate causes an increase in intelligence, it merely showed a correlation (Crichton, Elias, & Alkerwi, 2016). And as any science undergraduate can tell you: correlation does not equal causation.

When I looked through the 160 comments that can be found on the Washington Post website regarding the above-mentioned chocolate article (Ferdman, 2016b), only 11 comments (6.8% of total comments) were sceptical of the claims in the article, and out of these 11 only 2 commented on the flaws within the actual study. This clearly shows that the public generally accepts science journalism as fact. As pointed out by Carrie Figdor, the public is generally in no position to properly assess the results of scientific studies (Figdor, 2017). So, instead of assessing the research itself, they choose to assess the credibility of the source and then determine the research's credibility, based on who has reported the information. So, when readers of outlets such as The Washington Post read an article that presents a piece of research in a certain way, they are likely to believe whatever they read.

This puts a lot of pressure on science journalists. Not only do they need to focus on presenting the information in a manner that makes it accessible to the public, they also need to ensure that all the information is correctly conveyed. In the Code of Ethics of the National Association of Science Writers (NASW), the duties of science journalists are outlined and include the unbiased presentation of accurate scientific discoveries (Code of ethics for science writers, 2014). This might appear as a simple task, however more often than not, the individuals who write the science articles for mass media outlets do not have a background in science (Figdor, 2017). While the writers enjoy the trust of their readers, they themselves do not possess the experience and knowledge to assess scientific claims. Similarly to the trust that their readers put in them, these journalists put their trust in the scientists and journals to ensure that only quality research is published.

However, there is no perfect research. In many fields there is a lack of consensus on crucial findings and questionable research practices are widespread. These practices include p-value hacking in order to find an analysis that produces desirable results, adaptive sampling to either extend or shorten testing to produce the wanted effect, and not submitting papers for review that do not fit the current narrative (Fidgor, 2017). These things are hard or impossible to spot for the layman science journalist and are common, since there are generally no consequences for researchers and journals that implement such measures (Fidgor, 2017).

So, how can this problem be solved? Who has the responsibility of ensuring that the public receives correct information? Is it up to the public to ensure that they possess the expertise to analyze and assess the intricacies of scientific research practices? Do science journalists and mass media outlets have the responsibility to ensure that only qualified individuals are allowed to relay scientific information to the public? Or is it up to the researchers and scientific journals that bad science or inconclusive studies are not spread in the first place? We can debate about the ethical duties that each one of these groups have, but I personally believe that every single person involved in this scientific Chinese whispers has an obligation to ensure that they understand the information they are receiving and to distribute only the information they know is accurate. If accuracy cannot be guaranteed, others need to be made aware of this fact. I do not have a solution that could be implemented on a large scale to make the entire system fail safe, but instead I'm appealing to self-responsibility in this issue. We all have a role to play here and if we as young researchers understand this issue and try to avoid questionable practices in our own research and sharing misleading mass media science articles, then we can do our part.

References

Code of ethics for science writers. (2014, Oct 17). Retrieved from https://www.nasw.org

Crichton, G. E., Elias, M. F. & Alkerwi, A. (2016). Chocolate intake is associated with better cognitive function: the Maine-Syracuse longitudinal study. Appetite, 100, 126-132

Ferdman, R. A. (2016a, March 04). The magical thing eating chocolate does to your brain. Retrieved from https://www.washingtonpost.com

Ferdman, R. A. (2016b, March 07). Chocolate makes you cleverer: a 40-year psychology study proves that the sweet treat can boost our grey matter. Retrieved from https://www.independent.co.uk

Figdor, C. (2017). (When) Is science reporting ethical? The case for recognizing shared epistemic responsibility in science journalism. Frontiers in Communication, 2(3). doi: 10.3389/fcomm.2017.00003

Graham, C. (2016, March 08). Chocolate makes you smarter, study suggests. Retrieved from https://www.telegraph.co.uk

Implementing an improved processing pipeline for diffusion tensor imaging data to assess the effects of chemotherapy on white matter integrity in breast cancer survivors

Yasmin Mzayek

Supervisor: Dr. Michiel de Ruiter

Netherlands Cancer Institute

Amsterdam, Netherlands

ABSTRACT

Adjuvant chemotherapy for non-CNS cancer is associated with changes in brain structure and function. Brain white matter seems to be particularly vulnerable to neurotoxic effects of chemotherapy. Diffusion tensor imaging (DTI) allows for studying in vivo microstructural changes in white matter. The most often used DTI measure is fractional anisotropy (FA). An influential study by Deprez et al. (2012) showed that breast cancer patients who received chemotherapy were characterized by a decrease in FA, which can be interpreted as a decrease in white matter integrity. These results could not be replicated by Menning et al. (2017), who applied tract-based spatial statistics (TBSS), in which DTI data were spatially normalized to a standard FA template and then 'skeletonized' to correct for misregistration effects. This approach greatly reduces the overall white matter volume that is subjected to statistical analysis, leading to information loss. In the present study, we aimed to replicate the results of Deprez et al. by constructing a pipeline resembling their approach, but with an improved registration method in Advanced Normalization Tools (ANTs) and an improved eddy current distortion correction tool. These steps obviate the need to skeletonize the data, preserving the total white matter volume for statistical testing. Building up from the standard TBSS analysis done by Menning et al., we implemented and compared the following three pipelines, each systematically improved from the former:

1) Standard TBSS with omission of skeletonization (non-skeletonized TBSSa)

2) Standard TBSS with omission of skeletonization and improved eddy current correction (non-skeletonized TBSSb)

3) ANTs with omission of skeletonization, improved eddy current correction, and improved registration through an optimized registration algorithm and a T1-weighted GW template (multimodal ANTs-GW)

It was hypothesized that similar effects to Deprez et al. would be found in our sample with improvement of the processing pipeline. Though the results did not reflect the findings in Deprez et al., voxel-wise differences were found showing that breast cancer survivors, with and without chemotherapy, had significantly decreased FA compared to controls, with a much larger number of voxels showing a significant decrease in the chemotherapy group than the no chemotherapy group. These results were not found in Menning et al. The analyses demonstrated that improvement of DTI processing methods appear to make the data more sensitive to index decrease in brain white matter integrity in breast cancer patients. Further, the feasibility of integrating recent methods in the TBSS processing pipeline of longitudinal DTI data was established.

KEYWORDS

white matter, chemotherapy, breast cancer, TBSS, DTI, processing pipeline

INTRODUCTION

Several studies have used diffusion-weighted MR imaging (DWI) to examine potential side effects of chemotherapy on brain white matter structure of cancer patients and survivors, particularly those with breast cancer. The diffusion tensor imaging (DTI) technique is used to extract information from DWI data about the movement of water molecules along the x, y, and z axes in white matter (Le Bihan et al., 2001). This information is used to measure white matter integrity and can reveal possible injury. There are several ways to analyze DTI data and inconsistent findings in breast cancer survivor (BCS) may, to some extent, be attributed to divergent processing methods. To better determine the effects of chemotherapy on BCS, refined techniques need to be considered. A brief introduction will first be given about the BCS population and DTI before delving into the limitations of current processing tools and potential ways for improvement.

Adverse cognitive effects have been reported in BCS treated with adjuvant chemotherapy, a treatment received following surgery. These effects include learning and memory problems (Schagen et al., 2014; Deprez et al., 2013; Wefel et al., 2015). The impact of this usually mild cognitive impairment, presumed to be associated with chemotherapy treatment, can lead to everyday challenges (Simó et al., 2013). Although many patients recover, a subgroup will continue to experience these difficulties in the long-term (Conroy et al., 2013; de Ruiter et al., 2012). With the number of increasing survivors, addressing the long-term cognitive effects and quality of life impact of chemotherapy-related cognitive impairment (CRCI) on BCS is becoming more and more essential (Boykoff, Moieni, & Subramanian, 2009).

Studying the underlying neural correlates of chemotherapy treatment can indicate which patients are at risk for such long-term cognitive impairment. Conroy et al. (2013) showed that a group of BCS treated with chemotherapy revealed decreased gray matter density compared to controls up to 10 years post-treatment. These effects may be due to neurotoxic properties of chemotherapy, either indirectly via systemic inflammatory responses or oxidized DNA damage that affects the central nervous system (Ahles, Root, & Ryan, 2012; Pomykala et al., 2013) or directly through smaller or larger proportions of administered chemotherapy entering the brain despite protection by the blood brain barrier. White matter changes might also be associated with CRCI as it has been shown that oligodentrocytes, the cells responsible for insulating axons in white matter structure, are susceptible to the toxic properties of chemotherapy (Dietrich et al., 2006). Moreover, white matter correlates to gray matter injury have also been seen in populations with similar neurodegenerative effects, such as aging and multiple sclerosis (Draganski et al., 2011; Bodini et al., 2009). Thus, it is possible that white matter changes underlie the effects seen on gray matter as well as CRCI in BCS.

DTI information about white matter structure is captured with several parameter maps including fractional anisotropy (FA) and mean diffusivity (MD). These two parameters are the most commonly used and track various aspects of the anisotropic movement of molecules along the axon bundles in the brain allowing researchers to study white matter integrity. In a longitudinal study, Deprez et al. (2012) found widespread decreases in FA over time in BCS treated with chemotherapy compared to BCS who did not receive the treatment and healthy controls. Compatible results have been found in other cancer populations, such as testicular cancer (Amidi et al., 2017), but not in any other longitudinal studies of BCS and contrast with what was shown in a comparable longitudinal study assessing chemotherapy-treated BCS +/- endocrine treatment, BCS not exposed to any systemic treatment, and controls on the effects of chemotherapy on white matter integrity (Menning et al., 2017). In this study, subtle detrimental effects of chemotherapy +/- endocrine therapy vs unexposed BCS were found in region of interest (ROI) analyses but no overall differences between groups were found in a voxel-wise analysis of white matter.

There are drawbacks in the approach taken by Menning et al. (2017) that may have led to the different findings. They used a suboptimal tool (eddy_correct) to correct image distortions caused by eddy currents (EC) and head motion. A newer tool eddy has been developed and shown to provide a better-quality correction (Andersson & Sotiropoulos, 2016). They also used standard tract-based spatial statistics (TBSS; Smith et al., 2006), a common and well-established method to analyze DTI data. This method has several limitations including a suboptimal registration algorithm, an FA skeleton projection step, and a standard FA template. In comparison, Deprez et al. (2012) used a pipeline that excluded FA skeleton projection and used improved registration with a population-based FA template.

Registration in TBSS is done with the non-linear algorithm FNIRT (Andersson, Jenkinson, & Smith, 2007), developed specifically for use on brain images and can compensate for local brain differences. However, FNIRT performs only moderately compared to other image registration algorithms (Klein et al., 2009). More recent registration algorithms have been shown to optimize transformations by using intensity-based, diffeomorphic alignment leading to increased anatomical specificity (Acosta-Cabronero & Nestor, 2014). Thus, depending on the studied population or the expected effects, the use of FNIRT might not always be appropriate and could lead to misregistration.

After TBSS registration, FA skeleton projection is used to compensate for misalignment resulting from imperfect registration. It is also used to restrict analysis to white matter and to gain statistical power by this dimensionality reduction (Smith et al., 2006). However, this skeletonization only allows for the assessment of the effects of interest where local FA values are highest (Van Hecke et al., 2010; Bach et al., 2014). This limits the analysis by decreasing the sensitivity to detect affected voxels. Further, the findings from Deprez et al. (2012) suggest that white matter injury due to chemotherapy might be located on the borders of white matter structures, implying that the FA skeleton will not capture such differences. This means that with the use of FA skeleton projection, valuable information about FA integrity is potentially missed.

Also common to the TBSS pipeline is the use of a standard tem-

plate. The advantage of using a standard template is that the location of statistical effects can be reported in a standardized way and brain atlases can be used for reference. While this template is beneficial for having predefined anatomical regions and for comparability across studies, it is not representative of the study population and can thus lead to erroneous findings resulting from misalignment (Van Hecke, Leemans, & Emsell, 2016; Keihaninejad et al., 2012). To improve registration, many advocate for the use of a study-specific template known as a group-wise (GW) template. This template is an optimized average template derived from the brain images of the sample being studied. Although TBSS also offers the option to create a study-specific template, this was not done in Menning et al. (2017).

To address some of the challenges mentioned above, the focus of the current study is the omission of the FA skeleton projection step due to improved EC distortion correction and improved registration. Schwarz et al. (2014) showed that an improved registration algorithm and use of a GW template can decrease misalignment and increase anatomical specificity and detection sensitivity of DTI analysis, rendering skeleton projection unnecessary. They used Advanced Normalization Tools (ANTs; Avants et al., 2011) to develop a pipeline (ANTs-GW) suitable for use within the TBSS framework to improve the processing of DTI data. ANTs encompass an open-source package for working with imaging data. The main benefit they yield is a state-of-the-art diffeomorphic image registration algorithm known as Symmetric Normalization (SyN). This algorithm has been evaluated against 13 other registration algorithms for brain MRI and has been shown to be the most consistent and accurate (Klein et al., 2009).

Thus, the current study is intended to use advanced methods to establish an optimal pipeline for processing DTI data of BCS by reexamining and improving the assessment of Menning et al. (2017) on the effects of chemotherapy on white matter integrity. To reach this goal, we modified their standard TBSS analysis by constructing three pipelines that gradually built on each other. The first pipeline followed standard TBSS, but with omission of the FA skeleton (non-skeletonized TBSSa). The second also followed standard TBSS with omission of the FA skeleton, but used maps corrected with the newer tool eddy¬ instead of eddy_correct (non-skeletonized TBSSb). The third was an optimized ANTs-GW based pipeline with omission of the FA skeleton projection, eddy corrected motion artifacts, and improved registration (multimodal ANTs-GW). The first pipeline is the closest to that used by Menning et al., with non-skeletonization being the only alteration. Both the 1st and the 2nd pipeline risk introducing misregistration effects, but can provide information on how motion correction and skeletonization might affect the results. The 3rd pipeline utilized SyN as well as an improved GW template built from T1-weighted scans instead of FA scans to improve registration. The high-resolution scans used in this pipeline should result in a more accurate template for better alignment and reduce statistical bias (Wintermark et al., 2014; Tustison et al., 2014). Hence, this pipeline was referred to as multimodal ANTs-GW. For comparison with the pipelines from the present study, the analysis of Menning et al. (2017) will be referred to as 'standard TBSS' or 'original analysis' from here on.

Appraisal of the outcomes from each pipeline can reveal both consistencies and disparities that may be attributed to varying the individual steps along the image processing stream. It is anticipated that with improvement of the pipeline from the original analysis, similar effects will be seen as were reported in Deprez et al. (2012). It is expected that non-skeletonized TBSSa analysis will show closer results to the original analysis than non-skeletonized TBSSb since only the FA skeletonization was omitted. More sensitive and accurate registration in multimodal ANTs-GW along with the retention of the whole white matter structure as opposed to only the skeleton is expected to provide more information about the effects of chemotherapy on white matter structure of BCS. Therefore, following this pipeline, it is predicted that BCS treated with chemotherapy will show a significant decrease in FA and a significant increase in MD over time in widespread areas of white matter when compared to BCS without chemotherapy treatment and healthy controls. Such outcomes would imply that DTI processing choices affect the results, since they were not seen in the standard TBSS analysis. Moreover, this study will assess the feasibility of an improved processing pipeline for longitudinal DTI data of BCS by addressing weaknesses in standard TBSS.

METHODS

Participants

Participants were recruited as part of a Dutch Cancer Society funded study approved by the Institutional Review Board of the Netherlands Cancer Institute. Participants were breast cancer patients who were scheduled to receive adjuvant chemotherapy with or without endocrine treatment (Ch+), breast cancer patients who do not require chemotherapy (Ch-) or endocrine treatment, and age-matched healthy controls (HC). The eligibility criteria were met if patients were female, under the age of 70 years, had a diagnosis of primary breast cancer with no previous malignancies, no distant metastases, no treatment other than surgery at baseline measurement, and had sufficient command of the Dutch language. Patients were excluded if they were additionally scheduled to receive trastuzumab after chemotherapy because of extended duration for treatment and possible unknown cognitive side effects. Additionally, participants were excluded if they had a history of or current psychiatric disorders or used psychotropic medication that could affect cognitive function. Controls were recruited through patients and advertisements in participating hospitals. The study was held at the Academic Medical Center Spinoza Center for Neuroimaging, both affiliated with the University of Amsterdam. Written informed consent was acquired based on the Declaration of Helsinki and institutional guidelines.

Procedure

Data for the study were collected across two time points. For patients, baseline data was collected after surgery but before receiving adjuvant chemotherapy (t1). A follow-up session took place 6

months after the last cycle of chemotherapy for Ch+ and at matched intervals for the other two groups (t2). Participants received a T1-weighted three-dimensional magnetization prepared rapid gradient echo (MPRAGE) scan (TR/TE = 6.6/3.0ms. FOV 270 X 252 mm, 170 slices, voxel size 1.05 X 1.05 X 1.20mm, sagittal direction) and a diffusion-weighted MRI (DWI) scan (32 directions, TR/TE = 8136/94ms, FOV 250 X 250mm, 64 slices, voxel size 2.23 X 2.23 X 2.00mm, b-value: 1000s/mm2) at each time point. DWI scans were acquired in the transversal direction except for three controls whose data were collected in the sagittal direction at baseline. Data were acquired using a 3.0 Tesla Phillips Intera full-body MRI scanner and a 3.0 Tesla Phillips Achieva full-body MRI scanner. To optimize comparability, a SENSE 8-channel receiver head coil was used at both locations.

DWI preprocessing

Processing of the DWI data was done using FMRIB Software Library 5.0.9 (FSL; Jenkinson et al., 2012). In the original analysis and non-skeletonized TBSSa, data were corrected for motion and eddy currents using FSL tool eddy_correct. The newer tool eddy was used in non-skeletonized TBSSb and multimodal ANTs-GW. These tools were not systematically compared in this study, but research has shown that eddy provides a better correction for eddy-current distortion and subject movement (Graham et al., 2016; Yamada et al., 2014). The improved correction of eddy can be attributed to its use of nonparametric predictions based on the whole dataset of volumes to account for eddy currents and subject movement simultaneously as opposed to eddy_correct, which uses the b0 image as a reference for correction of all volumes (Graham et al., 2016). In this study, the tools were compared qualitatively and based on differences in the statistical outcomes. Brain extraction was done using BET toolbox in FSL. Then, dtifit was used to fit the diffusion tensor at each voxel (single tensor model), to produce diffusion tensor maps. Visual inspection of the data was done using FSLView.

DTI processing in TBSS

As mentioned above, the data was originally analyzed following standard TBSS in FSL. This pipeline has a cross-sectional framework which can be applied to longitudinal data and is briefly described here. First, all of the FA images from all subjects were non-linearly registered using FNIRT onto a common reference. This can be a study-specific template or a 1mm standard template (FMRIB58_FA), of which the latter was used in Menning et al. (2017). Second, the average of the aligned images was thinned into an FA skeleton. In this step, the mean FA image was eroded and only maximal FA values were retained. Third, each participant's FA image was then 'skeletonized' by projecting it onto the mean skeleton by searching perpendicularly from the skeleton for maximal FA values. Fourth, voxel-wise statistics were performed. MD maps were registered to the standard template using the same warps that registered the FA maps. The same steps were then taken to analyze the MD data.

Both non-skeletonized TBSS analyses followed the same procedure for FA and MD processing, but excluded FA skeleton projection. Instead, participants were compared on thresholded white matter maps (FA>0.2). To do this, normalized data were first blurred with a Gaussian kernel of sigma 1mm using FSL tool fslmaths. Then, the data were thresholded at FA>0.2. To ensure that the mask was representative of white matter structure, a mean FA mask was derived from thresholded data and then thresholded again at FA>0.2. The resulting thresholded mean FA mask was binarized and used to mask the normalized data.

Template building and registration in ANTs

For multimodal ANTs-GW, FA and MD maps were analyzed in ANTs (v2.0) for optimal GW template building and registration without skeletonization of the DTI data. A GW template in native space was created using the T1-weighted data collected for all participants at both time points. Native space was used because it has been shown to minimize partial volume effects compared to a standard template (Aribisala, He, & Blamire, 2011). T1-weighted maps were used because they minimize a statistical bias termed 'circularity bias'. Tustison et al. (2014) argue that the use of an FA template for normalization of FA images, as done in TBSS, introduces a bias that results from using image intensity values for alignment that are not independent of the intensity values used to assess group differences statistically. Direct FA-to-FA mapping has been shown to reduce the intensity variance in a studied population due to data dependency and, as a result, can lead to increased effect sizes. Instead, the ANTs team advocates for using independent images such as T1-weighted images that will not affect the data and, additionally, will yield a high-resolution template for better alignment. Thus, in contrast to the direct FA-to-FA mapping commonly used, FA-to-T1 mapping was used in multimodal ANTs-GW as an improvement.

Building the template is accomplished by an iterative linear and nonlinear registration method and encompasses several steps. Before the T1-weighted data is used to create the template, an N4 bias correction algorithm is applied to correct image inhomogeneity (Tustison et al., 2010). This algorithm is an improvement to the standard N3 bias correction that uses nonparametric non-uniform normalization (Sled, Zijdenbos, & Evans, 1998). The corrected images are used to build the template by averaging the T1-weighted images. Template construction utilizes ANTs registration to register the corrected T1-weighted images onto the template. For this registration, rigid and affine registration are performed for linear alignment and SyN is applied afterwards for non-linear alignment.

The T1-weighted template created in ANTs yields an unbiased average template (Zhan et al., 2013; Avants et al., 2010, Avants et al., 2008). This method of template building is said to be unbiased because the SyN algorithm does symmetric pair-wise mapping where mapping from one image to its target is consistent with the mapping of the target back to the image. Registration is also unbiased given that each image, regardless of time point, is independently transformed to the GW template with no preference towards a single image and no initial template used as a reference.

This is similar to what is done in TBSS, which also takes all time points independently and transforms them to a standard template. The result of both approaches, however, is the data being treated as cross-sectional. In other words, the time points of each participant are considered independently when they are actually dependent. The benefits and limitations of treating longitudinal data as such will be addressed in the discussion.

The multimodal ANTs-GW pipeline for processing FA maps is described in more detail below:

1. tbss_1_preproc, the initial step of TBSS, was used on FA images in order to remove outliers. This step is used in Schwarz et al. (2014) to erode the bright halo of voxels surrounding the FA images that typically results from eddy current distortions.
2. Baseline and follow-up skull stripped T1-weighted images were used as inputs to construct an unbiased and optimized average template with 4 iterations of rigid, affine, and non-linear (SyN) registration using the following command:

antsMultivariateTemplateConstruction2.sh -d 3 -f 4x2x1 -s 2x1x0vox -q 30x20x4 -t SyN -m CC -r 1 -c 2 -j 4 -o $output $T1inputs

The parameters called here include image dimension (-d), shrink factors (-f), smoothing factors (-s), max iterations at three resolutions (-q), transformation model (-t), similarity metric (-m), rigid-body registration (-r). -c and -j refer to the computing power and -o to the output. The settings for -f, -s, and -q are either defaults or what is commonly used in other studies. The initial rigid-body registration is recommended by the authors if no initial template is used. The similarity metric CC (cross-correlation) is also recommended by the authors for intra-modal image registration (Avants, Tustison, & Johnson, 2014; Avants et al., 2011).

3. Baseline and follow-up FA images were registered to their respective T1-weighted images using rigid, affine, and non-linear (SyN) registration as follows:

antsRegistration -d 3 -o [$transform] -t Rigid[0.1] -m MI[$T1, $FA] -c 30x20x10 -f 4x2x1 -s 2x1x0vox -t Affine[0.1] -m MI[$T1, $FA] -c 30x20x10 -f 4x2x1 -s 2x1x0vox -t SyN[0.25,3,0] -m MI[$T1, $FA] -c 30x20x10 -f 4x2x1 -s 2x1x0vox

Adding the non-linear transform algorithm in this step showed superior results to only performing linear registration. The options for the transforms (-t) were set using recommendations from the authors and what has been used in the literature. The -c parameter refers to convergence. All other parameters are the same as the script in step 2. Default parameter options were used here for -c, -f, and -s. The similarity metric MI (mutual information) is recommended by the authors for inter-modal image registration and is thus used here for FA to T1 mapping.

4. Transforms from steps 2 and 3 were applied to map FA and MD images to the template:

antsApplyTransforms -d 3 -i $FA -r $template -t $T1Warp -t $T1Affine -t $FAWarp -t $FAAffine.mat -n linear -o $output

5. Normalized data were blurred and limited to white matter following the same steps described above in the non-skeletonized TBSS analyses.

Table 1 shows an outline of the components of each pipeline.

Table 1 DTI processing pipelines

	Standard TBSS	Non-skeletonized TBSSa	Non-skeletonized TBSSb	Multimodal ANTs-GW
EC correction	*eddy_correct*	*eddy_correct*	*eddy*	*eddy*
Template	FMRIB58_FA (1mm)	FMRIB58_FA (1mm)	FMRIB58_FA (1mm)	study-specific
Registration	FNIRT	FNIRT	FNIRT	SyN
FA skeleton	Yes	No	No	No

Statistical Analysis

A one-sample t-test was first used in SPSS to assess change of mean FA and MD over time per group. The mean of FA and MD were taken by averaging across all white matter voxels for each participant for each time point and mean change was calculated by subtracting the baseline mean from the follow-up mean. Group differences in mean change were also analyzed using one-way ANOVA. Voxel-wise changes in FA and MD were then analyzed by comparing difference maps calculated from subtracting the baseline images from follow-up images. A nonparametric general linear model using randomise in FSL was applied to do paired group comparisons measuring voxel-wise differences in FA and MD change between groups and to perform one-sample t-tests assessing voxel-wise changes in FA and MD over time. The parameters for randomise included 1000 permutations, threshold-free cluster-enhancement, and voxel-wise corrected p-value images as output. White matter injury is inferred from lower FA values because they represent lower restriction of diffusion of water molecules. Increased MD suggests worse outcome given its association with edema. Age and scan direction were included as covariates to match the analyses done in the Menning et al. (2017). Scan direction was included because of the three participants that were scanned in the sagittal direction. Statistically significant outcomes were considered at a cluster level, FWE corrected threshold of $p<0.05$ (threshold-free cluster-enhancement). Outcomes concerning number of voxels were reported in volume (mm3 = 0.001 ml) given the different dimensions of the voxels in standard space (1 x 1 x 1mm) for the TBSS pipelines and in native space (1.2 x 1.055 x 1.055mm) for the ANTs pipeline.

RESULTS

Information about recruitment, participation, and patient demographics are described in previous reports (Menning et al., 2015; Menning et al., 2017). See Table 2 for details. The final sample in this study included 26 Ch+, 23 Ch-, and 30 HC with mean age of 50. There was no significant difference found in age between the groups. Time between t1 and t2 was also not significantly different between groups. No severe white matter abnormalities were found nor any significant group differences in white matter abnormalities at t1 or t2..

Table 2 Patient characteristics

	Ch+ (n = 26)	Ch- (n = 23)	HC (n = 30)	*p*
Age at t1 (years)	49.1 (8.7)	50.8 (6.5)	50.5 (8.0)	.734
Estimated IQ (NART)	100.1 (13.6)	103.9 (13.6)	107.6 (11.4)	.101
Education level (n, %)				
Low	0 (0)	0 (0)	0 (0)	
Middle	4 (15)	3 (13)	0 (0)	
High	22 (85)	20 (87)	30 (100)	
Interval t1 – t2 (days)	332 (70)	342 (33)	363 (59)	.119
Scan location at FU (n)	18/8	20/3	15/15	.017
Postmenopausal (n, %)				
t1	10 (38)	12 (52)	16 (53)	.484
t2	26 (100)	13 (57)	16 (53)	.001
Lifetime estrogen exposure (yrs)	31.4 (6.0)	33.9 (6.0)	32.6 (6.2)	.356
Medication use at t2 (n, %)				
Anti-diabetic		1 (4)	1 (3)	
Cardiovascular	3 (12)	5 (22)	7 (23)	
Psychotropic	6 (24)	1 (4)	3 (10)	
Breast cancer stage (n, %)				
0	0 (0)	12 (52)		
1	14 (54)	11 (48)		
2	11 (42)	0 (0)		
3	1 (4)	0 (0)		
Surgery (n, %)				.790
WLE	16 (62)	15 (65)		
Ablatio	10 (39)	8 (35)		
Radiotherapy (n, %)	21 (81)	15 (65)		
Tamoxifen (n, %)	17 (65)	NA		
Chemotherapy (n, %)				
AC[1]	3 (12)			
AC-docetaxel[2]	17 (65)			
AC-paclitaxel[3]	3 (12)			
FEC[4]	3 (12)			
Days since chemotherapy	201 (69)			

Values indicate mean ± SD unless indicated otherwise. BC+SYST, BC patients receiving systemic treatment; BC, BC patients not requiring systemic treatment; NC, no-cancer controls. Scan location at FU depicts number of participants at the two scan locations. Lifetime estrogen exposure was calculated by subtracting age at menarche from the age at menopause or current age, for each pregnancy an additional 0.75 year was subtracted (Schilder et al. 2010). WLE = wide local excision; Ablatio = breast amputation. AC = doxorubicin (Adriamycin), cyclophosphamide; FEC = 5-fluorouracil, epirubicin, cyclophosphamide. [1]4 or 6 cycles; [2]3 or 6 cycles; [3]4 cycles AC followed by 4 or 12 cycles of paclitaxel; [4]3 or 6 cycles.

Preprocessing

4D DWI volumes corrected with eddy showed noticeably less motion and smoothing with visual inspection as compared to the older eddy_correct tool used in Menning et al. (2017). The outcomes of the two techniques were not compared quantitatively because, as previously mentioned, research has already shown enhanced correction provided by the newer version. Optimal correction for EC and motion is important because such artifacts can affect the spatial resolution and estimation of the diffusion parameter maps leading to inaccurate outcomes (Jezzard et al., 1998). Applying dtifit on the corrected DWI data produced parameter maps for FA, MD, 3 eigenvectors, 3 eigenvalues, and the S0 image (raw T2 signal with no diffusion weighting = b0 image).

Template creation

High-resolution T1-weighted images were used in the current study to build the GW template from the whole sample (N=79), including both t1 and t2, totaling 158 images. The resulting high-resolution template was intended to minimize circularity bias, since it

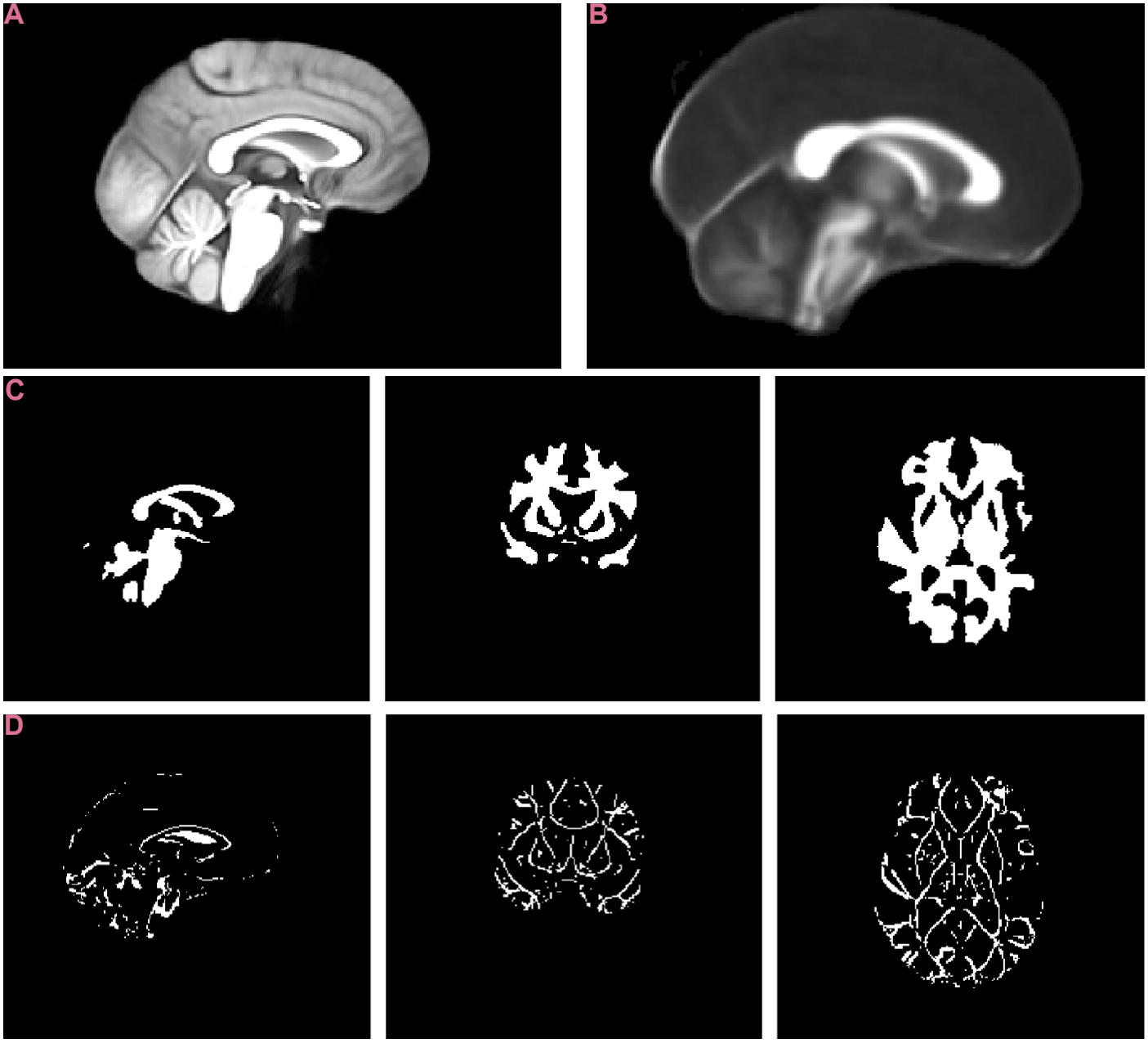

Fig. 1 **A:** Sagittal section of T1-weighted of GW template created with ANTs in native space. **B**: Sagittal section of FMRIB58_FA standard space (1mm) template in TBSS. **C**: Sagittal (left), coronal (middle), and transverse (right) sections of mean FA mask thresholded at 0.2 to limit the data to white matter in the multimodal ANTs-GW pipeline. **D:** Corresponding sections to **C** of the FA skeleton mask used in standard TBSS.

was created independently from the registered FA images. In TBSS, a standard template was used, which has a lower resolution than the T1-weighted GW template. (See Fig. 1A & 1B).

Registration

FA image registration using SyN in ANTs has been shown to be superior to many other registration algorithms including FNIRT. For this reason, we were able to exclude the FA skeleton with less concern for the potential effects of misregistration than with the non-skeletonized TBSS analyses. Nevertheless, without this skeleton, more white matter is preserved in all three pipelines. Compared to the FA skeleton used in standard TBSS with a volume of 124.7 ml, masked images in the improved pipelines included a considerably larger volume of 557.9 ml for non-skeletonized TBSSa, 507.9 ml for non-skeletonized TBSSb, and 512.7 ml for multimodal ANTs-GW (See Fig. 2C & 2D). The white matter mask had no voxels with FA lower than 0.2 and was visually checked for areas that might represent inclusion of gray matter (i.e. basal ganglia structures).

Statistical results

The one sample t-test for DTI values averaged across all voxels within the white matter mask in the standard TBSS and non-skeletonized TBSSa analyses showed significant decreases in mean FA in the Ch+ and HC groups. Additionally, both pipelines showed significant increases in MD in the healthy controls. The non-skeletonized TBSSb pipeline showed a significant decrease in mean FA in the Ch+ group. Similarly for the multimodal ANTs-GW pipeline, a significant decrease in FA was observed (-0.0015 ±0.0022, $p<0.001$), whereas no decrease was seen in Ch- nor controls. No significant changes in mean MD were seen in both pipelines. (See Table 3). There was a difference in mean FA change between groups approaching significance as determined by one-way ANOVA

Table 3 DTI means analysis

	Ch+ (n = 26)	Ch- (n = 23)	HC (n = 30)
Standard TBSS			
Mean FA (±)	-0.0031 (0.0062)*	-0.0013 (0.0046)	-0.005 (0.0094)**
Mean MD *1000 (±)	0.0013 (0.01)	0.0013 (0.0102)	0.0055 (0.0135)*
Non-skeletonized TBSSa			
Mean FA (±)	-0.001 (0.0019)*	-0.0005 (0.0015)	-0.0014 (0.0026)**
Mean MD *1000 (±)	-0.0134 (0.0658)	0.0003 (0.0044)	0.0026 (0.0051)**
Non-skeletonized TBSSb			
Mean FA (±)	-0.0015 (0.0023)**	-0.0006 (0.0019)	0.0003 (0.0043)
Mean MD *1000 (±)	0.0004 (0.0076)	0.001 (0.0056)	-0.0005 (0.0076)
Multimodal ANTs-GW			
Mean FA (±)	-0.0015 (0.0022)***	-0.0004 (0.0017)	-0.0001 (0.0026)
Mean MD *1000 (±)	0.0007 (0.0043)	0.001 (0.005)	-0.0001 (0.0038)

One sample t-test comparing mean FA and mean MD of white matter difference maps to 0 to assess changes over time
*p≤0.05, **p≤0.01, ***p≤0.001

Table 4 Voxel-wise paired group analysis

[a]Decrease	Ch+ vs. Ch-	Ch+ vs. HC	Ch- vs. HC
Standard TBSS			
FA (mm^3)	0	0	0
MD (mm^3)	0	0	0
Non-skeletonized TBSSa			
FA (mm^3)	28.68	0	0
MD (mm^3)	0	0	0
Non-skeletonized TBSSb			
FA (mm^3)	0	1569.18	5.91
MD (mm^3)	0	0	0
Multimodal ANTs-GW			
FA (mm^3)	0	13554.60	599.18
MD (mm^3)	0	0	0
[b]Increase	**Ch+ vs. Ch-**	**Ch+ vs. HC**	**Ch- vs. HC**
Standard TBSS			
FA (mm^3)	0	0	0
MD (mm^3)	0	0	0
Non-skeletonized TBSSa			
FA (mm^3)	0	0	0
MD (mm^3)	0	0	0
Non-skeletonized TBSSb			
FA (mm^3)	0	0	0
MD (mm^3)	0	0	0
Multimodal ANTs-GW			
FA (mm^3)	0	0	0
MD (mm^3)	0	0	0

[a]Proportion of volume in the first group that shows a significant decrease in FA or MD compared to the second group, FWE corrected at p<0.05.
[b]Proportion of volume in the first group that shows a significant increase in FA or MD compared to the second group, FWE corrected at p<0.05.
The proportion is calculated in relation to the total white matter analyzed in each pipeline and multiplied by 1000000.

(F (2,76) = 3.095, p = .051) seen only in the multimodal ANTs-GW pipeline. A Tukey post hoc test revealed that the Ch+ group had a significant decrease of mean FA over time (-0.0015 ± 0.0022, 0.047) compared to the HC group (-0.0001 ± 0.0026). There were no statistically significant differences between the clinical groups (p=0.203) or between the Ch- group and the HC group (p=0.844). There were no significant group differences in mean MD change over time following statistical analysis in any of the pipelines.

Table 4 shows the results of the voxel-wise analysis performed with randomise. Significant voxels were reported as a proportion of significant volume to total white matter volume because of the differences in the amount of white matter being compared in each pipeline. Standard TBSS as reported in Menning et al. (2017) showed no significant effects. Non-skeletonized TBSSa showed a small amount of volume with a significant decrease in FA in Ch+ compared to Ch-. No other effects were seen reflecting the results from the original analysis. For non-skeletonized TBSSb, both Ch+ and Ch- showed significantly decreased FA compared to HC but to a much lesser extent compared to the ANTs-GW analysis, which showed larger differences in FA over time in the cancer groups compared to the controls. Both Ch+ and Ch- groups showed a significant decrease in FA from t1 to t2 compared to the HC group (p<0.05) with the Ch+ comparison showing a considerably larger amount of affected volume than the Ch- comparison. These differences were seen lying outside of the FA skeleton, were concentrated in the splenium of the corpus callosum, and span parts of its trunk as well as parts of the posterior and superior white matter structure. (Fig.2).

Results of the voxel-wise one sample t-tests are shown in Table 5. Significant decreases in FA from t1 to t2 were found in the Ch+ and HC groups for all pipelines. In Ch+, these changes were consistently found in the left anterior and right posterior regions of white matter structure in all pipelines. For the HC group, the changes in FA were consistently located in the genu of the corpus callosum for all of the TBSS pipelines with additional areas in the right parietal region in non-skeletonized TBSSb. Multimodal ANTs-GW contrarily

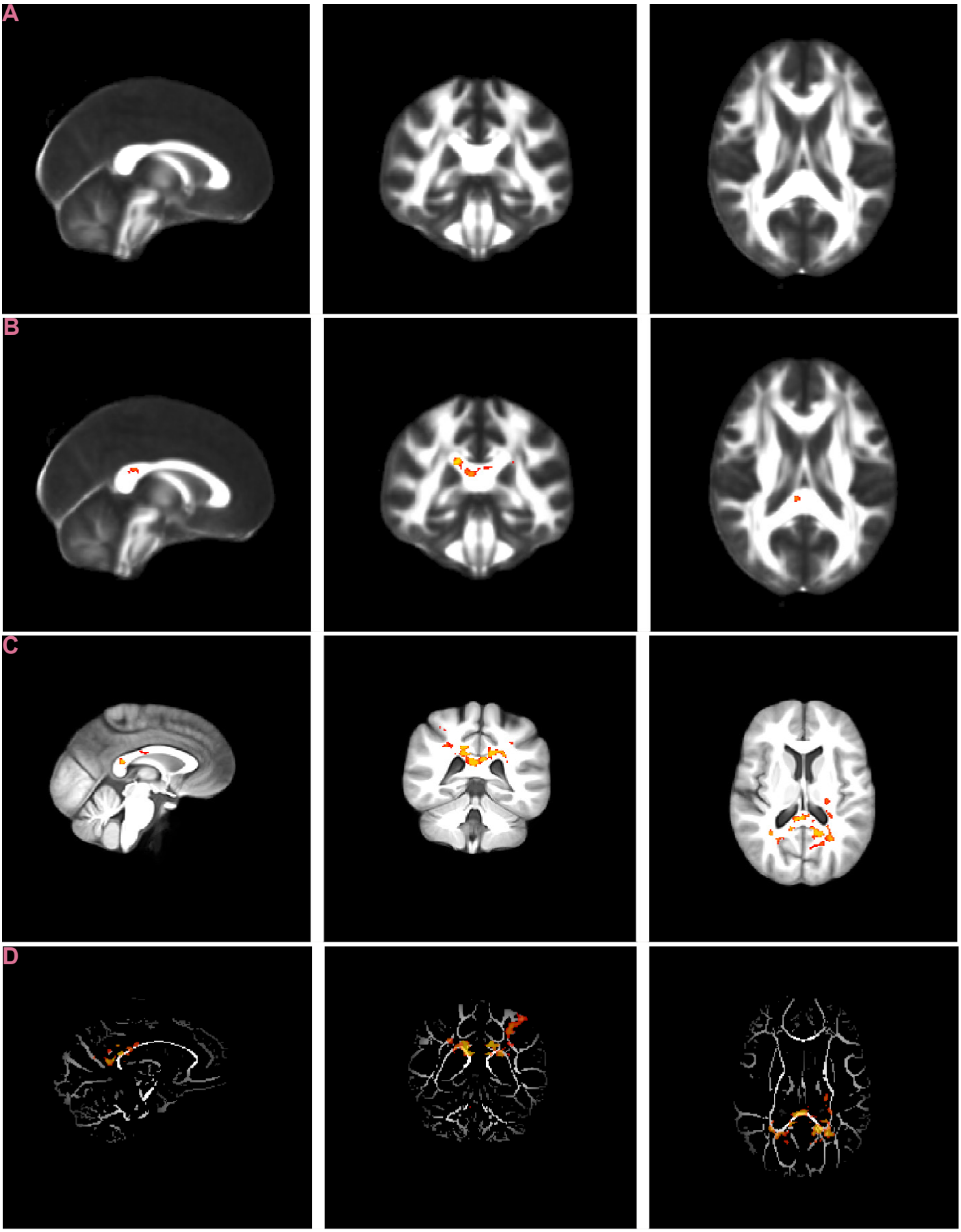

Fig. 2 **(A-C)**Results from the voxel-wise group analysis (CH+ < HC contrast) using randomise in FSL. **(A)** non-skeletonized TBSSa: Significant change in FA cannot be seen following the statistical analysis in this pipeline. **(B)** non-skeletonized TBSSb: Red-yellow voxels imposed on top of FMRIB58_FA standard template showing voxels with a significant decrease in FA in Ch+ compared to HC. **(C)** multimodal ANTs-GW: Red-yellow voxels imposed on top of T1-weighted GW template showing voxels with a significant decrease in FA in Ch+ compared to HC. **(D)** A sagittal, coronal, and transverse view of the FA skeleton in template space. Red-yellow voxels show significant decrease in FA from baseline to follow-up in Ch+ compared to HC in the ANTS pipeline. These effects lie mostly outside of the FA skeleton.

showed these changes in lateral anterior regions and right superior regions of white matter. Significant increases in MD were also found in all pipelines, but only for the HC group. These were seen in the left anterior regions for standatrd TBSS and non-skeletonized TBSSa. For both non-skeletonized TBSSb and multimodal ANTs-GW, these changes were seen in a large amount of voxels scattered in lateral and medial anterior parts of the white matter structure. Multimodal ANTs-GW also showed a significant increase in FA in the HC group in the splenium of the corpus callosum and anterior and superior parts of the white matter structure.

Table 5 Voxel-wise one sample t-test

	Ch+ (n=26)	Ch- (n=23)	HC (n=30)
Decrease (t2<t1)			
Standard TBSS			
FA (mm^3)	32.07	0	481.09
MD (mm^3)	0	0	0
Non-skeletonized TBSSa			
FA (mm^3)	2037.90	0	4109.86
MD (mm^3)	0	0	0
Non-skeletonized TBSSb			
FA (mm^3)	1708.97	0	2287.81
MD (mm^3)	0	0	0
Multimodal ANTs-GW			
FA (mm^3)	1909.58	0	3597.71
MD (mm^3)	0	0	0
Increase (t2>t1)			
Standard TBSS			
FA (mm^3)	0	0	0
MD (mm^3)	0	0	192.44
Non-skeletonized TBSSa			
FA (mm^3)	0	0	0
MD (mm^3)	0	0	5930.88
Non-skeletonized TBSSb			
FA (mm^3)	0	0	0
MD (mm^3)	0	0	60386.80
Multimodal ANTs-GW			
FA (mm^3)	0	0	5499.47
MD (mm^3)	0	0	51865.94

Proportion of volume containing either a significant increase or decrease over time per group when compared to 0, FWE corrected at $p<0.05$. The proportion is calculated in relation to the total white matter analyzed in each pipeline and multiplied by 1000000.

DISCUSSION

Overall, all the pipelines showed a significant decrease in mean FA (averaged across all white matter voxels) over time in the Ch+ group, but the effect was most pronounced in the multimodal ANTs-GW analysis. The HC group showed significant decreases in mean FA and increases in mean MD following the analyses of standard TBSS and non-skeletonized TBSSa. Such patterns are a common finding in the DTI literature and can be attributed to normal aging (Barrick et al., 2010). As expected, the non-skeletonized TBSSa analysis did not show any notable group differences in FA or MD reflecting the original analysis of Menning et al. (2017). The non-skeletonized TBSSb analysis showed similar decreases in FA in the clinical groups compared to HC as multimodal ANTs-GW, but the effects were to a lesser degree in terms of statistical significance. It was expected that Ch+ would show decreased FA over time compared to both Ch- and HC, however, significant differences between the clinical groups were not observed. Compared to the amount of volume (0.60 ml) showing a decrease in FA when Ch- is compared to HC, the effect does seem more pronounced in the Ch+ vs. HC comparison as it is seen in a much larger area (13.55 ml).

These results suggest that white matter effects may be related to the cancer itself with chemotherapy possibly having an added effect. However, results from the voxel-wise one sample t-test of multimodal ANTs-GW showed that HC had an increase in FA in voxels located in the same location where some of the group differences were found between the clinical groups and the HC. Thus, this increase probably contributed to the group differences found in FA. Nevertheless, significant group differences were seen in additional areas where HC did not show an increase in FA such as a wider area of the corpus callosum and frontal parts of the white matter structure. Therefore, it is possible that the cancer groups experienced more white matter injury compared to healthy controls where these effects did not overlap.

Even though patterns of decreased FA and increased MD are expected with aging (Rathee, Rallabandi, & Roy, 2016), it was surprising that both effects were seen only in the HC group. In general, HC are used as a reference for patient groups and are not always an informative comparison. However, some speculations may explicate these findings. It is possible that the HC group share a characteristic confound that was not controlled for in this study. The increase in FA seen in HC was also surprising and difficult to explain. This could potentially be due to scanner drift artifacts that were not controlled for in this study. Over time, scanners can experience a drift or a decay of signal that can affect the quality of the data (Takao et al., 2011). Thus, the change found in HC may be due to variability in the signal that is caused by scanner hardware. It is also possible that patterns of these effects are seen in all pipelines but only endure correction in the optimized pipeline due to its increased sensitivity. A closer look at uncorrected analyses can inform why these effects were found only in the multimodal ANTs-GW.

It seems that with each improvement of the processing steps of standard TBSS results became closer to the optimized analysis run in multimodal ANTs-GW. For example, the similarity of results between the non-skeletonized TBSSa and standard TBSS and between non-skeletonized TBSSb and ANTs-GW analysis from the means analysis suggests that more similar processing steps will lead to more similar outcomes. Thus, the results imply some consistency between the different pipelines, yet the level of agreement decreases as the pipelines become more different. However, unlike the findings in Deprez et al. (2012), the results did not support our expectation that chemotherapy is exclusively linked to loss of white matter integrity since the clinical groups do not differ statistically from each other in any of the analyses. This may be due to a lack of statistical power seeing as the Ch+ group showed much more significant voxels in comparison to HC than did the Ch- group.

Given the mixed findings in the literature and the findings from this study, the true effects of chemotherapy on white matter integrity in BCS are still inconclusive. Differences in findings can be at-

tributed to several other limitations concerning the sample itself or study design. For example, a sample of BCS in any given study could present with different cognitive problems or have differences in the degree in which the sample experiences these problems (i.e. Menning et al., 2017 and Deprez et al., 2012). Also, it is still difficult to parse out the effects of chemotherapy from other cancer-related effects because many studies do not use a group of BCS that did not receive chemotherapy (Wefel et al., 2011). For example, Koppelmans et al. (2014) assessed the effects of chemotherapy on BCS by comparing chemotherapy-treated BCS with healthy controls only and found negative effects of chemotherapy on white matter structure with time since treatment. However, without using proper control groups, some of the outcomes associated with white matter integrity can alternatively be attributed to the cancer itself, hormonal treatment, and anxiety and depression that survivors may experience after undergoing cancer treatment. It also makes it difficult to compare such results to other studies that compare multiple groups with specific treatment regimens (Stouten-Kemperman et al., 2015). Finally, many of the studies in BCS are cross-sectional limiting the interpretation of any differences found between groups.

Longitudinal studies like the study described in this thesis are especially important because they increase certainty that observed effects are truly the result of chemotherapy and not attributable to some pre-existent group differences. Also, they can provide information about the progression of impairment and recovery, direction of change, and identification of small effects. As explained below, the pipelines constructed for the present thesis did not exploit the possibilities of longitudinal data to its full extent. A way to analyze longitudinal data is by registering, on single subject basis, follow-up images to the previous time point until baseline is reached. This is done so that the same warp (from baseline to template) is used to register all the images to the template in order to keep within-subject longitudinal differences (Madhyastha et al., 2014). In this way, however, baseline and follow-up images are processed differently and lead to an interpolation bias. Interpolation asymmetry arises when the baseline images are used as a reference and are consequently left unaffected while the follow-up images are smoothed when warped back to the baseline (Reuter & Fischl, 2011). To address this asymmetry, many studies treat all the images from all the time points the same as was done in the present thesis. For all pipelines presented, baseline and follow-up images are not defined as such, which results in all the images being registered individually to the template. While this can be said to be unbiased, it handles the longitudinal data like cross-sectional data.

Another challenge that comes with longitudinal image processing is inverse inconsistency. Inverse inconsistency occurs when the transforms are inconsistent in each direction (Reuter & Fischl, 2011). Given two images that need to be registered to each other, the transform from image 2 to image 1 should be the inverse of the transform going from image 1 to image 2. However, this is usually not the case in many studies because of the way many registration algorithms are designed. Even when symmetric registration is used as in SyN, the bias still arises when baseline and follow-up images are biased as a result of interpolation asymmetry. If both a symmetric registration algorithm is used and interpolation asymmetry is resolved then image warps can be said to have inverse consistency.

In the different approaches used in this study and in TBSS generally, interpolation issues still play a minimal role in the sense that some individual brain scans are more distant from the template and therefore are interpolated to a larger extent than others, but no consistent bias is introduced by registering all images to one time point as is done in some 'truly' longitudinal pipelines. Because of this, image processing does not take advantage of the benefits of having dependent data, mainly the reduction of variance. The next step would be to modify the multimodal ANTs-GW pipeline to optimize it for longitudinal data. An unbiased longitudinal DTI pipeline was developed by Keihaninejad et al. (2013) that uses a within-subject template. In the first step, all the time points of each subject are registered together in a mean space to create a within-subject template. Then, the subject's images are registered to this template and averaged yielding one image per subject. The average images are used to create a GW template through iterative linear and non-linear registration. Finally, the transforms of a subject's baseline and follow-up images from native space to the within-subject template and from there to the GW template are combined to bring each image to the GW template. This approach can also be applied in the TBSS pipeline (Madhyastha et al., 2014; Engvig et al., 2012). However, it has not been fully developed in an ANTs framework yet to our knowledge.

Despite the challenges that remain, improvements on processing DTI were made on multiple levels in this study compared to standard TBSS. First, we created a GW template instead of using a standard template. Moreover, the template was based on the inclusion of structurally detailed, high-resolution T1-weighted images. which aid in alignment and minimize circularity bias. To our knowledge, this has not been done in any study looking at the effects of chemotherapy in BCS. Second, the registration algorithm used led to unbiased and optimal normalization of the DTI maps increasing the chances for finding true effects. Third, because of better registration we could exclude the FA skeleton and retain whole white matter structure. As implicated by the Deprez et al. findings, our results showed that brain changes in BCS seem to be located on the periphery of white matter structure and cannot be fully captured using an FA skeleton.

The current study presents with several limitations. As discussed above, the longitudinal data is not treated as such in the registration step. An unbiased pipeline for longitudinal data has been implemented in several studies using different processing programs. Though it has not been applied in ANTs, it is theoretically feasible and would be the next step for optimizing ANTs-GW for longitudinal analysis. Another limitation is a lack of quantified comparisons of the tools used in the different pipelines. The improved methods have already been quantitatively assessed in previous research and were not the focus of this research. Also, a template in native space was used in the final pipeline (multimodal ANTs-GW) making direct comparisons regarding the spatial localization of effects as compared to the other pipelines not straightforward. However, using such template is believed to lead to more accurate registration. Finally, scanner drift and other possible confounds were not included

as covariates in the statistical model. Inclusion of this variable, as well as a more thorough investigation into the characteristics of the HC group, might explain some of the unexpected effects that were found. In addition to addressing these limitations, future work should focus on the application of multimodal ANTs-GW in other non-CNS cancer survivors treated with chemotherapy who show similar cognitive impairment as BCS (e.g. testicular and colon cancer; Schagen et al., 2014).

By comparing the results from the different pipelines used in this study, it can be concluded that the systematically varying preprocessing steps regarding EC and motion correction tool, template choice, registration method, and skeletonization influence the processing and results of DTI analyses in a predictable way, with more accurate methods leading to more reliable results. Moreover, this shows how important it is to address the limitations of current standardized DTI data processing approaches and to validate new techniques that can improve existing pipelines or lead to new ones. Since the differing pipelines make it difficult to compare across studies, the results might not altogether be contradictory to each other or to what has been previously found.

CONCLUSION

Our findings suggest a possible effect of cancer and its treatments on white matter integrity, however, further investigation is needed to confirm the outcomes of this study. We were able to improve standard TBSS analysis of DTI data by establishing the feasibility of a DTI processing pipeline with a new EC and motion correction tool, a T1-weighted GW template and improved registration (SyN) applied in ANTs, and no skeletonization. While not yet ideal for longitudinal data, this approach takes an unbiased and improved approach that is appropriate for DTI data of BCS.

REFERENCES

Acosta-Cabronero, J., & Nestor, P. J. (2014). Diffusion tensor imaging in Alzheimer's disease: insights into the limbic-diencephalic network and methodological considerations. Frontiers in Aging Neuroscience, 6, 266. https://doi.org/10.3389/fnagi.2014.00266

Ahles, T. A., Root, J. C., & Ryan, E. L. (2012). Cancer- and cancer treatment-associated cognitive change: an update on the state of the science. Journal of Clinical Oncology: Official Journal of the American Society of Clinical Oncology, 30(30), 3675–3686. https://doi.org/10.1200/JCO.2012.43.0116

Amidi, A., Hosseini, S. M. H., Leemans, A., Kesler, S. R., Agerbæk, M., Wu, L. M., & Zachariae, R. (2017). Changes in Brain Structural Networks and Cognitive Functions in Testicular Cancer Patients Receiving Cisplatin-Based Chemotherapy. JNCI: Journal of the National Cancer Institute, 109(12). https://doi.org/10.1093/jnci/djx085

Andersson, J. L. R., & Sotiropoulos, S. N. (2016). An integrated approach to correction for off-resonance effects and subject movement in diffusion MR imaging. NeuroImage, 125, 1063–1078. https://doi.org/10.1016/j.neuroimage.2015.10.019

Andersson J.L.R., Jenkinson M., & Smith S. (2007) Non-linear registration, aka spatial normalisation. FMRIB Technial Report TR07JA2. https://www.fmrib.ox.ac.uk/datasets/techrep/tr07ja2/tr07ja2.pdf

Aribisala, B. S., He, J., & Blamire, A. M. (2011). Comparative study of standard space and real space analysis of quantitative MR brain data. Journal of Magnetic Resonance Imaging, 33(6), 1503–1509. https://doi.org/10.1002/jmri.22576

Avants, B. B., Tustison, N. J., & Johnson H. (2014). Advanced normalization tools (ANTs), version 2.x. Retrieved from http://stnava.github.io/ANTsDoc/

Avants, B. B., Tustison, N. J., Song, G., Cook, P. A., Klein, A., & Gee, J. C. (2011). A Reproducible Evaluation of ANTs Similarity Metric Performance in Brain Image Registration. NeuroImage, 54(3), 2033–2044. https://doi.org/10.1016/j.neuroimage.2010.09.025

Avants, B. B., Yushkevich, P., Pluta, J., Minkoff, D., Korczykowski, M., Detre, J., & Gee, J. C. (2010). The optimal template effect in hippocampus studies of diseased populations. NeuroImage, 49(3), 2457–2466. https://doi.org/10.1016/j.neuroimage.2009.09.062

Avants, B. B., Epstein, C. L., Grossman, M., & Gee, J. C. (2008). Symmetric diffeomorphic image registration with cross-correlation: evaluating automated labeling of elderly and neurodegenerative brain. Medical Image Analysis, 12(1), 26–41. https://doi.org/10.1016/j.media.2007.06.004

Bach, M., Laun, F. B., Leemans, A., Tax, C. M. W., Biessels, G. J., Stieltjes, B., & Maier-Hein, K. H. (2014). Methodological considerations on tract-based spatial statistics (TBSS). NeuroImage, 100, 358–369. https://doi.org/10.1016/j.neuroimage.2014.06.021

Barrick, T. R., Charlton, R. A., Clark, C. A., & Markus, H. S. (2010). White matter structural decline in normal ageing: A prospective longitudinal study using tract-based spatial statistics. NeuroImage, 51(2), 565–577. https://doi.org/10.1016/j.neuroimage.2010.02.033

Bodini, B., Khaleeli, Z., Cercignani, M., Miller, D. H., Thompson, A. J., & Ciccarelli, O. (2009). Exploring the relationship between white matter and gray matter damage in early primary progressive multiple sclerosis: an in vivo study with TBSS and VBM. Human Brain Mapping, 30(9), 2852–2861. https://doi.org/10.1002/hbm.20713

Boykoff, N., Moieni, M., & Subramanian, S. K. (2009). Confronting chemobrain: an in-depth look at survivors' reports of impact on work, social networks, and health care response. Journal of Cancer Survivorship: Research and Practice, 3(4), 223–232. https://doi.org/10.1007/s11764-009-0098-x

Conroy, S. K., McDonald, B. C., Smith, D. J., Moser, L. R., West, J. D., Kamendulis, L. M., … Saykin, A. J. (2013). Alterations in brain structure and function in breast cancer survivors: effect of post-chemotherapy interval and relation to oxidative DNA damage. Breast Cancer Research and Treatment, 137(2), 493–502. https://doi.org/10.1007/s10549-012-2385-x

de Ruiter, M. B., Reneman, L., Boogerd, W., Veltman, D. J., Caan, M., Douaud, G., … Schagen, S. B. (2012). Late effects of high-dose adjuvant chemotherapy on white and gray matter in breast cancer survivors: converging results from multimodal magnetic resonance imaging. Human Brain Mapping, 33(12), 2971–2983. https://doi.org/10.1002/hbm.21422

Deprez, S., Amant, F., Smeets, A., Peeters, R., Leemans, A., Van Hecke, W., … Sunaert, S. (2012). Longitudinal assessment of chemotherapy-induced structural changes in cerebral white matter and its correlation with impaired cognitive functioning. Journal of Clinical Oncology: Official Journal of the American Society of Clinical Oncology, 30(3), 274–281. https://doi.org/10.1200/JCO.2011.36.8571

Deprez, S., Billiet, T., Sunaert, S., & Leemans, A. (2013). Diffusion tensor MRI of chemotherapy-induced cognitive impairment in non-CNS cancer patients: a review. Brain Imaging and Behavior, 7(4), 409–435. https://doi.org/10.1007/s11682-012-9220-1

Dietrich, J., Han, R., Yang, Y., Mayer-Pröschel, M., & Noble, M. (2006). CNS progenitor cells and oligodendrocytes are targets of chemotherapeutic agents in vitro and in vivo. Journal of Biology, 5(7), 22. https://doi.org/10.1186/jbiol50

Draganski, B., Ashburner, J., Hutton, C., Kherif, F., Frackowiak, R. S. J., Helms, G., & Weiskopf, N. (2011). Regional specificity of MRI contrast parameter changes in normal ageing revealed by voxel-based quantification (VBQ). NeuroImage, 55(4), 1423–1434. https://doi.org/10.1016/j.neuroimage.2011.01.052

Engvig, A., Fjell, A. M., Westlye, L. T., Moberget, T., Sundseth, Ø., Larsen, V. A., & Walhovd, K. B. (2012). Memory training impacts short-term changes in aging white matter: a longitudinal diffusion tensor imaging study. Human Brain Mapping, 33(10), 2390–2406. https://doi.org/10.1002/hbm.21370

Graham, M. S., Drobnjak, I., & Zhang, H. (2016). Realistic simulation of artefacts in diffusion MRI for validating post-processing correction techniques. NeuroImage, 125, 1079–1094. https://doi.org/10.1016/j.neuroimage.2015.11.006

Jenkinson, M., Beckmann, C. F., Behrens, T. E. J., Woolrich, M. W., & Smith, S. M. (2012). FSL. NeuroImage, 62(2), 782–790. https://doi.org/10.1016/j.neuroimage.2011.09.015

Jezzard, P., Barnett, A. S., & Pierpaoli, C. (1998). Characterization of and correction for eddy current artifacts in echo planar diffusion imaging. Magnetic Resonance in Medicine, 39(5), 801–812. https://doi.org/10.1002/mrm.1910390518

Keihaninejad, S., Ryan, N. S., Malone, I. B., Modat, M., Cash, D., Ridgway, G. R., … Ourselin, S. (2012). The Importance of Group-Wise Registration in Tract Based Spatial Statistics Study of Neurodegeneration: A Simulation Study in Alzheimer's Disease. PLOS ONE, 7(11), e45996. https://doi.org/10.1371/journal.pone.0045996

Keihaninejad, S., Zhang, H., Ryan, N. S., Malone, I. B., Modat, M., Cardoso, M. J., … Ourselin, S. (2013). An unbiased longitudinal analysis framework for tracking white matter changes using diffusion tensor imaging with application to Alzheimer's disease. NeuroImage, 72, 153–163. https://doi.org/10.1016/j.neuroimage.2013.01.044

Klein, A., Andersson, J., Ardekani, B. A., Ashburner, J., Avants, B., Chiang, M.-C., … Parsey, R. V. (2009). Evaluation of 14 nonlinear deformation algorithms applied to human brain MRI registration. NeuroImage, 46(3), 786–802. https://doi.org/10.1016/j.

neuroimage.2008.12.037

Koppelmans, V., de Groot, M., de Ruiter, M. B., Boogerd, W., Seynaeve, C., Vernooij, M. W., … Breteler, M. M. B. (2014). Global and focal white matter integrity in breast cancer survivors 20 years after adjuvant chemotherapy. Human Brain Mapping, 35(3), 889–899. https://doi.org/10.1002/hbm.22221

Le Bihan, D., Mangin, J. F., Poupon, C., Clark, C. A., Pappata, S., Molko, N., & Chabriat, H. (2001). Diffusion tensor imaging: concepts and applications. Journal of Magnetic Resonance Imaging: JMRI, 13(4), 534–546.

Madhyastha, T., Mérillat, S., Hirsiger, S., Bezzola, L., Liem, F., Grabowski, T., & Jäncke, L. (2014). Longitudinal reliability of tract-based spatial statistics in diffusion tensor imaging. Human Brain Mapping, 35(9), 4544–4555. https://doi.org/10.1002/hbm.22493

Menning, S., de Ruiter, M. B., Veltman, D. J., Boogerd, W., Oldenburg, H. S. A., Reneman, L., & Schagen, S. B. (2017). Changes in brain white matter integrity after systemic treatment for breast cancer: a prospective longitudinal study. Brain Imaging and Behavior. https://doi.org/10.1007/s11682-017-9695-x

Menning, S., de Ruiter, M. B., Veltman, D. J., Koppelmans, V., Kirschbaum, C., Boogerd, W., … Schagen, S. B. (2015). Multimodal MRI and cognitive function in patients with breast cancer prior to adjuvant treatment — The role of fatigue. NeuroImage : Clinical, 7, 547–554. https://doi.org/10.1016/j.nicl.2015.02.005

Pomykala, K. L., Ganz, P. A., Bower, J. E., Kwan, L., Castellon, S. A., Mallam, S., … Silverman, D. H. S. (2013). The association between pro-inflammatory cytokines, regional cerebral metabolism, and cognitive complaints following adjuvant chemotherapy for breast cancer. Brain Imaging and Behavior, 7(4), 511–523. https://doi.org/10.1007/s11682-013-9243-2

Rathee, R., Rallabandi, V. P. S., & Roy, P. K. (2016). Age-Related Differences in White Matter Integrity in Healthy Human Brain: Evidence from Structural MRI and Diffusion Tensor Imaging. Magnetic Resonance Insights, 9, 9–20. https://doi.org/10.4137/MRI.S39666

Reuter, M., & Fischl, B. (2011). Avoiding asymmetry-induced bias in longitudinal image processing. NeuroImage, 57(1), 19–21. https://doi.org/10.1016/j.neuroimage.2011.02.076

Schagen, S. B., Klein, M., Reijneveld, J. C., Brain, E., Deprez, S., Joly, F., … Wefel, J. S. (2014). Monitoring and optimising cognitive function in cancer patients: Present knowledge and future directions. EJC Supplements, 12(1), 29–40. https://doi.org/10.1016/j.ejcsup.2014.03.003

Schwarz, C. G., Reid, R. I., Gunter, J. L., Senjem, M. L., Przybelski, S. A., Zuk, S. M., … Alzheimer's Disease Neuroimaging Initiative. (2014). Improved DTI registration allows voxel-based analysis that outperforms tract-based spatial statistics. NeuroImage, 94, 65–78. https://doi.org/10.1016/j.neuroimage.2014.03.026

Simó, M., Rifà-Ros, X., Rodriguez-Fornells, A., & Bruna, J. (2013). Chemobrain: a systematic review of structural and functional neuroimaging studies. Neuroscience and Biobehavioral Reviews, 37(8), 1311–1321. https://doi.org/10.1016/j.neubiorev.2013.04.015

Sled, J. G., Zijdenbos, A. P., & Evans, A. C. (1998). A nonparametric method for automatic correction of intensity nonuniformity in MRI data. IEEE Transactions on Medical Imaging, 17(1), 87–97. https://doi.org/10.1109/42.668698

Smith, S. M., Jenkinson, M., Johansen-Berg, H., Rueckert, D., Nichols, T. E., Mackay, C. E., … Behrens, T. E. J. (2006). Tract-based spatial statistics: voxelwise analysis of multi-subject diffusion data. NeuroImage, 31(4), 1487–1505. https://doi.org/10.1016/j.neuroimage.2006.02.024

Stouten-Kemperman, M. M., de Ruiter, M. B., Koppelmans, V., Boogerd, W., Reneman, L., & Schagen, S. B. (2015). Neurotoxicity in breast cancer survivors ≥10 years post-treatment is dependent on treatment type. Brain Imaging and Behavior, 9(2), 275–284. https://doi.org/10.1007/s11682-014-9305-0

Takao, H., Hayashi, N., & Ohtomo, K. (2011). Effect of scanner in longitudinal studies of brain volume changes. Journal of Magnetic Resonance Imaging, 34(2), 438–444. https://doi.org/10.1002/jmri.22636

Tustison, N. J., Avants, B. B., Cook, P. A., Kim, J., Whyte, J., Gee, J. C., & Stone, J. R. (2014). Logical circularity in voxel-based analysis: normalization strategy may induce statistical bias. Human Brain Mapping, 35(3), 745–759. https://doi.org/10.1002/hbm.22211

Tustison, N. J., Avants, B. B., Cook, P. A., Zheng, Y., Egan, A., Yushkevich, P. A., & Gee, J. C. (2010). N4ITK: improved N3 bias correction. IEEE Transactions on Medical Imaging, 29(6), 1310–1320. https://doi.org/10.1109/TMI.2010.2046908

Van Hecke, W., Leemans, A., & Emsell, L. (2016). DTI Analysis Methods: Voxel-Based Analysis. In Diffusion Tensor Imaging (pp. 183–203). Springer, New York, NY. Retrieved from https://link.springer.com/chapter/10.1007/978-1-4939-3118-7_10

Van Hecke, W., Leemans, A., De Backer, S., Jeurissen, B., Parizel, P. M., & Sijbers, J. (2010). Comparing isotropic and anisotropic smoothing for voxel-based DTI analyses: A simulation study. Human Brain Mapping, 31(1), 98–114. https://doi.org/10.1002/hbm.20848

Wefel, J. S., Kesler, S. R., Noll, K. R., & Schagen, S. B. (2015). Clinical characteristics, pathophysiology, and management of noncentral nervous system cancer-related cognitive impairment in adults. CA: A Cancer Journal for Clinicians, 65(2), 123–138. https://doi.org/10.3322/caac.21258

Wefel, J. S., Vardy, J., Ahles, T., & Schagen, S. B. (2011). International Cognition and Cancer Task Force recommendations to harmonise studies of cognitive function in patients with cancer. The Lancet. Oncology, 12(7), 703–708. https://doi.org/10.1016/S1470-2045(10)70294-1

Wintermark, M., Huss, D. S., Shah, B. B., Tustison, N., Druzgal, T. J., Kassell, N., & Elias, W. J. (2014). Thalamic connectivity in patients with essential tremor treated with MR imaging-guided focused ultrasound: in vivo fiber tracking by using diffusion-tensor MR imaging. Radiology, 272(1), 202–209. https://doi.org/10.1148/radiol.14132112

Yamada, H., Abe, O., Shizukuishi, T., Kikuta, J., Shinozaki, T., Dezawa, K., … Imamura, Y. (2014). Efficacy of distortion correction on diffusion imaging: comparison of FSL eddy and eddy_correct using 30 and 60 directions diffusion encoding. PloS One, 9(11), e112411. https://doi.org/10.1371/journal.pone.0112411

Zhan, J., Dinov, I. D., Li, J., Zhang, Z., Hobel, S., Shi, Y., … Liu, S. (2013). Spatial-temporal atlas of human fetal brain development during the early second trimester. NeuroImage, 82, 115–126. https://doi.org/10.1016/j.neuroimage.2013.05.063

Animal Testing from a Philosophical Perspective

by Nikos Kolonis

The place of non-human animals in the philosophical tradition has not always been ideal. From Aristotle to Kant, the animals' inability to reason has been reason enough to justify their use as a means to an end. Descartes has even gone as far as saying that animals are machines, incapable of thinking or feeling pain. The first moral system to include animals as moral agents has been utilitarianism, where, according to Jeremy Bentham, the criterion for ethical consideration should not be the ability to reason, but the capacity to feel pain.

Animal use for experimentation dates back to the 17th century, when William Harvey researched the heart's role in blood flow, by performing thoracotomy in animals while they were still alive, to observe the contractions of their hearts (Besterman, 2004). Today, animals are used mainly for biomedical research, but also toxicology and medical training purposes, with a majority of the scientific community supporting its necessity. The human species, they would say, is in a much better place now thanks to animal testing. If it were not for animal testing, we would not be able to do blood transfusions, produce insulin, use anaesthetics and much more (Sandøe & Christiansen, 2008). So, for most people, although animal testing as a practice is not really desirable, its benefits seem to make it indispensable. That is, until good enough alternatives have been developed in the future. This perspective on the issue appears valid, but there is one key assumption within it that needs to be made explicit.

In general, those who tend to follow this line of thought are those with preconceived ideas of non-human animals being somehow inferior to humans and there to serve their needs. This is a categorical distinction that is made automatically but also, one could argue, arbitrarily. Peter Singer (2009) has popularized the term speciesism, to refer to this exclusion from moral consideration based on morally irrelevant differences between species, like differences in mental capabilities (p. 9). Similar to racism or sexism, speciesism is a logically invalid prejudice against members of other species. He further argues that, even if mental capability were a relevant feature for ethical consideration, it is not something that is distinctive of certain species, as large variability is observed, even within the same species. Justifying the right to use an animal for your own gain based on its limited mental capabilities, can also justify making the same use of a person who for some reason might have limited mental capabilities in comparison to others.

Instead of focusing on the differences, Singer argues that we should be focusing on the similarities among different species and on our shared basic interests. Following Bentham's utilitarian philosophy, he argues that the main similarity is the ability to feel pain and the consequential interest in avoiding pain (Singer, 2009, p. 5). This common interest seems to equate human and non-human animals and require equal ethical interest in the way they are treated, especially considering animals are often subject to pain during experimentation, whether physical or psychological.

One grey area in Singer's argumentation relates to the ethical issues of euthanizing animals. Whereas the ethical importance of avoiding pain is made clear, it is not clear whether death should be similarly considered. That is, if we consider an ideal scenario where animals used for research have a completely painless death, would that death then be morally justifiable? When evaluating the life of an animal, one thing that should be taken into consideration, according to philosopher Warwick Fox (2012), is an animal's ability to have an autobiographical sense of self, that is to be aware of its existence in time. For that animal, death would be a discontinuation in its temporal experience. Humans are par excellence autobiographical beings, as they are aware of a continuation of the self in time, expect the future and make plans for it and are aware of their own mortality. According to Fox, humans are the only autobiographical beings, as he argues that being linguistically enabled is a prerequisite for it. This assertion is grounded on evidence from people who gained their linguistic ability at an older than normal age and claim to have been originally unable to make a distinction between past, present and future experiences. If we consider this to be the case, then every non-human animal cannot be autobiographical and, consequently, its death is not morally unacceptable.

However, it still remains an open question whether language is indeed the main factor and it might be safer to assume that an autobiographical sense of self is a continuum, that different animals have in different rates, according to their place in the evolutionary timeline. Indeed, according to cognitive ethologist Donald Griffin, animals other than humans do possess some sort of self-awareness, in the sense that they are aware of their own body and actions and are able to distinguish them from the bodies and actions of others (Griffin, 2001). Despite lacking awareness of their existence in time, they still have an interest in perpetuating their existence and getting to the next second of consciousness. No matter which of the two holds true, whether only humans or also non-human animals can possess some sort of self-awareness, it should always be taken into account that the death of an animal is in most cases

a cause of psychological pain for others associated with the deceased animal. Even though death might not be a deprivation for a certain animal, it could still be for others, thus making the life of that animal indirectly valuable.

> "As humans, we are historically poor at challenging our ideas of superiority over others and the case of animal testing is no exception."

Going one step further, the philosopher Tom Regan tries to prove that both causing pain and causing death should be considered morally wrong (Regan, 2012). He claims that both humans and most non-human animals should be recipients of some basic moral rights, such as the right to life and to physical integrity. He invokes findings concerning the similarities in mammal nervous systems, which he argues give them similar conscious experiences. All mammals, according to Regan, independent of their variability in mental capabilities, have an interest for what they experience and what they are deprived of. All mammals enjoy certain experiences and find others painful, share cognitive abilities (like the ability to learn from experience, remember the past and anticipate the future) and share emotional experiences (like fear, jealousy and sadness). The psychological complexity of these animals requires that we consider them as "subjects-of-a-life" and ascribe to them some basic rights, that prohibit causing them any form of harm and, thus, performing any sort of experimentation on them.

Regan makes a distinction between mammals and simpler living organisms, considering the latter as morally irrelevant. The physiology of non-mammals shows that they lack a basic capability of having a conscious experience and they are characterized by a mental and emotional simplicity. Such a claim, though, is slowly being refuted, as accumulating evidence over the past few years shows that certain non-mammals, like the octopus, do actually possess a quite complex nervous system and a range of behaviours that implies a much higher cognitive complexity than previously thought. Such observations have led many to claim that these animals are actually conscious in a similar way to mammals (Godfrey-Smith, 2016). However, it is irrelevant whether this is eventually proven to be true or not, the basis of Regan's argumentation remains unaffected, in the sense that a distinction for ascribing moral relevance can still be made between the animals that we know to be capable of conscious experience and the ones that lack this capability, even though this distinction might not be between mammals and non-mammals.

During the last few decades, considerable progress has been made in reducing pain in animals used for experimentation. Moreover, the categorical distinction between more and less morally relevant species seems to be moving backwards in the evolutionary timeline, with stricter regulations being implemented for experimentation in mammals and even with the complete elimination of testing for some primates. In the near future, it is highly probable that the dilemma of whether animal testing is ethically justifiable or not will become irrelevant, before a consensus on it is reached. Many alternatives have and are being developed. Engineered cell cultures and tissues, as well as computer simulations are already replacing animal testing and inventions like the "organ on a chip" are holding a lot of promise for the future. As alternatives become more and more prominent and affordable, it is logical to assume that they will eventually replace all experimentation on living organisms.

However, at present, for animals used for experimentation purposes, physical pain has not been completely eliminated and psychological pain still remains at a considerably high level. As for the distinction according to mental capability, it still seems to remain entrenched in the scientific mentality, making the use of certain animals more morally acceptable than others. As humans, we are historically poor at challenging our ideas of superiority over others and the case of animal testing is no exception. Scientists should always remind themselves to take a step back and consider the morality of their actions, taking into account what distinguishes them from the animals they experiment on. They will most probably fail in finding a distinguishing factor that matters.

References

Besterman, E. M. M. (2004). William Harvey and his discovery of the circulation of the blood. West Indian Medical Journal. https://doi.org/10.1097/00007611-199112000-00019

Fox, W. (2012). Forms of Harm and Our Obligations to Human and Other Animals. In E. D. Protopapadakis (Ed.), Animal Ethics – Past and Present Perspectives (pp. 198-210). Berlin: Logos Verlag.

Godfrey-Smith, P. (2016). Other Minds: The Octopus, The Sea, and the Deep Origins of Consciousness. US: Farrar, Straus and Giroux.

Griffin, D. R. (2001). Chapter 1: In Favor of Animal Consciousness. In Animal Minds: Beyond Cognition to Consciousness. US: University of Chicago Press.

Regan, T. (2012), Empty Cages: Animal Rights and Vivisection. In J. R. Garrett (Ed.), The Ethics of Animal Research: Exploring the Controversy. MIT Press.

Singer, P. (2009). Animal Liberation (Updated Edition). New York: HarperCollins.

Sandøe, P., & Christiansen, S. B. (2008). Chapter 7: The Use of Animals in Experiments. In Ethics of Animal Use (p. 104). UK: Blackwell Publishing.

The role of Lin41 in cortical development, adult neurogenesis and ependymal cell fate specification

Iris Marchal

Supervisor: Dr. Claudia Marini

ABSTRACT

First described in the nematode C. elegans as a regulator of the larval-to-adult transition, Lin41 is now known as a key regulator of developmental processes that is highly conserved in a wide range of animal species. Next to its role in development, Lin41 has recently been found to show recurring expression in the postnatal central nervous system (CNS). In the postnatal brain, Lin41 expression is exclusively found in the ependymal cells lining the walls of the four ventricles. The timing and localization of this expression pattern implicates a potential role for Lin41 in cortical development, adult neurogenesis and ependymal cell fate specification. In the present study, I further investigate the temporal and spatial expression pattern of postnatal Lin41 and its potential roles in the murine CNS. Performing immunostaining on coronal slides and whole mount lateral ventricle preparations I show that lack of Lin41 does not lead to cortical deficits, disorganization of the adult neurogenic niche, ependymal cell specification or the progenitor population of the V-SVZ. The notion that Lin41 is dispensable for these processes in the adult brain raises new questions regarding possible other functions of this ancient regulator in the postnatal murine CNS.

KEYWORDS

lin41, cell, ependymal, postnatal, neurogenesis

INTRODUCTION

First described in the nematode Caenorhabditis elegans (C. elegans) as a regulator of the larval-to-adult transition, Lin41 is now known as a key regulator of developmental processes that is highly conserved in a wide range of animal species (Slack et al., 2000). As a target of the differentiation-associated microRNA (miRNA) let-7, Lin41 has historically been studied as a model miRNA target (Slack et al., 2000). However, more recently the developmental and molecular functions of Lin41 have received increasing attention and are beginning to be unravelled (Ecsedi & Großhans, 2013). Research has identified Lin41 as an important regulator of cell proliferation and inhibitor of differentiation in vertebrate and invertebrate development (Chang et al., 2012; Rybak et al., 2009; Worringer et al., 2013). In murine development, it is most highly expressed during the earliest stages of development, with the earliest expression detectable around embryonic day 8 (E8). At this stage, Lin41 is expressed in all but the heart tissue. Expression declines from that time on. With the exception of a late niche of putative expression in the male germ line (Rybak et al., 2009), Lin41 expression in other regions is undetectable from E11.5 (Schulman, Esquela-Kerscher, & Slack, 2005). Lin41 was shown to be essential for numerous processes during embryogenesis such as chick and murine limb development (Lancman et al., 2005), adequate timing of zebrafish embryonic development (Lin et al., 2007) and the maintenance of murine neuronal progenitors (Chen, Lai, & Niswander, 2012). Additionally, early expression of Lin41 in mouse development was found to be required for embryonic viability and neural tube closure, with embryos lacking Lin41 displaying a lethal phenotype beginning at E9.5. Although, the cause of embryonic lethality has not yet been fully elucidated, neural tube closure defects might be caused

by the role of LIN41 as E3 ubiquitin ligase controlling the balance between self-renewal, differentiation and cell death (Chen et al., 2012; Cuevas, Rybak-Wolf, Rohde, Nguyen, & Wulczyn, 2015; Thi et al., 2017).

Next to its role in embryogenesis, a recent study using a new gene trap mouse line deficient in Lin41 investigated expression patterns in the postnatal central nervous system (CNS) (Cuevas et al., 2015). Lin41 was found to be expressed not only during embryonic development until E13.5 but also at later stages beginning from postnatal day 10 (P10) and extending into adulthood. To date, the potential role of Lin41 expression in late-embryonic stages of development and of its recurring expression at adult stages in the CNS has not been investigated.

Development of the CNS starts with the formation of the neural plate: a structure that folds and fuses thereby forming a cavity – known as the neural tube – filled with cerebrospinal fluid (CSF), constructing the first framework of what is to become the ventricular system (Götz & Huttner, 2005). The neural plate and neural tube are composed of a single layer of neural progenitor cells named neuroepithelial cells, which form the neuroepithelium. With the switch to neurogenesis, neural progenitor cells begin asymmetric cells divisions, exit the cell cycle, and migrate away from the lumen giving rise to a tissue of multiple cell layers containing neurons,astrocytes and oligodendrocytes (Götz & Huttner, 2005). During this process, neuroepithelial cells are the origin of a distinct cell type: radial glial cells. Radial glial cells constitute the ventricular zone (VZ). As compared to neuroepithelial cells, radial glial cells are more fate-restricted. Consequently, most of the neurons and glia in the brain are derived – both directly and indirectly – from radial glial cells. Next to the formation of radial glial cells, another type of neural progenitors emerges at the onset of neurogenesis, known as the basal progenitors. At later stages, these cells form a mitotic cell layer immediately below the VZ known as the subventricular zone (SVZ) (Götz & Huttner, 2005; Molyneaux, Arlotta, Menezes, & Macklis, 2007). In mice, the process of corticogenesis starts around E12.5 and is completed by birthdate. Late-embryonic Lin41 expression – from E9.5 to E13.5 – is mainly restricted to the neuroepithelium (Cuevas et al., 2015). This timing and localization pattern of late-embryonic Lin41 expression indicates a potential role in the proliferation, specification or patterning of cortical progenitors. Lack of Lin41 could lead to deficiencies in neural progenitor cell proliferation, cell fate changes or defects in patterning, and may disrupt cortical development, leading to defects in cortical morphology postnatally.

Within the postnatal brain, Lin41 expression is exclusively found in the ependymal cells lining the walls of the four ventricles (Cuevas et al., 2015). Ependymal cells form the interface between the ventricular lumen and the brain parenchyma and are typically rectangular cuboidal and multiciliated. During embryogenesis, ependymal cells are born from radial glial cells between E14 and E16. Interestingly, the maturation of ependymal cells and the formation of cilia occur significantly later, during the first postnatal week (Spassky, 2005). Staining and live cell imaging of primary cell cultures resembling the time course of ependyma generation in the brain show that onset of Lin41 promotor activity is induced upon ependymal cell differentiation and coincided with the induction of ependymal lineage markers and the formation of functional motile cilia (Cuevas et al., 2015). These results suggest that Lin41 might play a functional role in ependymal cell specification or function. In healthy conditions, cilia in the apical side of the ependymal cells regulate the unidirectional and synchronized movement of the CSF through the ventricular system (Cathcart & Worthington, 1964). Defects in cilia can cause hydrocephalus, a condition characterized by CSF accumulation and enlargement of the ventricle cavities (Ibañez- Tallon et al., 2004; Paez-Gonzalez et al., 2011). If Lin41 is essential for the proper function of ependymal cells, it could be expected that lack of Lin41 would lead to dysregulation of CSF flow resulting in a hydrocephalus-like phenotype.

Next to their role in CSF flow, ependymal cells are also considered to be essential for the process of adult neurogenesis. After birth, new neurons and glia cells continue to be born in restricted germinal regions, of which the largest is the SVZ surrounding the walls of the lateral ventricles (Alvarez-Buylla & Lim, 2004). In the adult mammalian brain the SVZ in the lateral walls generates new neurons migrating along the rostral migratory stream (RMS) to become granule and periglomerular neurons in the olfactory bulb (OB) (Zhao, Deng, & Gage, 2008). Additionally, adult neurogenesis in the SVZ niche produces oligodendrocytes in corpus callosum, fimbria, and striatum (Jackson & Alvarez-Buylla, 2008; Menn et al., 2006). The adult brain lateral ventricles show compelling resemblance to the VZ in the embryonic neuroepithelium (Guillemot, 2005). Three types of precursor cells can be identified in the postnatal SVZ (Zhao et al., 2008). Firstly, neural stem cells (NSCs) in the postnatal brain have been identified as a subpopulation of astrocytes – which are derived from radial glia – and are also known as type B1-cells (Doetsch, Caillé, Lim, García-Verdugo & Alvarez-Buylla, 1999). Additionally, the SVZ is populated with type C cells – or intermediate progenitors – which are the progeny of B cells that give rise to type A migrating neuroblasts. Some studies have suggested ependymal cells to be the adult NSCs responsible for neurogenesis in the SVZ (Coskun et al., 2008; Johansson, Svensson, Wallstedt, Janson, & Frisén, 1999). However, this notion is still highly debated and most studies in the mammalian brain report that ependymal cells are postmitotic and do not directly contribute to neurogenesis (Mirzadeh, Merkle, Soriano-Navarro, Garcia-Verdugo, & Alvarez- Buylla, 2008; Spassky, 2005). Still, ependymal cells are believed to play at least supportive roles in the process of adult neurogenesis. For example, the bone morphogenic protein (BMP) antagonist Noggin is expressed by ependymal cells, thereby promoting neurogenesis (Lim et al., 2000). Additionally, ependymal cells may promote NSCs self-renewal through secretion of pigment epithelium-derived factor (Ramírez-Castillejo et al., 2006). Interestingly, ependymal cells are also critical for the correct migration of new-born neurons towards the OB, as neuroblast migration parallels CSF flow (Sawamoto et al., 2006). Furthermore, ependymal cells form an important component of the cellular arrangement of the adult neurogenic niche (Mirzadeh et al., 2008; Paez-Gonzalez et al., 2011). Within the niche, ependymal cells are distributed in the ventricle wall in a so-called 'pinwheel' structure

surrounding a single GFAP positive NSC (B1 cell). This pinwheel organization might be fundamental to neurogenesis – enabling stem cells to stay in direct contact with the ventricle through its apical primary cilium – and suggests a supporting role for ependymal cells within the niche. Moreover, contact with the ventricular fluid provides NSCs with access to signals like Noggin (Lim et al., 2000). The supporting roles of ependymal cells in the organization and function of the neurogenic niche could be partly regulated by Lin41 expression, creating an environment that promotes proliferation or inhibits differentiation of NSCs.

In the present study, I further investigate the temporal and spatial expression pattern of postnatal Lin41 in the wild-type (WT) murine CNS. Moreover, I examine the possible role of Lin41 in late embryonic cortical development, adult neurogenesis and the specification of ependymal cells via the use of an Emx1-Cre induced Lin41 knock out mouse model. The Lin41 expression pattern observed in NMRI WT mice is similar to previous reports, in which Lin41 mRNA and protein is increased around P7 and remains present up to adulthood. Performing immunostaining on coronal slides and whole mount ventricular preparations I show that lack of Lin41 does not lead to disorganization of the adult neurogenic niche and the progenitor population of the VZ-SVZ. The notion that Lin41 might be dispensable for the proper performance of ependymal cells in the neurogenic niche and the subsequent progenitor population raises new questions regarding possible other functions of this ancient regulator in the adult murine CNS.

METHODS

Animals

C57BL/6 animals lacking Lin41 expression in all Emx1 positive cells were generated by crossing Lin41lox/+;Emx1-Cre+/- to Lin-41loxlox-;Emx1-Cre-/- mice (Supplementary Figure 2.1). Offspring generated Lin41lox/-;Emx1-Cre+/- mice – also referred to as Lin41 conditional knock out (cKO) – inactivating the functional Lin41 allele from E10,5 in all Emx1 positive cells. NMRI WT, Lin41lox/-;Emx1-Cre-/-, Lin41lox/+;Emx1-Cre+/- or Lin41lox ;Emx1-Cre-/- were taken as controls. All generated C57BL/6 offspring as well as WT NMRI mice were maintained under standard condition of rodent husbandry. All animal experiments were carried out in consonance with the applicable European and German laws, following the Animal Welfare Act and the European legislative Directive 86/609/EEC were approved by the Animal Welfare Committee of the Charité, Berlin. The number of sacrificed animals and their stress and discomfort were kept to a minimum.

Quantitative real-time PCR

Postnatal Lin41 mRNA expression was determined by qRT-PCR on independent samples (n = 2 per time point). RNA was isolated from brain tissue at different post-natal time points (P2, P4, P7, P10, P14, P17, P21, P28 and adult) using TRIZOL reagent (Ambion, #15596026) in accordance with manufacturer's instructions. Total RNA concentration was determined using the photometer (NanoDrop) and 15.5 µl of total RNA for each sample was subjected to DNase treatment using RQ1 RNase-free DNase (Promega #M6101) for 30 min at 37 °C. cDNA was synthesized using random hexamer primers and the RevertAid Premium Reverse Transcriptase (Thermo Scientific) kit. Subsequently, cDNA was used for qPCR with the RT2 SYBR® Green qPCR Mastermix (QIAGEN) in a 1:3 dilution performed on a StepOnePLus Real-Time PCR system (Applied Biosystems). The housekeeping gene Oaz1 was used for normalization of loaded cDNA.

Western Blotting

To assess postnatal LIN41 protein expression using western blot, brains from WT NMRI or C57BL/6 offspring from the Lin41+/-;Emx1-Cre+/- x Lin41lox/lox;Emx1-Cre-/- mice were collected via cervical dislocation and each hemisphere was snap frozen in liquid nitrogen. Subsequently, tissue was lysed for protein extraction using 50mM Tris; pH 7,4, 150 mM NaCl, 0,5% NP-40 and 5 mM EDTA as lysis buffer. Total protein concentration was determined using a Bradford assay with bovin albumin serum as calibration standard (0 - 2,0 µg/µl) at 595 nm wavelength in the photometer (Nanodrop). To separate proteins by means of their molecular weight samples were run on an SDS-PAGE gel (10%) followed by wet transfer to a nitrocellulose membrane. After blocking (5% skimmed milk powder in PBST), membranes were exposed to primary antibodies against LIN41 (OriGene) and GADPH (Millipore). After washing, membranes were incubated with the appropriate secondary antibodies conjugated to horseradish peroxidase (1:1000) for 1 hour at room temperature. All membranes were developed using ECL substrate Bio-Rad Clarity and the imaging system ImageQuant LAS (GE Healthcare) to visualize labelled bands. After development, all blots were stained using the Coomassie staining protocol to assess protein loading.

Tissue preparation

P27 mice were administered a lethal dose of pentobarbital solution via intra-peritoneal injection. Animals were then subjected to intracardiac perfusion with PBS, followed by approximately 15 ml of 4% PFA to fix brain tissue. For immunohistochemistry and in situ hybridization purposes, brains were post-fixed in 4% PFA overnight at 4 °C and treated for cryo-protection in increasing sucrose solutions (10-20%). Subsequently, tissue was embedded in gelatine and frozen using dry ice. Tissue blocks were stored at -30 °C until they were cryo-sectioned on a Leica cryostat (Leica Biosystems) at -20 °C in approximately 12 µm thick slides. For vibratome analysis, following perfusion brains were post fixed in 4% PFA overnight. Subsequently, each brain was embedded in 5% agarose blocks (in PBS) and cut in 200 µm-thick serial coronal vibratome sections.

Immunohistochemistry

Tissue was washed in PBS to remove excessive gelatine and where then incubated in blocking and permeabilization buffer (3% BSA, 0,25 % Triton-x, 0,3M Glycine in PBS) for 1 hour at R/T. Sections were then incubated in a humid, Parafilm covered chamber with primary antibodies diluted in blocking buffer O/N at 4 °C. Primary antibodies were the as follows: mouse anti-FoxJ1 (eBiosci-

ence), rat anti-CD133 (eBioscience), rabbit anti-LIN41 (OriGene) rat anti-L1CAM
(Millipore), rabbit anti-PAX6 (R&D Systems) and chicken anti-TBR2 (Chemicon). The following day they were washed three times with 1x PBS and then incubated with appropriate secondary antibodies (1:500) in blocking buffer for 3 hours at R/T in a dark chamber. Subsequently, the sections were incubated with DAPI in 1x PBS for 1 hour at R/T to counterstain for cell nuclei. Following three more washing steps in 1x PBS the sections were mounted on a slide with fluoro-protective mounting medium DABCO (Sigma, 10,981) and a coverslip.

mRNA in situ hybridization

In situ hybridization was performed with a modified protocol that has been described previously by Silahtaroglu et al. (2007) using the Tyramide Signal Amplification (TSA) system as method of probe detection. Briefly, after tissue preparation tissue slices were post-fixed in 4% PFA for 10 minutes and acetylated using acetylation buffer (0.6 % acetic anhydride, 0.35 % 6N HCl, 1.35 % triethanolamine in RNase free H2O). To pre-hybridize, tissue sections were incubated in hybridization buffer (50% formamide, 5x SSC, 0.1 mg/ml yeast tRNA, 0,5 mg/ml salmon sperm (Sigma), 0,1mg/ml heparin, 0,1 Tween, 10% dextran sulphate, 5x Denhardts solution) at hybridization temperature (53-55 °C) for at least 1 hour. Hybridization was carried out overnight with probes diluted in the hybridization solution. The next day, slides were washed in 1x SSC at 6-8 °C above hybridization temperature for 30 minutes and in 5x SSC at RT
for 10 minutes. To quench endogenous peroxidases, slides were incubated in a 3% H2O2 solution (in 1xPBS) for 10 minutes. Subsequently, slides were blocked with blocking solution (3% BSA in TBST) for at least 1 hour. This was followed by overnight incubation of anti-DIG antibody (Roche) in blocking solution (1:400) at 4 °C in a humid chamber covered with Parafilm. Sections were developed using the TSA-plus Cyanine 3 Kit (PerkinElmer) as described in the manufacturer's instructions, counterstained with DAPI and mounted with DABCO mounting medium (Sigma, 10,981). For the experiments on HEK cell cultures the same protocol was applied to ascertain comparable results.

Whole-Mount dissection and staining

After cervical dislocation, brains were extracted fresh in cold PBS. Whole mounts of the lateral ventricle were obtained as reported by Mirzadeh and colleagues (2010). In short, brains were sectioned in two halves to separate the hemispheres. Subsequently, the lateral ventricle was dissected from the caudal aspect of the telencephalon, and the hippocampus and septum were removed. The dissected lateral wall was fixed in 4% PFA overnight at 4 °C. Thereafter, the ventricular walls were further dissected from underlying parenchyma as slices of 200 to 300 µm thick tissue. Primary antibodies were incubated overnight at 4 °C. Primary antibodies were the following: mouse anti-ß-catenin (1:100, BD Biosciences), chicken anti-GFAP (1:1000, SYSY) and rabbit anti-ϑ-tubulin (1:1000, Sigma). Appropriate secondary antibodies conjugated to Alexa 488, Cy3 or Cy5 were used for visualization (all diluted 1:500) and incubated for 3 hours at room temperature. Following staining, tissue was mounted on a slide with fluoro-protective mounting medium DABCO and a coverslip.

Imaging and image analysis

Images were captured using a Leica SP8 confocal microscope. Comparable image parameters were maintained to obtain images from all brains in each experiment. Z-stacks were taken individually for each channel and then collapsed to get maximum intensity projections. Images were analysed using ImageJ (Wayne Rasband, National Institutes of Health, USA). Coronal vibratome sections were imaged using a Leica MZ16FA stereomicroscope.

Statistical analysis

All values were expressed as mean±SEM. Student's t-tests and one-way ANOVA followed by the Tukey's post hoc multiple comparison tests were used for statistical analysis. P-values less than 0.05 were considered statistically significant. Statistical analysis was performed using GraphPad Prism version 5.02 for Windows (GraphPad Software, Inc.).

RESULTS

Analysis of temporal Lin41 expression pattern in the postnatal murine CNS

Previous observations on Lin41 expression pattern show an onset of promotor activity in the ventricular walls of the postnatal CNS from as early as P7 that is maintained throughout adulthood. Additionally, immunostaining of adult WT brain showed protein expression of LIN41 in the apical layer of ependymal cells surrounding the lateral ventricles (Cuevas et al., 2015). To address in more detail the temporal expression of Lin41, qPCR analysis on extracts of brain tissue from NMRI WT mice was performed on different postnatal time points from P2 to adult. In NMRI WT mice, Lin41 mRNA expression

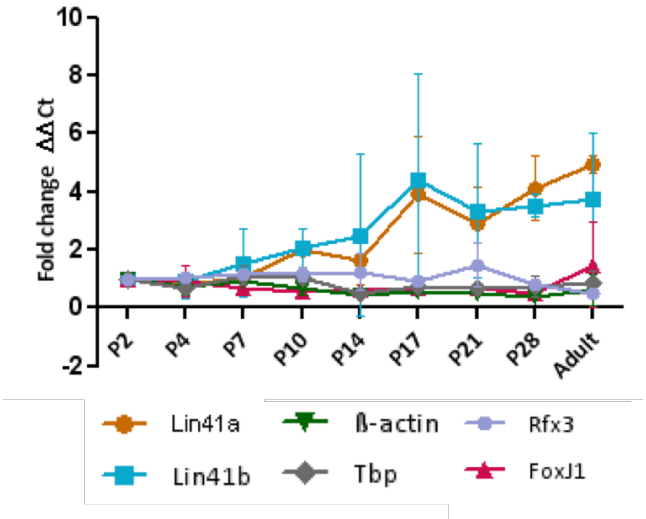

Fig. 3.1 Lin41 mRNA expression in the postnatal murine brain. Lin41 mRNA was analysed by qRT-PCR with two primer pairs Lin41a and Lin41b using Oaz1 as a standard. Expression is plotted relative to P2 set as one. Results from both primer pairs reveal increased Lin41 mRNA expression from P7 compared to P2 with continued expression up to adulthood. Lin41 mRNA expression reaches a plateau from P17 with approximately a 5-fold change compared to P2.

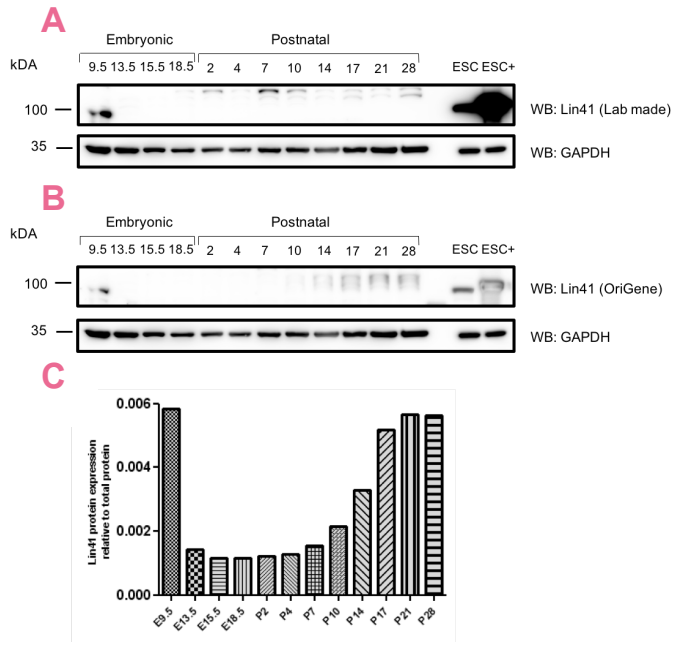

Fig. 3.2 A time course of developing embryo and brain lysates from NMRI WT mice from E9.5 to P28 to investigate the temporal expression pattern of LIN4 protein. Western blot analysis was performed using the following antibodies against LIN41: anti-LIN41 (lab-made) in the upper blot **A** and anti-LIN41 (OriGene) in the lower blot **B**. In each blot, the bottom panel shows the result with anti-GAPDH antibody as a loading control. **A** LIN41 protein was highly expressed in E9.5 (lane 1) and undetectable at later embryonic time points from E13.5 to E18.5 (lane 2 – 4). ESC lysates either under normal conditions (lane 14) or overexpressing LIN41 (lane 15) were used as positive controls. No LIN41 protein was detected in any postnatal extracts (lane 5 – 12). **B** LIN41 protein was detected in E9.5 (lane 1) and undetectable at later embryonic stages from E13.5 to E18.5 (lane 2 – 4). ESC lysated either under normal conditions (lane 14) or overexpressing LIN41 (lane 15) were used as positive controls. Postnatal extracts reveal a protein band that runs slightly higher than the expected 93 kDA from P10 to P28 (lane 8 – 12). **C** Protein expression was quantified using the total protein loading as determined via Coomassie staining as reference. Assuming the higher band is LIN41 specific (for further information see Results), quantification of the LIN41 (OriGene) blot shows LIN41 protein expression in E9.5 and increased protein expression from P10 to P28.

was increased from P7 compared to P2 and showed continued expression that was maintained up to adulthood (Figure 3.1).

Immunostaining was performed on P7 and P27 Lin41 cKO mice and littermate controls to assess postnatal LIN41 protein expression and the effect of Emx1-Cre driven Lin41 knock out on expression levels in the ependymal cells of the lateral ventricle. However, problems with specificity of the anti-LIN41 antibodies led me to examine other methods of postnatal LIN41 protein detection (Supplementary Figure 3.1).

As an alternative, temporal LIN41 protein expression was assessed via western blot analysis of protein lysates from brain tissue of NMRI WT mice covering a time course from E9.5 to adulthood. For this purpose, several anti-LIN41 antibodies available in the laboratory were tested for their effectiveness in recognizing LIN41 in the lysed tissue samples. The rabbit anti- LIN41 antibody developed by our laboratory – further referred to as anti-LIN41 (lab made) – has previously found to recognize LIN41 in embryonic tissue and embryonic stem cells cultures. In accordance with these previous observations, anti-LIN41 (lab made) recognized LIN41 at E9.5 and ESCs either under normal conditions (ESC) or with induced LIN41 overexpression (ESC+). However, the antibody did not show a specific band corresponding to LIN41 in postnatal brain lysates (Figure 3.2A). Additionally, the commercial rabbit anti-LIN41 (OriGene) antibody revealed a LIN41 protein band in embryonic tissue at E9.5 and in both ESCs cell cultures, and showed multiple slightly higher bands in postnatal tissue lysates (Figure 3.2B). Due to the consistency of this pattern in multiple experiments it was hypothesized that these bands could be LIN41 specific, indicating the potential presence of a different isoform or post-translational modifications of LIN41 in the postnatal brain.

To further investigate whether the observed band in postnatal extracts of the western blot analysis using anti-LIN41 (OriGene) could be LIN41 specific or was a cross-reaction to another protein, additional western blot analysis was performed on the four genotypes generated from the Lin41+/-;Emx1-Cre+/- x Lin41lox/lox-;Emx1-Cre+/- breeding. As in the time course experiment, LIN41 protein expression was high in E9,5 and in both ESC lysates. All four genotypes revealed a protein band that ran slightly higher compared to the positive controls (Figure 3.3A). Emx1- Cre driven Lin41 knock out did not lead to complete absence of this protein band. Assuming this protein band is LIN41 specific, this observation is in line with the notion Emx1-Cre driven knock out does not lead to complete depletion of LIN41 in the adult brain. As Emx1 is only expressed by dorsal telencephalic radial glial cells, not all Lin41 expressing ependymal cells are Emx1 positive. The remaining LIN41 expression might be a result of Lin41 positive ependymal cells in the wall of ventricles not targeted by the Emx1-Cre driven knock out (Cecchi & Boncinelli, 2000). Repetition of the experiment revealed high variation of protein expression between animals of the same genotype, indicating that Emx1-Cre driven LIN41 depletion or the introduction of a Lox-P site into the Lin41 gene might be subject to high variation in number

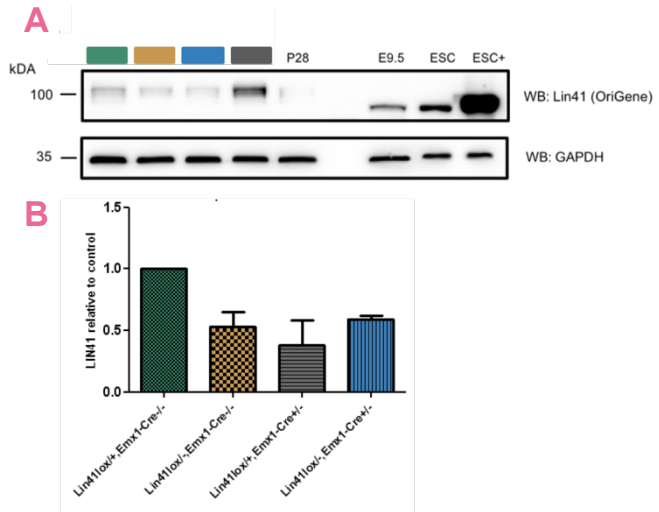

Fig. 3.3 LIN41 protein expression in the Lin41+/-;Emx1-Cre+/- x Lin41lox/lox;Emx1-Cre+/- offspring reveals high variation of a protein expression that likely – but yet to be validated – corresponds to LIN41. Western blot analysis was performed using the anti-LIN41 (OriGene) antibody. The bottom panel shows the result with anti-GAPDH antibody as a loading control. **A** LIN41 protein was expressed in E9,5 (lane 7) and in both ESC extracts either under normal conditions (lane 8) or overexpressing LIN41 (lane 9), which served as positive controls. **A** High variation of protein expression was observed between Lin41lox+-;Emx1-Cre-/- (green), Lin41lox/-;Emx1-Cre-/- (yellow), Lin41lox/+;Emx1-Cre+/- (grey) and Lin41lox/- ;Emx1-Cre+/- (blue) of a band that ran slightly higher than the expected 93 kDA. Emx1-Cre driven LIN41 depletion did not result in complete loss of this protein band. **B** Protein expression was quantified using the total protein loading as determined via Coomassie staining as reference. Assuming the higher band is LIN41 specific (for further information see Results), quantification shows LIN41 expression in Lin41 cKO (blue), Lin41lox/+;Emx1-Cre+/- (grey) and Lin41lox/-;Emx1-Cre-/- (yellow) is reduced compared to the Lin41lox+-;Emx1-Cre-/- (green) control.

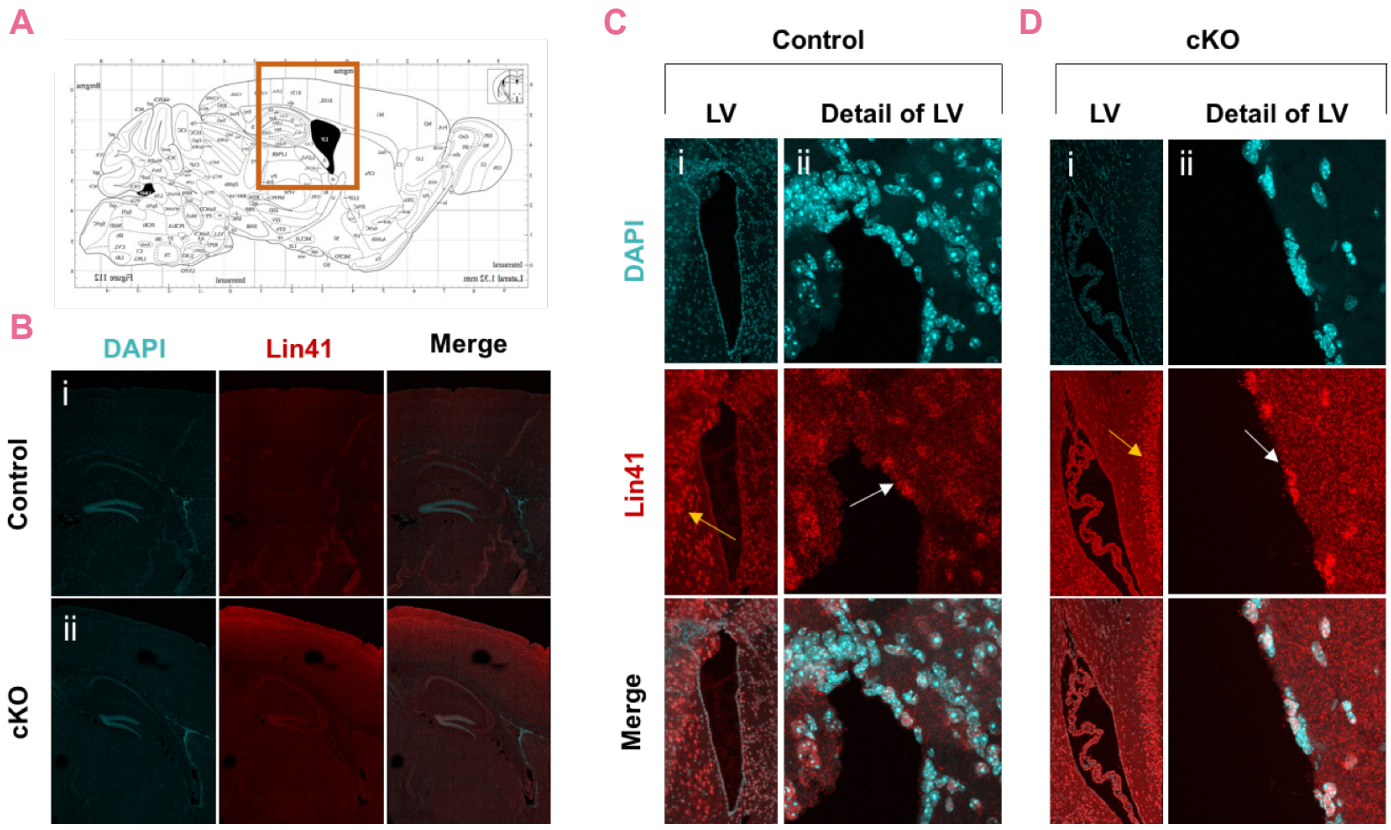

Fig. 3.4 In situ hybridization using TSA shows high background and low to undetectable specific binding. Brains from P27 control and Lin41 cKO mice were hybridized to an LNA probe specific for Lin41, which was visualized by TSA. **A** Sagittal sections are shown with anterior to the left. Overview pictures of the lateral ventricle, hippocampus and cortex were taken covering a selected area as depicted by the red box. **B** Fluorescent signal (red) was detected across the whole section in control **i** and Lin41 cKO **ii** conditions with strongest signal detectable in the cortex. **C-D** Higher magnification images of the lateral ventricle showed low to undetectable specific binding of the Lin41 probe to ependymal cells lining the ventricular wall (Control **i** and **ii**). Signal that could be considered specific (**white arrows**) was observed in both control and Lin41 cKO tissue. However, the high unspecific signal observed in the surrounding tissue (**yellow arrows**) complicated the interpretation of the results.

of affected cells or brain areas (Figure 3.3B). The observation that this particular higher protein band shows high variation between the four genotypes strengthens our hypothesis that it might be LIN41 specific. However, other explanations, such as a cross-reaction of the antibody to a different protein, are possible. To further investigate whether the observed protein band is corresponding to LIN41 our group is currently performing immunoprecipitation essays.

Analysis of spatial Lin41 expression pattern in the postnatal murine CNS

The current results confirm the previous findings by Cuevas and colleagues (2015) and provide additional details regarding the temporal expression of Lin41 in the postnatal murine CNS. To further characterize spatial Lin41 expression in the postnatal brain in both control and Lin41 cKO conditions, the distribution of Lin41 mRNA expression was assessed using in situ hybridization (ISH). For this purpose, a high sensitive commercial Lin41 LNA probe was used in an immunofluorescence ISH essay on sagittal sections of P27 control and Lin41 cKO brains. Following the protocol as described by Silahtaroglu et al. (2007) signal detection was first revealed by AP-Fast Red chromogenic reaction. However, the low sensitivity and dotted signal of the Fast Red dye did not provide satisfactory results. High background signal and evenly distributed red precipitate covering all sections complicated assessment of specific binding (Supplementary Figure 3.2). Signal detection in subsequent experiments was conducted using the tyramide signal amplification (TSA) reaction. This method of detection provides enzymatic fluorescent signal amplification that is known to be ideal for low-abundance RNA targets such as Lin41. ISH with TSA helped to overcome the problem of red precipitate (Supplementary Figure 3.2). However, sections showed high background and low to undetectable specific signal (Figure 3.4).

As an attempt to reduce unspecific background and to increase specific signal changes were made considering hybridization temperature and efficiency of the washing steps. Furthermore, probe concentrations were adjusted to half of the original (from 5.0 pmoles to 2.5 pmoles). However, the decrease in probe concentration did not lower non-specificity of the staining and did not increase the specific signal in the ependymal cells lining the ventricular wall (Figure 3.5).

Because changing the experimental parameters did not lead to any improvement in the outcome of the experiment, as a next step I decided to investigate the efficacy of the used protocol – originally described for microRNAs – and to validate the specificity of the Lin41 probe. Therefore, a HEK cell transfection essay was performed in which HEK cells were transfected with either Lin41 or Arpp21. As previous findings in our lab have shown that the LNA probe specific for Arpp21 results in specific signal in the current ex-

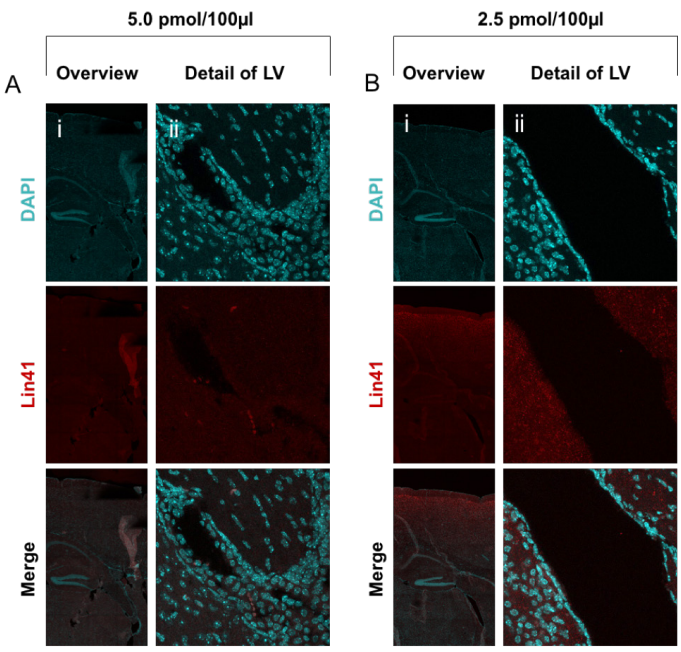

Fig. 3.5 In situ hybridization with different experimental parameters to increase signal to noise ratio. Images of the Lin41 probe in P27 control mice using different concentrations **A** 5.0 pmol/100 µl and **B** 2.5 pmol/100 µl. **i** overview image of the selected area as described in Figure 3.4A. As observed previously, unspecific fluorescent signal (red) was detected in the whole section, best noticeable in the cortex. **ii** Detail of the lateral ventricle. The decrease in probe concentration from 5.0 pmol/100µl **A** to 2.5 pmol/100µ **B** did not lower non- specificity of the signal and did not increase the specific signal in the ependymal cells lining the ventricular wall.

perimental set-up, Arpp21 functioned as a positive control. In the Arpp21 overexpressing HEK cells, all cells that showed a positive signal for the Arpp21 probe were transfected – thus overexpressing Arpp21. Therefore, ISH using the Arpp21 probe resulted in specific binding, validating the efficacy of the used protocol for LNA probes under the current experimental conditions. However, it should be noted that hybridization efficiency was low – since only ±10% of all transfected cells were hybridized – and the experimental conditions could thus be optimized. As in the Arpp21 condition, Lin41 overexpressing HEK cells showed low hybridization efficiencies. However, Lin41 overexpressing HEK cells showed an irregular hybridization pattern. Firstly, unspecific background staining was higher as compared to the Arpp21 condition (Figure 3.6). Second, a subset of cells that showed a positive signal for Lin41 probe hybridization were found to be not transfected. This false positive result lead to the conclusion that – in this experimental set-up – the Lin41 probe might not be working properly (Figure 3.6 white arrows). Therefore, the probe will next be sequenced to validate the binding potential of the probe to Lin41 mRNA. Additionally, alternative detection methods such as the highly sensitive chromogenic substrates nitro blue tetrazolium (NBT) and 5-bromo-4-chloro-3-indolyl phosphate (BCIP) will be investigated.

Lin41 cKO does not affect corticogenesis

Late-embryonic Lin41 is mainly restricted to the neuroepithelium, indicating a potential role in proliferation, specification or patterning of cortical progenitors. To assess whether lack of Lin41 disrupts cortical development – leading to defects in cortical morphology postnatally – morphological parameters were measured in coronal sections of all Lin41+/-;Emx1-Cre+/- x Lin41lox/lox;Emx1-Cre+/- offspring (N = 28). Measurements included total brain area and thickness of the cortex and corpus callosum. Each measurement was performed at specific stereotaxic coordinates which were selected by the use of 'The mouse brain atlas' (Franklin and Paxinos, 2007). For a detailed description of selected areas and method of measurements see Supplementary Figure 3.3. There were no differences in total brain area between Lin41lox/-;Emx1-Cre+/-, and control conditions. Also, no differences were found between the Lin41lox/+;Emx1-Cre+/- and Lin41lox/- ;Emx1-Cre-/- conditions – possessing only one functional Lin41 allele – and Lin41lox/+;Emx1-Cre- /- animals (Figure 3.7). Additionally, cortical thickness was assessed on three different coronal sections covering the primary somatosensory cortex (S1), the barrel cortex (BC) and the auditory cortex (AuD) (Supplementary Figure 3.3). From each individual animal, cortical thickness at each area was assessed in both the left and right hemisphere. Similar to total brain area, there were no significant differences found between any of the experimental conditions (Figure 3.7). Furthermore, a slight

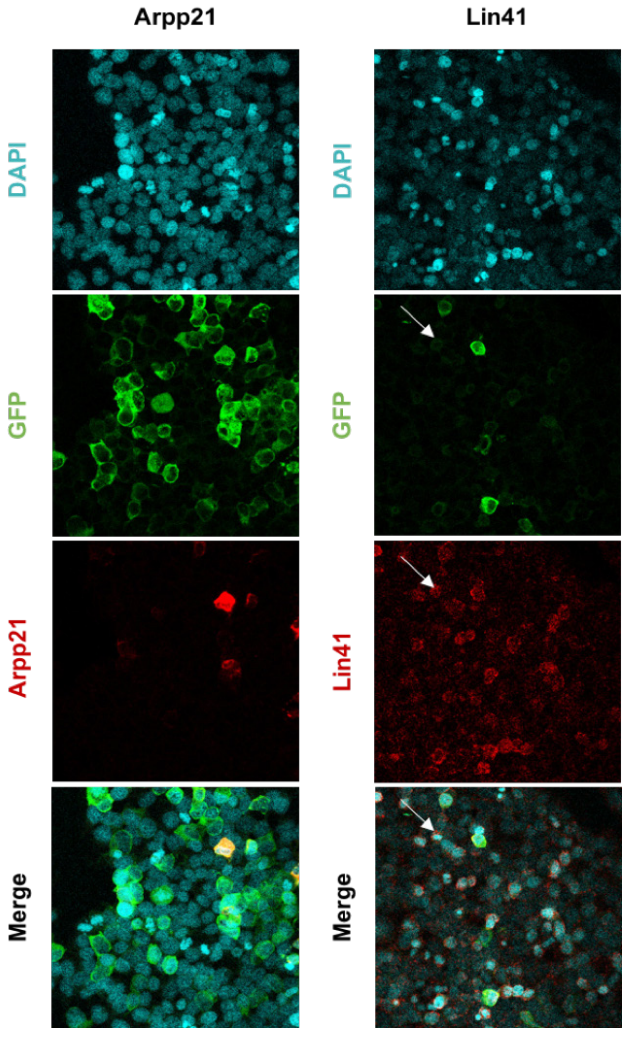

Fig. 3.6 HEK cell transfection essay to test specificity of the Lin41 probe. HEK cells overexpressing either Arpp21 or Lin41 are hybridized with the corresponding probe specific for Arpp21 and Lin41 respectively. Transfected cells are GFP positive, cells that are not transfected within the same sample serve as the negative control. Despite suboptimal hybridization efficiency of the Arpp21 probe (<10 %), Arpp21 signal was restricted to GFP+ cells overexpressing Arpp21. However, HEK cells overexpressing Lin41 showed signal in cells that were not transfected- (**white arrows**) indicating unspecific hybridization of the Lin41 probe. This false positive result led to the conclusion that – in contrast to the Arpp21 probe – the Lin41 probe does not function properly in this experimental design.

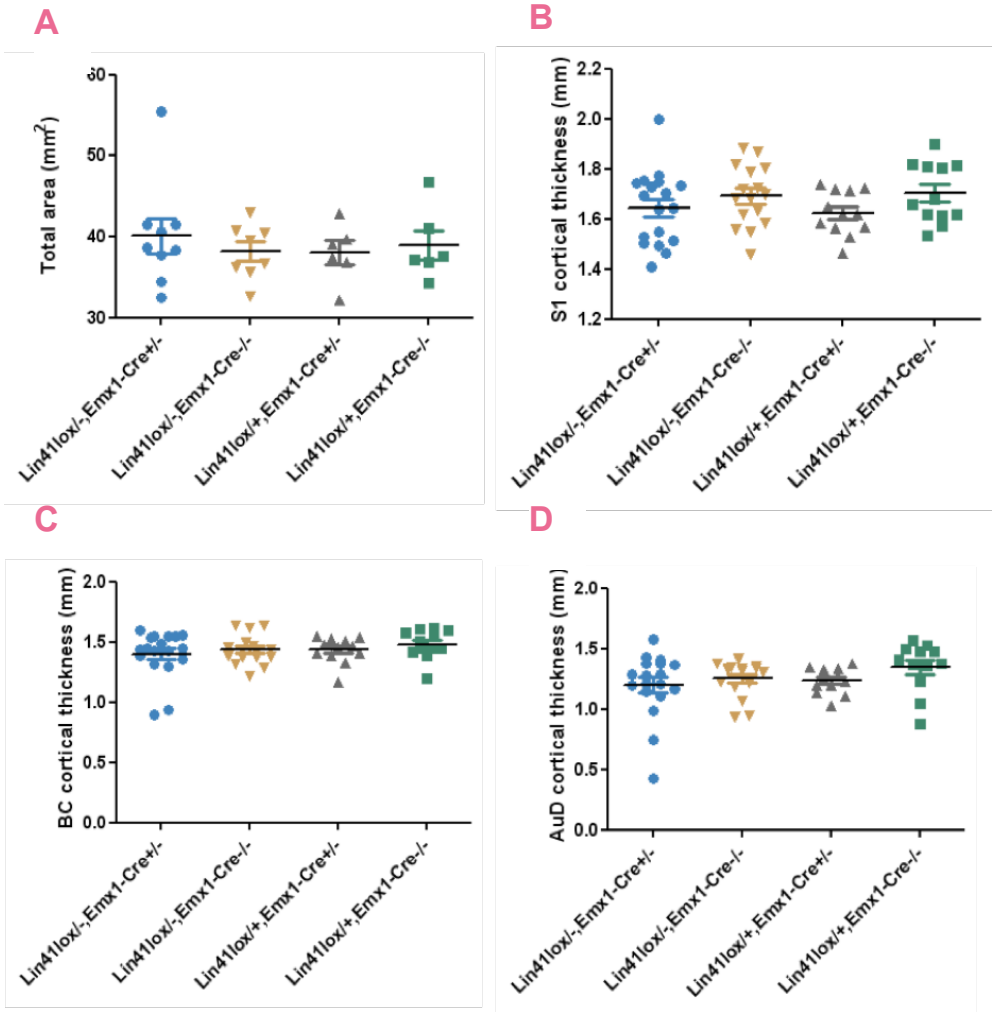

Fig. 3.7 Morphometric analysis of total brain area and cortical thickness. Analysis was performed on Lin41lox/-;Emx1-Cre+/- (N = 9), Lin41lox/-;Emx1-Cre-/- (N = 8), Lin41lox/+;Emx1-Cre+/- (N = 6) and Lin41lox/-;Emx1-Cre-/- (N = 6). **A** Analysis of Variance revealed that no differences were found between groups for total brain area ($F(3, 54)=0{,}315$, $P = 0.814$). Additionally, no differences were found in cortical thickness in **B** S1 ($F(3, 54)= 1{,}218$, $P = 0.312$), **C** BC ($F(3, 54)=0{,}771$, $P = 0.515$) and **D** AuD ($F(3, 54)= 1{,}425$, $P = 0.246$).

reduction in corpus callosum thickness was observed in immunostainings using the L1CAM antibody (Supplementary Figure 3.4). To further assess corpus callosum morphology thickness of the corpus callosum was measured at both at the intersection between the two hemispheres and laterally. Again, no significant differences were observed between any of the four conditions (Supplementary Figure 3.5). These results indicate that deletion of Lin41 from E10.5 in Emx1 positive cells does not affect embryonic corticogenesis to an extent at which it causes major morphological deficits postnatally. Interestingly, Lin41lox/- ;Emx1-Cre+/- did show significant reduction of body weight compared to the control condition (Supplementary Figure 3.5G).

Lin41 cKO exhibits a low-penetrance hydrocephalus phenotype

In healthy conditions, ependymal cilia regulate the flow of CSF through the ventricles. If Lin41 is essential for the proper function of ependymal cells, it could be expected that lack of Lin41 would lead to dysregulation of CSF flow resulting in a hydrocephalus-like phenotype. To assess the potential presence of a hydrocephalus-like phenotype as a consequence of any defects in ependymal cell function, I next assessed size of the lateral ventricle. Analysis of ventricular size showed a non-significant trend towards differences between groups ($F(3,54)=2.242$, $P=0.076$) (Figure 3.8). One animal within the Lin41 cKO condition showed severe hydrocephalus exhibiting ventricles up to approximately 42 times bigger compared to the group average (Figure 3.8, upper two outliers).

Considering the presence of the hydrocephalic phenotype in the Lin41lox/- ;Emx1-Cre+/- group – also observed in two other animals of this condition that were used for other purposes – and the absence of any other major morphological deficits that could be caused by developmental defects further research focused on the investigation of the role of postnatal Lin41 expression in ependymal cells and their immediate environment – the adult neurogenic niche of the VZ-SVZ – at the cellular level.

Lin41 and the adult VZ/SVZ progenitor population

Defects in adult neurogenesis as a result of Emx1-Cre driven Lin41 knock out might lead to a disruption in neural progenitor cell population in the neurogenic niche of the VZ-SVZ. Immunostaining with a group of specific antibodies was used to map the different cellular identities of the cell population residing in the VZ-SVZ. For this experiment, Pax6 was used as a marker for early progenitor cells in the VZ and Tbr2 as a marker for intermediate progenitors of the SVZ. Coronal brain sections from Lin41 cKO and control littermates at P7 (N = 2) and P27 (N = 3) were stained to visualize early progenitor and intermediate progenitor cell populations. Tbr2 and Pax6 are known to be mainly expressed in the dorsal region

of the lateral ventricle (Bril et al., 2009). Here, I observed Tbr2 and Pax6 expression to be mainly restricted to the dorsal and medial part of the lateral ventricle (Supplementary Figure 3.6; Figure 3.9). Comparing expression patterns between P7 and P27 control tissue revealed no differences in Pax6 expression (Figure 3.9). This is in line with the notion that Pax6 is known to be expressed from the earliest postnatal stages up to adulthood (Roybon et al., 2009, Saha 2012). Moreover, Tbr2 positive cells were found at both postnatal time points, with higher expression at P7 as compared to P27 in both Lin41 cKO and control mice (Figure 3.9). Although the functional role of Tbr2 in the postnatal and adult brain is still unknown, it is found not to be required for establishment of SVZ progenitor cells (Arnold et al., 2008). Tbr2 is expressed by a subpopulation of glutamatergic progenitors. Glutamatergic OB neurogenesis mainly occurs in early postnatal stages and adult neurogenesis is found to be mainly GABAergic (Bril et al., 2009, Hsieh 2012). Based on these notions, the observed reduction in Tbr2 expression at later postnatal stages might be a result of a decrease in glutamatergic neurogenesis. Additionally, quantification of Tbr+ and Pax6+ cells in both postnatal stages revealed no differences in expression between Lin41 cKO and control mice (Supplementary Figure 3.6). These results indicate that lack of Lin41 in the ependymal cells in the postnatal brain does not induce disruptions in the postnatal progenitor population of the VZ-SVZ.

Lin41 is not essential for the organization of the neurogenic niche

In the normal postnatal brain, ependymal cells are known to form an important component of the cellular arrangement of the neurogenic niche, in which they are organized in a pinwheel- structure surrounding a single GFAP+ NSC. This structure is believed to be fundamental for the process of adult neurogenesis. To study the potential role of Lin41 in the organization of ependymal cells into pinwheel structures a comparative study of whole mount preparations of the lateral ventricle wall was performed in control and Lin41 cKO mice using confocal imaging. Pinwheel organization was assessed in the posterior dorsal and ventral anterior regions of the lateral wall, which are known to be specifically rich in these structures (Mirzadeh et al., 2008). Visualization of the pinwheel organization in these regions was established using antibodies against ß-catenin, ϐ-tubulin and GFAP to stain for cell membranes, basal bodies of cilia and NSCs respectively. Emx1-Cre driven Lin41 knock out did not affect the organization of ependymal cells into pinwheel structures (Figure 3.10). Three independent experiments showed that pinwheels with centrally located NSCs apical endings surrounded by ependymal cells could be identified in both conditions in the anterior ventral as well as posterior dorsal wall of the lateral ventricle. Thus, Lin41 is not essential for the organization of ependymal cells into pinwheel structures in the lateral ventricular wall.

DISCUSSION

The recent discovery of the presence of Lin41 in ependymal cells lining the wall of the ventricles of the adult brain has raised some intriguing questions concerning the functional consequences of Lin41 expression in this time and space. In the present study, I further investigated the temporal and spatial expression pattern of postnatal Lin41, and examined the possible role of Lin41 in corticogenesis, adult neurogenesis and ependymal cell specification.

Using NMRI WT mice, I obtained similar results to those of Cuevas et al. (2015) observing that Lin41 in the postnatal brain is increased from P7 and shows continued expression up to adult stages. Despite the fact that our qPCR data reinforced the evidence of the presence of Lin41 mRNA in the postnatal brain, the encountered issues with the western blot antibodies, the in situ hybridization procedure and the immunostainings have complicated our assessment of the expression pattern of Lin41 in the postnatal CNS in WT conditions. Considering our western blot data, the potential presence of a different LIN41 isoform or post-translational modifications in postnatal tissue could be a possible explanation for the failure of the antibodies and the inability of the Lin41 probes to bind to Lin41 mRNA. However, alternative explanations should be considered. For example, the observed band in postnatal brain lysates on the western blots might be a result of cross-reactivity to a different protein. Alternatively, as research antibodies are often screened and optimized for narrow conditions, the used antibodies might simply not have worked correctly in the current experimental context (Baker, 2015).

Using the Emx1-Cre driven Lin41 cKO mouse model, I performed morphological analysis, immunohistochemistry and whole mount preparation of the lateral ventricle to assess the possible role of Lin41 in corticogenesis, adult neurogenesis and ependymal cell specification and function. The obtained results showed that Emx1-Cre driven Lin41 knock out does not result in any major cortical defects. Additionally, no effect of Lin41 knock out on the progenitor cell population or the organization of the neurogenic niche was ob-

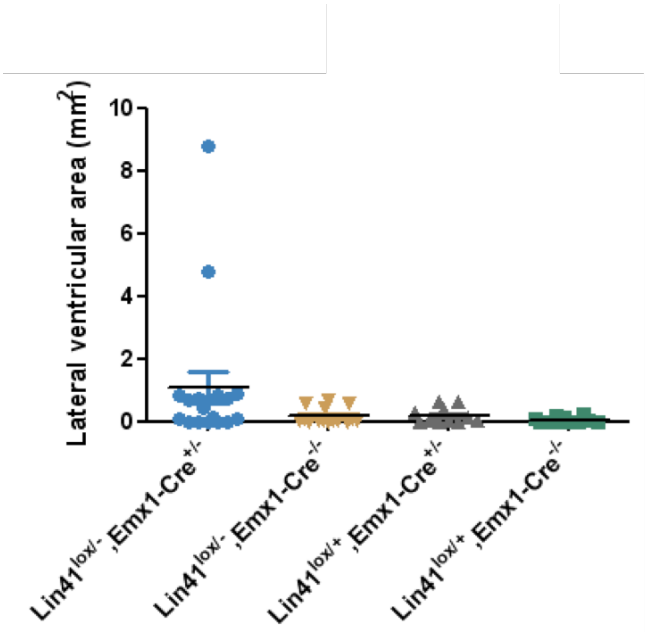

Fig. 3.8 Analysis of hydrocephalus in Lin41 cKO mice using coronal vibratome sections. Morphometric analysis of ventricular size for Lin41lox/-;Emx1-Cre+/- (N = 9), Lin-41lox/-;Emx1- Cre-/- (N= 8), Lin41lox/+;Emx1-Cre+/- (N = 6) and Lin41lox/-;Emx1-Cre-/- (N = 6). No differences were found between groups for lateral ventricular size ($F(3, 54)=2,242$, $P = 0.076$). In the Lin41lox/-;Emx1-Cre+/- group one animal exhibited severe hydrocephalus expressed by an approximately 42 times bigger ventricle as compared to the group average (two upper outlying data points).

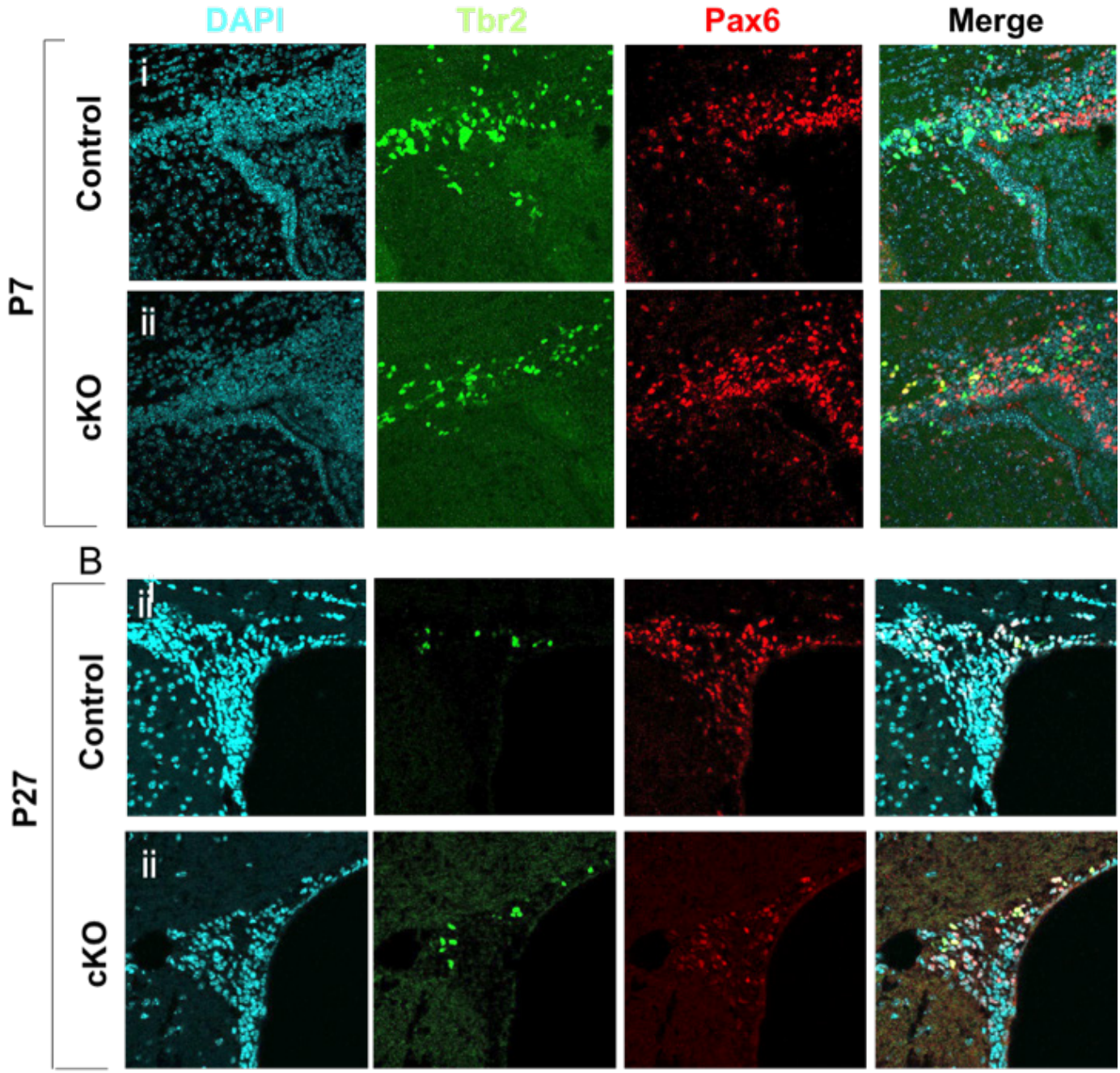

Fig. 3.9 Analysis the effect of Lin41 knock out on the progenitor VZ-SVZ population in the postnatal brain. P7 and P27 coronal brain sections were stained with antibodies against Pax6 and Tbr2 to investigate the postnatal progenitor population (N=2 and N=3 respectively). Compared to the later postnatal time point (P27), P7 brains appeared to show higher expression of Tbr2, but a similar expression of Pax6 was observed in P7 and P27 brains. At both P7 and P27, no differences in Tbr2 and Pax6 expression were observed between control and Lin41 cKO conditions.

served in any of the experiments. Nor were there any deficits observed in ependymal cell specification, with unaffected pinwheel organization of the neurogenic niche in Lin41 knock out conditions. A detailed investigation of ependymal cell function such as the beating capacity, length, density and directionality of their motile cilia and a quantitative analysis of planar cell polarity (both rotational and translational) was beyond the scope of this project. Therefore, the current data do not exclude the possibility of any deficits on these levels. Given the observed low-penetrance hydrocephalus phenotype and the remarkable temporal and spatial overlap between Lin41 expression and ependymal cell differentiation, the potential role of Lin41 in ependymal function certainly requires additional investigation. This is therefore currently a mayor focus within our research group.

The current study results lead to the conclusion that – despite it's known function as a key regulator of neurogenesis during embryonic development – late-embryonic Lin41 and postnatal Lin41 expression in the ependymal cells of the murine CNS is not essential in the process of corticogenesis, ependymal cell specification or adult neurogenesis under normal conditions. This notion raises new questions regarding possible other functions of this ancient regulator in the postnatal CNS. The recent research developments into the molecular functions of Lin41, and its role in embryonic development and IPSC reprogramming all indicate a specific role for Lin41 in keeping cells in a stem cell like state by inhibition of apoptosis and differentiation and by promoting proliferation (Cuevas et al., 2015; Thi et al., 2017; Worringer et al., 2013). Why would a protein that is so strongly related to stemness be expressed in cells that are considered to be post mitotic and not to contain any neural stem

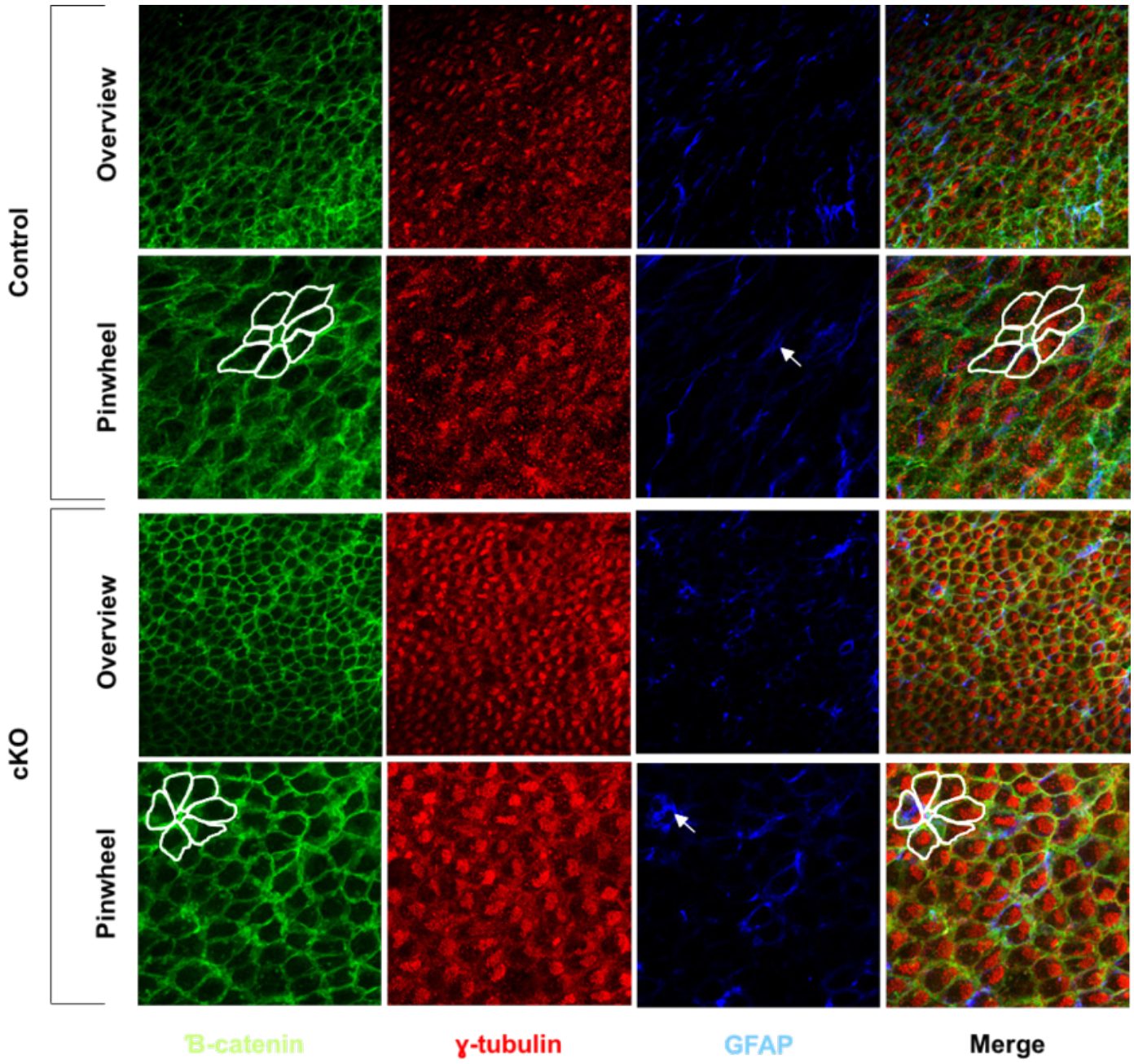

Figure 3.10 Lack of Lin41 does not affect ependymal cell assembly into pinwheels in the neurogenic niche of the SVZ. Whole mount sections of the lateral ventricle wall of Lin41 cKO and control animals were stained with ß-catenin, ɣ-tubulin and GFAP to stain for cell membranes, basal bodies of cilia and NSC respectively. Three independent experiments were performed for each condition. Pinwheel structures – multiciliated ependymal cells surrounding the GFAP+ apical ending of a NSC – were observed in both control and cKO conditions in each individual whole mount (white lines = ependymal pinwheel, white arrow = GFAP+ apical ending of NSC).

cell capacities?

The issue whether ependymal cells are neural stem cells in the adult brain is still highly controversial. Ependymal cells in the SVZ of the adult brain are found to be quiescent and do not contribute to neurogenesis under normal conditions. However, several studies investigating the neural stem cell capacity of ependymal cells after injury – such as stroke or spinal cord injury – showed that under these conditions ependymal cells can contribute to regenerative neurogenesis. For example, a study by Carlen et al (2009) showed that ependymal cells can give rise to neuroblasts and astrocytes in response to stroke. Under these circumstances, the ependymal cell population was depleted and failed to self-renew sufficiently to maintain its population. It was proposed that ependymal cells can serve as a back-up reservoir that can only be recruited in case of insults. Studies into the role of ependymal cells as contributors to regenerative neurogenesis in spinal cord injuries (SCI) have revealed that ependymal cells can generate large numbers of cells of multiple fates such as scar-forming glial cells and oligodendrocytes as a response to injury (Barnabé-Heider et al., 2010; Meletis et al., 2008). These examples illustrate a remarkable activation potential and fate plasticity of ependymal cells. Based on this notion, we could propose an alternative role for ependymal cells as a separate class of cells that are fate-restricted NSCs that under normal conditions are quiescent but can act as neural stem cells after injury. In this case, Lin41 in the ependymal cells of the lateral ventricular wall might play a role in this type of regenerative neurogenesis, and could act to push ependymal cells back into a more undifferentiated state to generate new neurons after brain injury. However, more recent studies

into the neural stem cell capacity of ependymal cells after injury provide contradicting evidence showing that ependymal-derived progeny after SCI remains local, does not migrate and contribute few cells of any kind (Ren et al., 2017; Young et al., 2013). Highly contradicting results as exemplified here illustrate the research controversies concerning the role of ependymal cells in neurogenesis under normal conditions and after injury and their potential stem cell capacity. For this reason, research into ependymal cells over the past years has been – to say the least – somewhat neglected. The weight of the evidence suggests that ependymal cells are post-mitotic, terminally differentiated and do not transdifferentiate even after injury. However, cell fate restriction seems to be less strict than thought and stemness after injury inducible in cells that physiologically never do so.

Another constraint regarding studies into ependymal cells lies in the absence of a biological marker that is exclusively expressed by ependymal cells. Subsequently, difficulties arise with the attempt to create a mouse model in which all ependymal cells of the lateral wall are targeted for the conditional Lin41 knock out. Our current model, in which Cre recombination of the 4th exon of Lin41 is driven by the expression of Emx1, is based on the notion that radial glia cells in the dorsal telencephalic neuroepithelium are Emx-1 positive and thus their progeny – among which are ependymal cells of the lateral ventricle – will be affected by the Cre recombination (Simeone et al., 1992). However, we have currently not validated whether the knock out is successful in all ependymal cells lining the wall of the lateral ventricle. The high standard variation observed in my western blot data might indicate that the current method of Emx1-Cre driven knock out is prone to high variation between individuals. Moreover, the notion that the Emx1 positive lineage gives rise to most cortical neurons and the observation the Emx1-Cre driven Lin41 knock out does not lead to any defects of the cortex or corpus callosum raises further questions concerning the validity of the current approach (Cecchi & Boncinelli, 2000). To test whether the current model knocks out Lin41 in the lateral ventricle in a consistent and effective fashion, our group is currently breeding Lin41lox/WT;Emx1-Cre+/- with a reporter mouse line that expresses tdTomato upon Cre recombination.

Nevertheless, as the current study shows no indication for developmental deficits as a consequence of late-embryonic Lin41 knock out and because we strive to further investigate the potential role of Lin41 in the adult brain, alternative mouse models could be proposed for future research purposes. The most common marker to target ependymal cells is CD133. However, this method is undesirable for our current research goals as CD133 is also expressed by both quiescent and activated NSCs (Llorens-Bobadilla et al., 2015). Additionally, ependymal cells are often identified by the expression of FoxJ1, as this is a key transcription factor regulating the differentiation of radial glia into ependymal cells of the lateral wall and a subset of astrocytes in the adult brain (Jacquet et al., 2009). Our group recently started working with a new mouse model, in which Lin41 knock out can be established upon tamoxifen induced expression of CreERT2 in FoxJ1+ cells. This model will enable us to specifically knock out Lin41 at any postnatal time point in ependymal cells of the lateral ventricle, and provides a more precise method to further study the role of Lin41 in ependymal cell function and its possible role in neurogenesis as a response to brain injury. In conclusion, the presence of Lin41 in ependymal cell of the postnatal brain remains a highly intriguing observation. Future research into this topic will help to further elucidate the role of Lin41 in regulating cellular fate and may provide insight into the importance of ependymal cells in the adult neurogenic niche.

REFERENCES

Alvarez-Buylla, A., & Lim, D. A. (2004). For the Long Run: Maintaining Germinal Niches in the Adult Brain. Neuron, 41(5), 683–686. http://doi.org/10.1016/S0896-6273(04)00111-4

Baker, M. (2015). Reproducibility crisis: Blame it on the antibodies. Nature, 521(7552), 274–276. http://doi.org/10.1038/521274a

Barnabé-Heider, F., Göritz, C., Sabelström, H., Takebayashi, H., Pfrieger, F. W., Meletis, K., & Frisén, J. (2010). Origin of New Glial Cells in Intact and Injured Adult Spinal Cord. Cell Stem Cell, 7(4), 470–482. http://doi.org/10.1016/j.stem.2010.07.014

Cathcart, R. S., & Worthington, W. C. (1964). Ciliary Movement in the Rat Cerebral Ventricles: Clearing Action and Directions of Currents. Journal of Neuropathology and Experimental Neurology, 23(4), 619–634. http://doi.org/10.1097/00005072-196410000-00003

Cecchi, C., & Boncinelli, E. (2000). Emx homeogenes and mouse brain development. Trends in Neurosciences, 23(8), 347–352. http://doi.org/10.1016/S0166-2236(00)01608-8

Chang, H.-M., Martinez, N. J., Thornton, J. E., Hagan, J. P., Nguyen, K. D., & Gregory, R. I. (2012). Trim71 cooperates with microRNAs to repress Cdkn1a expression and promote embryonic stem cell proliferation. Nature Communications, 3(May), 923. http://doi.org/10.1038/ncomms1909

Chen, J., Lai, F., & Niswander, L. (2012). The ubiquitin ligase mLin41 temporally promotes neural progenitor cell maintenance through FGF signaling. Genes and Development, 26(8), 803–815. http://doi.org/10.1101/gad.187641.112

Coskun, V., Wu, H., Blanchi, B., Tsao, S., Kim, K., Zhao, J., ... Sun, Y. E. (2008). CD133+ neural stem cells in the ependyma of mammalian postnatal forebrain. Proceedings of the National Academy of Sciences of the United States of America, 105(3), 1026–1031. http://doi.org/10.1073/pnas.0710000105

Cuevas, E., Rybak-Wolf, A., Rohde, A. M., Nguyen, D. T. T., & Wulczyn, F. G. (2015). Lin41/Trim71 is essential for mouse development and specifically expressed in postnatal ependymal cells of the brain. Frontiers in Cell and Developmental Biology, 3(April), 20. http://doi.org/10.3389/fcell.2015.00020

Doetsch, F., Caillé, I., Lim, D. A., García-Verdugo, J. M., & Alvarez-Buylla, A. (1999). Subventricular Zone Astrocytes Are Neural Stem Cells in the Adult Mammalian Brain. Cell, 97(6), 703–716. http://doi.org/10.1016/S0092-8674(00)80783-7

Ecsedi, M., & Großhans, H. (2013). LIN-41 / TRIM71 : emancipation of a miRNA target LIN-41 / TRIM71 : emancipation of a miRNA target, 581–589. http://doi.org/10.1101/gad.207266.112

Götz, M., & Huttner, W. B. (2005). The cell biology of neurogenesis. Nat Rev Mol Cell Biol, 6(10), 777–788. http://doi.org/10.1038/nrm1739

Guillemot, F. (2005). Cellular and molecular control of neurogenesis in the mammalian telencephalon. Current Opinion in Cell Biology, 17(6), 639–647. http://doi.org/10.1016/j.ceb.2005.09.006

Ibañez-Tallon, I., Pagenstecher, A., Fliegauf, M., Olbrich, H., Kispert, A., Ketelsen, U. P., ... Omran, H. (2004). Dysfunction of axonemal dynein heavy chain Mdnah5 inhibits ependymanl flow and reveals a novel mechanism for hydrocephalus formation. Human Molecular Genetics, 13(18), 2133–2141. http://doi.org/10.1093/hmg/ddh219

Jackson, E. L., & Alvarez-Buylla, A. (2008). Characterization of adult neural stem cells and their relation to brain tumors. Cells Tissues Organs, 188(1–2), 212–224. http://doi.org/10.1159/000114541

Jacquet, B. V., Salinas-Mondragon, R., Liang, H., Therit, B., Buie, J. D., Dykstra, M., ... Ghashghaei, H. T. (2009). FoxJ1-dependent gene expression is required for differentiation of radial glia into ependymal cells and a subset of astrocytes in the postnatal brain. Development (Cambridge, England), 136(23), 4021–31. http://doi.org/10.1242/dev.041129

Johansson, C. B., Svensson, M., Wallstedt, L., Janson, A. M., & Frisén, J. (1999). Neural Stem Cells in the Adult Human Brain. Experimental Cell Research, 253(2), 733–736. http://doi.org/10.1006/excr.1999.4678

Lancman, J. J., Caruccio, N. C., Harfe, B. D., Pasquinelli, A. E., Schageman, J. J., Pertsemlidis, A., & Fallon, J. F. (2005). Analysis of the regulation of lin-41 during chick and mouse limb development. Developmental Dynamics, 234(4), 948–960. http://doi.

org/10.1002/dvdy.20591

Lim, D. A., Tramontin, A. D., Trevejo, J. M., Herrera, D. G., García-Verdugo, J. M., & Alvarez-Buylla, A. (2000). Noggin antagonizes BMP signaling to create a niche for adult neurogenesis. Neuron, 28(3), 713–726. http://doi.org/10.1016/S0896-6273(00)00148-3

Lin, Y. C., Hsieh, L. C., Kuo, M. W., Yu, J., Kuo, H. H., Lo, W. L., ... Li, W. H. (2007). Human TRIM71 and its nematode homologue are targets of let-7 microRNA and its zebrafish orthologue is essential for development. Molecular Biology and Evolution, 24(11), 2525–2534. http://doi.org/10.1093/molbev/msm195

Llorens-Bobadilla, E., Zhao, S., Baser, A., Saiz-Castro, G., Zwadlo, K., Martin-Villalba, A., ... al., et. (2015). Single-Cell Transcriptomics Reveals a Population of Dormant Neural Stem Cells that Become Activated upon Brain Injury. Cell Stem Cell, 17(3), 329–340. http://doi.org/10.1016/j.stem.2015.07.002

Meletis, K., Barnabé-Heider, F., Carlén, M., Evergren, E., Tomilin, N., Shupliakov, O., & Frisén, J. (2008). Spinal Cord Injury Reveals Multilineage Differentiation of Ependymal Cells. PLoS Biology, 6(7), e182. http://doi.org/10.1371/journal.pbio.0060182

Menn, B., Garcia-Verdugo, J. M., Yaschine, C., Gonzalez-Perez, O., Rowitch, D., & Alvarez-Buylla, A. (2006). Origin of Oligodendrocytes in the Subventricular Zone of the Adult Brain. Journal of Neuroscience, 26(30), 7907–7918. http://doi.org/10.1523/JNEUROSCI.1299-06.2006

Mirzadeh, Z., Doetsch, F., Sawamoto, K., Wichterle, H., & Alvarez-Buylla, A. (2010). The Subventricular Zone En-face: Wholemount Staining and Ependymal Flow. J. Vis. Exp, 39, 1938. http://doi.org/10.3791/1938

Mirzadeh, Z., Merkle, F. T., Soriano-Navarro, M., Garcia-Verdugo, J. M., & Alvarez-Buylla, A. (2008). Neural Stem Cells Confer Unique Pinwheel Architecture to the Ventricular Surface in Neurogenic Regions of the Adult Brain. Cell Stem Cell, 3(3), 265–278. http://doi.org/10.1016/j.stem.2008.07.004

Molyneaux, B. J., Arlotta, P., Menezes, J. R. L., & Macklis, J. D. (2007). Neuronal subtype specification in the cerebral cortex. Nature Reviews. Neuroscience, 8(6), 427–37. http://doi.org/10.1038/nrn2151

Paez-Gonzalez, P., Abdi, K., Luciano, D., Liu, Y., Soriano-Navarro, M., Rawlins, E., ... Kuo, C. T. (2011). Ank3-Dependent SVZ Niche Assembly Is Required for the Continued Production of New Neurons. Neuron, 71(1), 61–75. http://doi.org/10.1016/j.neuron.2011.05.029

Ramírez-Castillejo, C., Sánchez-Sánchez, F., Andreu-Agulló, C., Ferrón, S. R., Aroca-Aguilar, J. D., Sánchez, P., ... Fariñas, I. (2006). Pigment epithelium–derived factor is a niche signal for neural stem cell renewal. Nature Neuroscience, 9(3), 331–339. http://doi.org/10.1038/nn1657

Ren, Y., Ao, Y., O'Shea, T. M., Burda, J. E., Bernstein, A. M., Brumm, A. J., ... Sofroniew, M. V. (2017). Ependymal cell contribution to scar formation after spinal cord injury is minimal, local and dependent on direct ependymal injury. Scientific Reports, 7, 41122. http://doi.org/10.1038/srep41122

Rybak, A., Fuchs, H., Hadian, K., Smirnova, L., Wulczyn, E. A., Michel, G., ... Wulczyn, F. G. (2009). The let - 7 target gene mouse lin - 41 is a stem cell specific E3 ubiquitin ligase for the miRNA pathway protein Ago2. Nature Cell Biology, 11(12), 1411–1420. http://doi.org/10.1038/ncb1987

Sawamoto, K., Wichterle, H., Gonzalez-Perez, O., Cholfin, J. A., Yamada, M., Spassky, N., ... Alvarez- Buylla, A. (2006). New Neurons Follow the Flow of Cerebrospinal Fluid in the Adult Brain. Science, 311(5761), 629–632. Retrieved from https://ntp.neuroscience.wisc.edu/neuro670/reqreading/NewNeuronsFollowTheFlowOfCerebrospinalFluidInTheAdultBrain.pdf

Schulman, B. R. M., Esquela-Kerscher, A., & Slack, F. J. (2005). Reciprocal expression of lin-41 and the microRNAs let-7 and mir-125 during mouse embryogenesis. Developmental Dynamics, 234(4), 1046–1054. http://doi.org/10.1002/dvdy.20599

Silahtaroglu, A. N., Nolting, D., Dyrskjøt, L., Berezikov, E., Møller, M., Tommerup, N., & Kauppinen, S. (2007). Detection of microRNAs in frozen tissue sections by fluorescence in situ hybridization using locked nucleic acid probes and tyramide signal amplification, 2–10. http://doi.org/10.1038/nprot.2007.313

Simeone, A., Gulisano1, M., Acampora, D., Stornaiuolo, A., Rambaldi, M., & Boncinellil, E. (1992). Two vertebrate homeobox genes related to the Drosophila empty spiracles gene are expressed in the embryonic cerebral cortex. The EMBO Journal, 1(7), 2541–2550. Retrieved from https://www.ncbi.nlm.nih.gov/pmc/articles/PMC556729/pdf/emboj00092-0178.pdf

Slack, F. J., Basson, M., Liu, Z., Ambros, V., Horvitz, H. R., & Ruvkun, G. (2000). The lin-41 RBCC Gene Acts in the C. elegans Heterochronic Pathway between the let-7 Regulatory RNA and the LIN-29 Transcription Factor. Molecular Cell, 5(4), 659–669. http://doi.org/10.1016/S1097-2765(00)80245-2

Spassky, N. (2005). Adult Ependymal Cells Are Postmitotic and Are Derived from Radial Glial Cells during Embryogenesis. Journal of Neuroscience, 25(1), 10–18. http://doi.org/10.1523/JNEUROSCI.1108-04.2005

Thi, D., Nguyen, T., Richter, D., Michel, G., Mitschka, S., Kolanus, W., ... Wulczyn, F. G. (2017). The ubiquitin ligase LIN41 / TRIM71 targets p53 to antagonize cell death and differentiation pathways during stem cell differentiation, 24(6), 1063–1078. http://doi.org/10.1038/cdd.2017.54

Worringer, K. A., Rand, T. A., Hayashi, Y., Sami, S., Takahashi, K., & Tanabe, K. (2013). Article The let-7 / LIN-41 Pathway Regulates Reprogramming to Human Induced Pluripotent Stem Cells by Controlling Expression of Prodifferentiation Genes. Stem Cell, 14(1), 40–52. http://doi.org/10.1016/j.stem.2013.11.001

Young, C. C., van der Harg, J. M., Lewis, N. J., Brooks, K. J., Buchan, A. M., & Szele, F. G. (2013). Ependymal Ciliary Dysfunction and Reactive Astrocytosis in a Reorganized Subventricular Zone after Stroke. Cerebral Cortex, 23(3), 647–659. http://doi.org/10.1093/cercor/bhs049

Zhao, C., Deng, W., & Gage, F. H. (2008). Mechanisms and Functional Implications of Adult Neurogenesis. Cell, 132(4), 645–660. http://doi.org/10.1016/j.cell.2008.01.033

Supplementary Fig. 2.1 Breeding strategy to obtain Lin41 cKO and control animals. Lin41+/-;Emx1-Cre- +/- mice expressing Cre recombinase under the promotor of the Emx1 gene obtained from previous breedings were crossed with Lin41lox/lox mice – having two alleles with loxP sites flanking the fourth exon – to obtain Lin41 cKO mice ( ) and control conditions. In this way, the Lin41 cKO mice possess one functional Lin41 allele with two inserted loxP sites on the flanks of the fourth exon. So, the fourth exon of the functional Lin41 allele in this mouse will be removed upon Cre recombination. Cre is located under the promotor of Emx1, a gene which is expressed in all radial glia cells of the dorsal telencephalic neuroepithelium from E10.5. As Emx1 expression is induced at E10.5, Cre recombination will remove the fourth exon of Lin41 in all Emx1 positive cells and their progeny. Emx1 positive cells are the radial glia cells in the dorsal telencephalic neuroeptihelium and their progeny are believed to include most cortical neurons and the ependymal cells lining the wall of the lateral ventricles (Simeone et al., 1992). This design allows us to overcome embryonic lethality due to neural tube closure defects before E9.5 and provides a viable mouse model to study the effect of late-embryonic Lin41 expression and Lin41 expression in the ependymal cells of the postnatal brain.

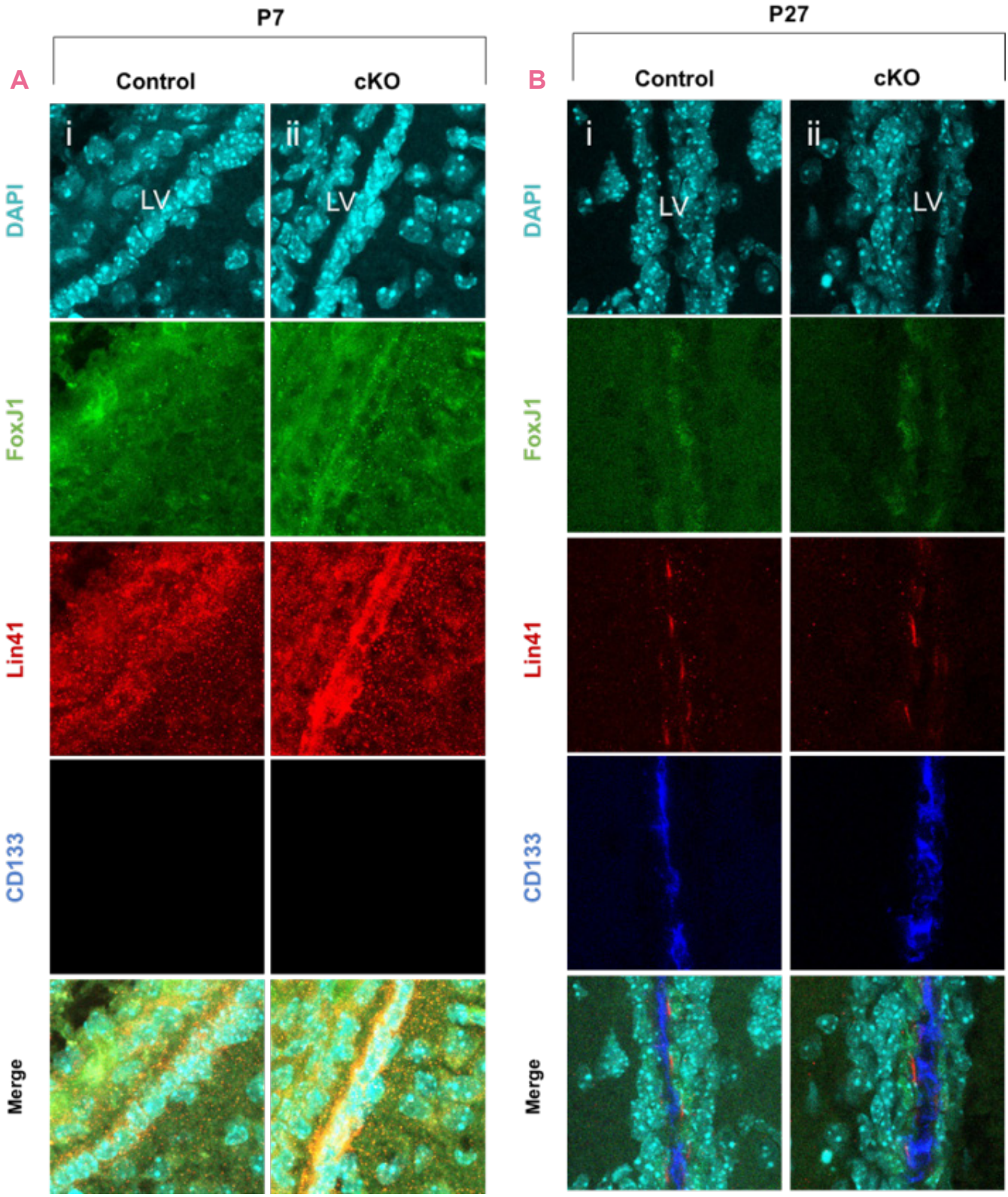

Supplementary Fig. 3.1 Immunostainings to asses LIN41 in ependymal cells of the postnatal lateral ventricular wall. Immunostaining of P7 and P27 brains with mouse anti-FOXJ1 (green), rabbit anti-LIN41 (red P7: lab made; P27: OriGene) and rat anti-CD133 (blue). FoxJ1 – a marker for ependymal cells – showed high background in both P7 **A** and P27 **B** samples. Additionally, no specific signal was detected at P27 stage, when ependymal cells are considered to be fully matured. This disabled us to distinguish the ependymal cell layer lining the ventricular wall from other cell types residing in the SVZ. LIN41 at P27 **B** showed staining of cells surrounding the lateral ventricle in both control **i** and cKO **ii** conditions. However, LIN41 protein is located in the cytoplasm, and should therefore not stain only the apical side of cells. Based on our qPCR results and previously published data, LIN41 is absent at P7. Thus, the high red signal seen in P7 **A** control **i** and cKO **ii** brains must be considered unspecific background. Together, these notions lead to the conclusion that the LIN41 staining pattern seen in P27 conditions should be considered unspecific. The surface protein CD133 is known to label ependymal cells in the adult SVZ (Coskun et al.,2008). Indeed, CD133 positive cells were observed at P27 stage **B** in both control **i** and cKO **ii** conditions. Absence of CD133 positive cells at P7 stages **A** is in line with the notion that ependymal cells remain undifferentiated until the second week after birth (Spassky et al., 2005).

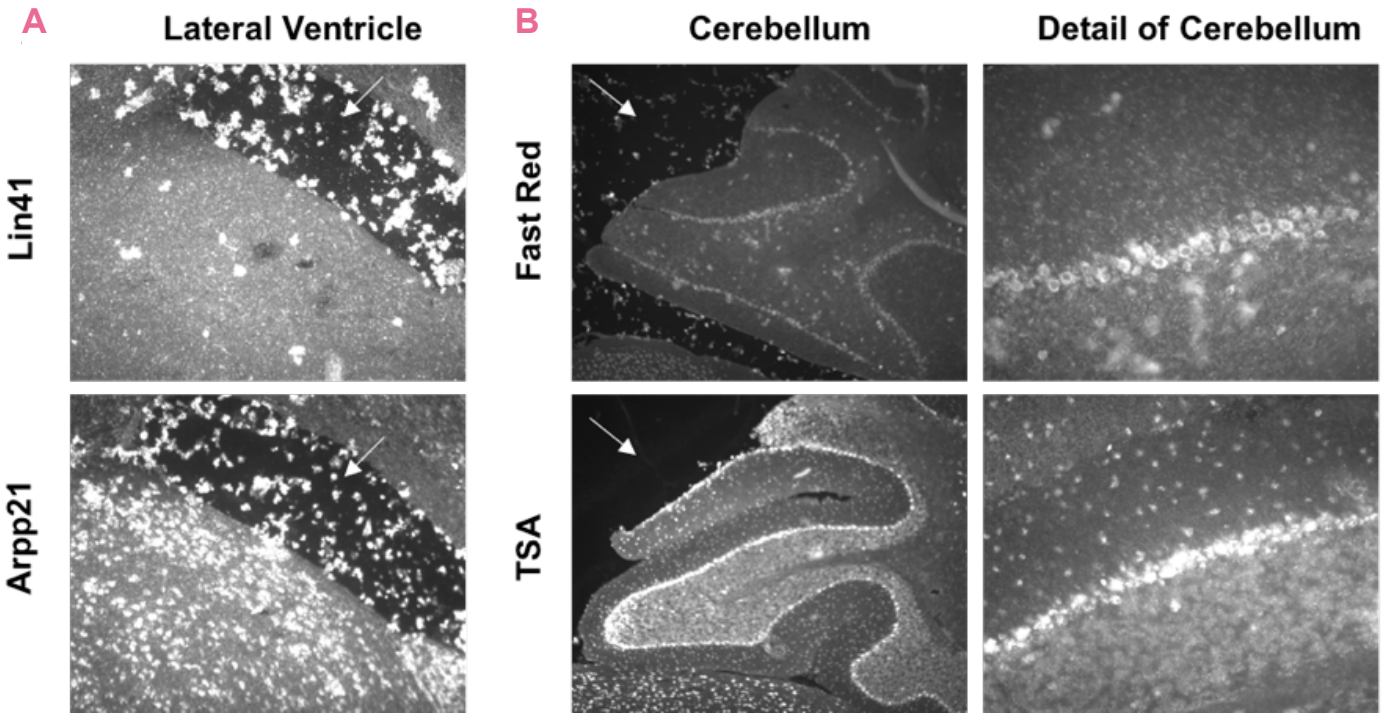

Supplementary Fig. 3.2 In situ hybridization using Fast Red tablets vs. TSA as detection method. High background was observed in all sections regardless of which probe was used. **A** example of Lin41 and Arpp21 probe in a sagittal section depicting part of the lateral ventricle after Fast Red development. Precipitate throughout the whole sample (best visible in the lateral ventricular lumen, **white arrows**) complicated assessment of potential specific binding. **B** Example of cerebellum and detail of cerebellum of after Fast Red vs. TSA development. Precipitate as consistently observed in the Fast Red method was absent in the TSA method (**white arrows**).

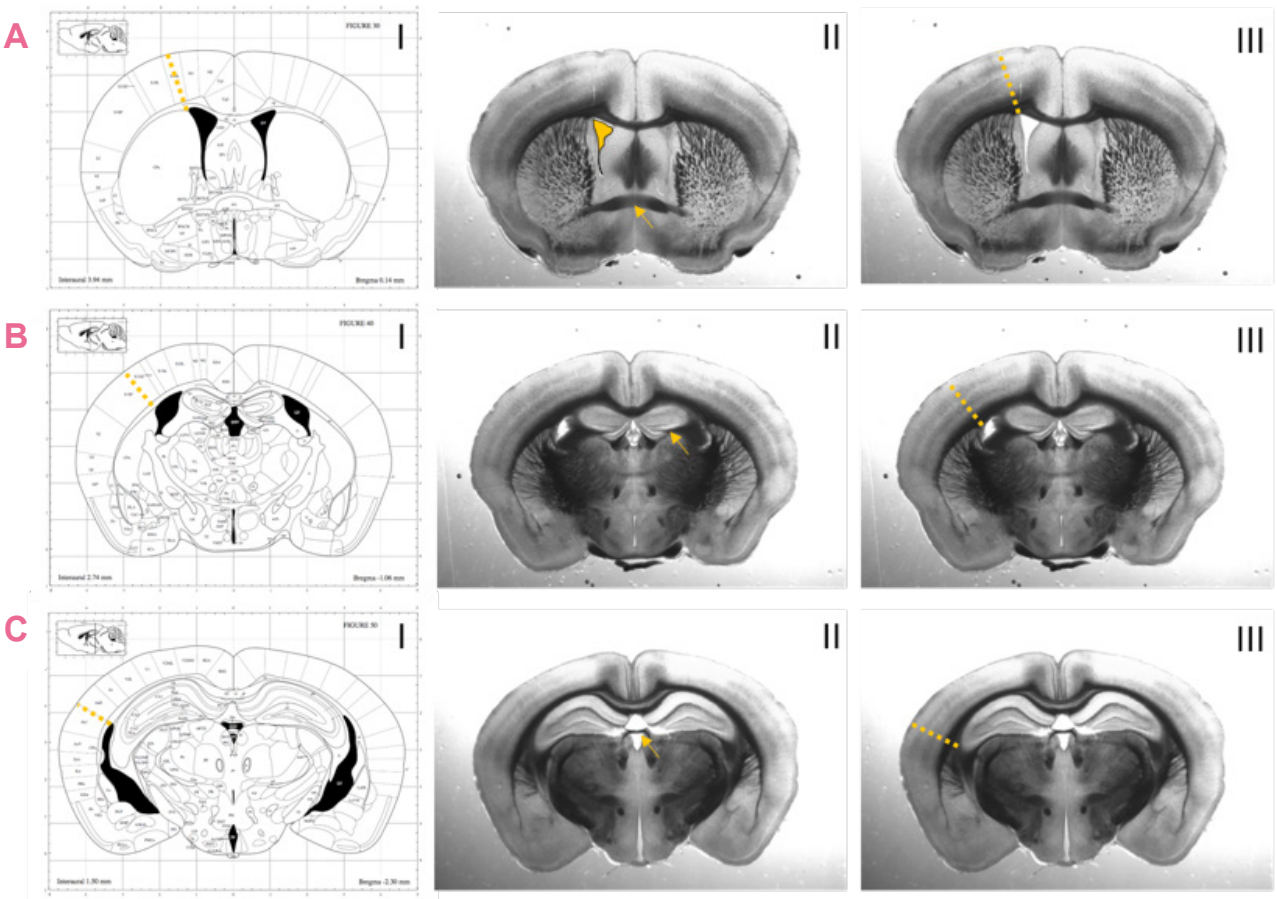

Supplementary Fig. 3.3 Detailed description of selected areas and methods to obtain morphometric measurements from coronal vibratome sections (200 µm thick). From anterior to posterior, three coronal sections were selected for each individual using the following criteria: **A-II** the first section in which the right and left anterior commissure fuse (**yellow arrow**); **B-II** the first section in which the hippocampus occurs (**yellow arrow**); and **C-II** the first section in which the right and left posterior commissure fuse (**yellow arrow**). Section A-I was used to obtain total brain area, CC thickness, lateral ventricle area and cortical thickness of the primary somatosensory cortex (S1). Section B-I and C-I were used to obtain additional cortical thickness measurements of the Barrel cortex (BC) and Auditory cortex (AuD). The dotted lines **A; B; C – I and III** indicate the exact location of each measurement. **A-I** Cortical thickness measurement of the S1 was taken from the intersection of the medial and lateral wall of the lateral ventricle to the pia. **B-I** Cortical thickness measurement of the BC was taken from the intersection of the lateral ventricle and the striatum to the pia.**C-I** Cortical thickness measurement of the AuD was taken from the intersection of the hippocampus with the lateral ventricle to the pia. Image adapted from 'The mouse brain atlas' (Franklin and Paxinos, 2007)

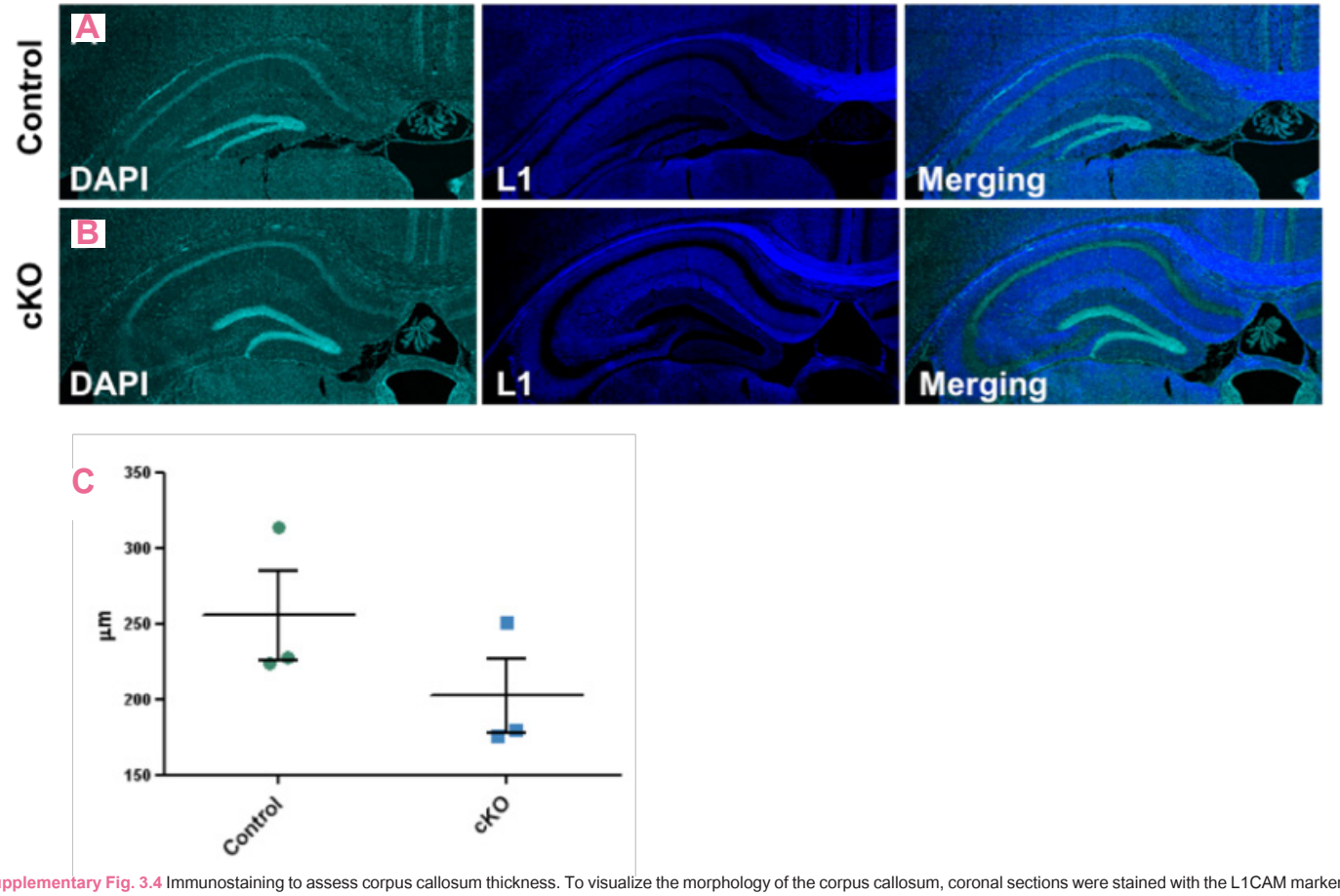

Supplementary Fig. 3.4 Immunostaining to assess corpus callosum thickness. To visualize the morphology of the corpus callosum, coronal sections were stained with the L1CAM marker (**blue**). Images were obtained from the first coronal section in which the hippocampal fissure was visible. Qualitatively, no major differences in corpus callosum morphology were observed between control **A** and cKO **B** mice at P27. **C** Quantification showed a trend toward decreased corpus callosum thickness in Lin41 cKO mice (202.3 ± 24.36; N=3) compared to control (255.3 ± 29.36; N=3) that was not significant (P = 0.2371).

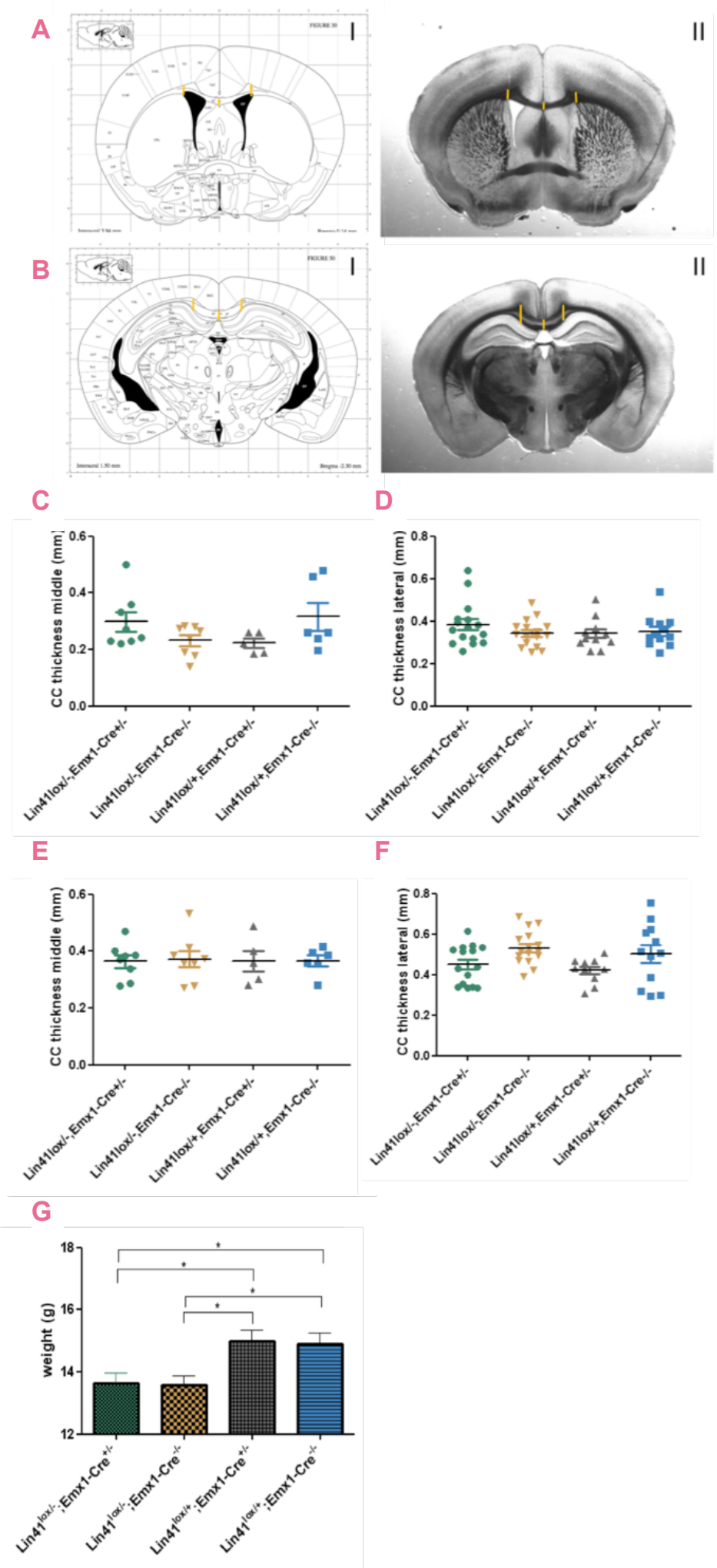

Supplementary Fig. 3.5 Analysis of corpus callosum thickness and body weight. Morphometric analysis of corpus callosum thickness of Lin41lox/-;Emx1-Cre+/- (N = 8), Lin41lox/-;Emx1-Cre-/- (N= 8), Lin41lox/+;Emx1-Cre+/- (N = 5) and Lin41lox+-;Emx1-Cre-/- (N = 6). **A** Yellow lines depict the position from which the measurements were taken. **B** No differences were found between groups for corpus callosum thickness in either the middle part connecting the two hemispheres (P = 0.152) or in the lateral areas **C** (P = 0.439). **D** Lin41 cKO mice differed significantly in weight from Lin41lox+-;Emx1-Cre+/- and Lin41lox+- ;Emx1-Cre-/- and Lin41lox/-;Emx1-Cre- /- weight differed significantly from Lin-41lox+-;Emx1-Cre+/- and Lin-41lox+- ;Emx1-Cre-/- (N=29, * P < 0.05)

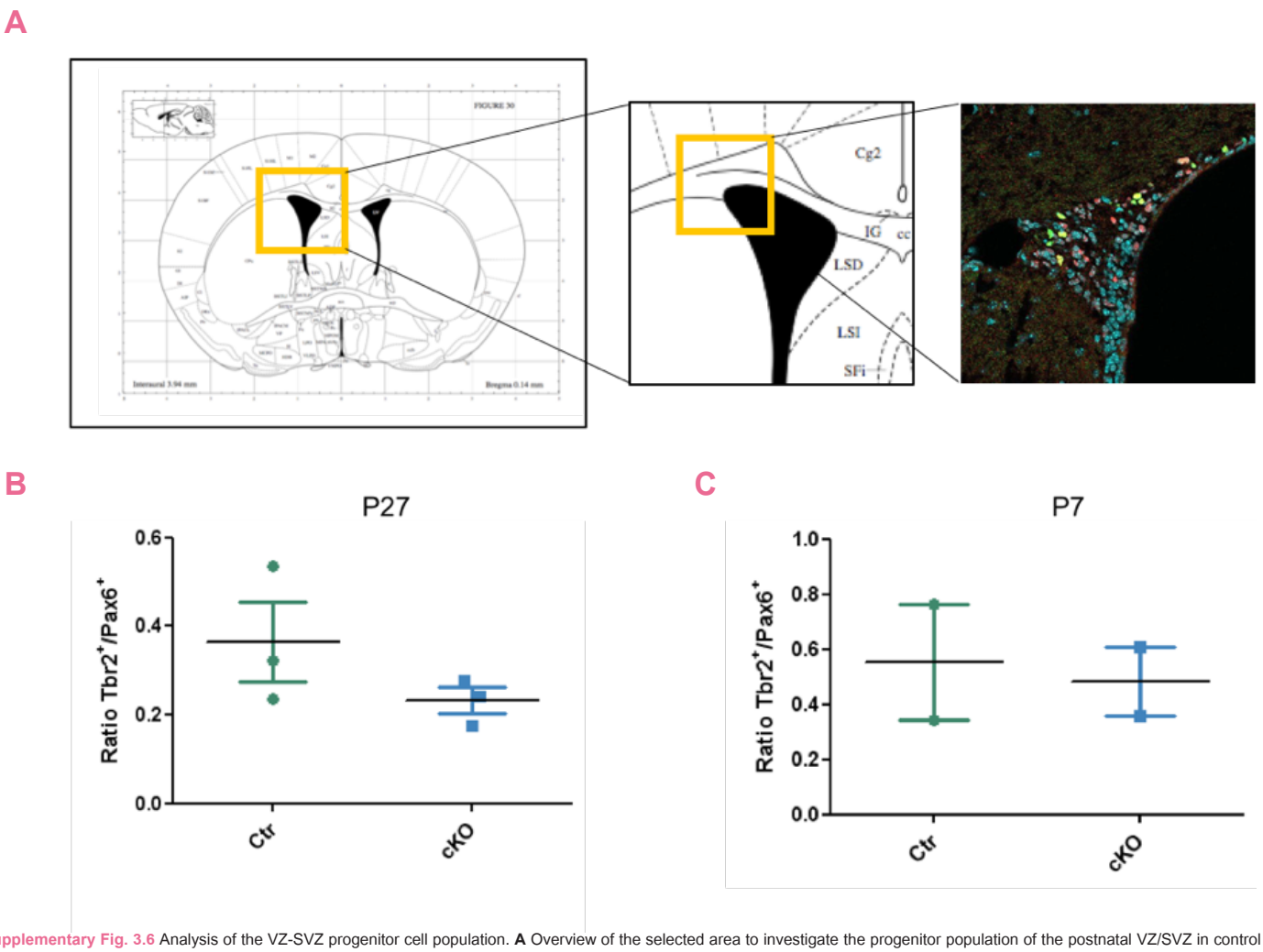

Supplementary Fig. 3.6 Analysis of the VZ-SVZ progenitor cell population. **A** Overview of the selected area to investigate the progenitor population of the postnatal VZ/SVZ in control and Lin41 cKO conditions. As Tbr2 and Pax6 were found to be most highly expressed in the dorsal and medial wall of the lateral ventricle, Tbr2 and Pax6 positive cells were counted from a selected area of the dorsal-medial wall. Image adapted from 'The mouse brain atlas' (Franklin and Paxinos, 2007) **B** Ratio of Tbr2+/Pax6+ cells showed no significant differences between control and Lin41 cKO at P27 ($P = 0.231$), **C** nor at P7 ($P = 0.804$). However, increasing the current sample size (N=2 for P7 and N=3 for P27) might be necessary to exclude any effects of Lin41 knock out on the progenitor cell population with certainty.

INTERVIEW Q&A

with Pim Haselager

by Steven Voges

Willem F.G. "Pim" Haselager is a neuroethicist and philosopher who works as an associate professor at the Donders Institute for Brain, Cognition and Behaviour, at the Radboud University Nijmegen. We talked with him about neuroethics, ethics education, artificial intelligence, and the Cambridge Analytica scandal.

Neuroethics is a very niche topic, what is your educational background and how did you get started in neuroethics?

I'm a philosopher and psychologist by training. I did my bachelors at the University of Amsterdam in psychology, then I did my master in philosophy at the University of Amsterdam and my masters in psychology at the Free University. After that I did my doctorate in philosophy of mind/cognitive science again at the Free University and in the mean time I started working as a teacher in the cognitive science department in Nijmegen teaching philosophy. Since then I've been working at Radboud University. Although I am a philosopher I work at the Donders institute where I am the only philosopher surrounded by neuroscientists, psychologists, and experts in Artificial Intelligence (AI). In a way, I am the in-house philosopher, but I didn't actually focus much on ethics until around 2008. There was a big group working on Brain-Computer Interfaces (BCIs) and the people working in that field started consulting me about the implications of the technology they were developing, about informed consent, how to communicate expected results to the media, consequences for views on free will, agency, and especially issues that had legal implications. Since my philosophical focus had always been on addressing practical questions that needed practical answers my work in neuroethics really took off from there. I believe that my perspective is unique in philosophy because I start with empirical research and look at how philosophy can help concretely. I also don't usually start with the history of philosophy, e.g. refer to Aristotle or similar philosophers, unless it is expressly relevant to the research. Philosophy is traditionally, and to a certain extent still, quite focused on its own history. This isn't necessarily a bad thing but often impractical. Nowadays, my ethics work is moving much more towards ELSI or Ethical, Legal and Societal Implications of neuroscience and AI. I also work in the field of neurolaw where we look at all sorts of legal consequences of neuroscience going from lie detection to the existence of free will. We even receive questions on whether there could be neuroscientific methods to test American jury-members for biases. So now I work with many ministries like the ministry of security and justice here in the Netherlands on what neuroscience or AI brings in terms of ethical, legal and societal consequences and how can we could stimulate responsible and avoid irresponsible usage of all these developing technologies. I also give lectures for big companies like Price Waterhouse Cooper or ASML on issues like super-intelligence. The field is really exploding and I am getting busier and busier every day.

The topic of ethics came up for the journal through a desire to increase ethics education across our master's program. How do you as a neuroethicist train the next generation of neuroscientist?

Here in the AI and Cognitive neuroscience programs at the Donders institute we have obligatory courses on the ethical and societal implications of current research. I think it's important that students really get a proper training because these days society expects new professionals to not only be good in their field but also to understand possible societal implications and secondly to have the capacity to communicate this to non-experts. This is something that I focus on with my students as well to not only learn how to communicate with other experts but really how to translate their expertise to the general public. I try to prepare my students to master effective strategies for communication. I currently teach a course called Science and Society on the AI Masters which is 3 ECTS at the moment but the university values it so much that they've doubled it to 6 ECTS for the upcoming year. One of the assignments for this course is a research brief that is written for non-experts which needs to have a 200-word executive summary. Another plan I have for the future is to collaborate with a journalism school to get student interviews with journalism students to gain experience with communicating to the media and learning how to answer questions and avoid being forced to say things they don't want to say. Two elements I emphasize for communication are the time frame and the stakeholder. By time I mean the future, are you discussing technology as it is now or 5 years from now, or over 50 years, 200? This is important because if you want to communicate with people you need to know what time frame they are actually interested in. This is something you really need to keep clear. The second is what stakeholders you are communicating to. There is a big difference in discussing AI and privacy with the ministry of justice or amnesty international. You will be addressing the same topic but the concerns and possibilities to take action will vary greatly. When talk about supportive technology you might be talking to healthcare providers, the organizations, or individual caregivers, those who care for the elderly. They will be interested in different aspects of the technology. All of these things you can prepare beforehand.

At the rate neuroscience is advancing it is often difficult to keep an ethical perspective on the research we do. Someone researching empathy to help people with autism could end up helping the military develop super soldiers who are callous to the emotions of their enemies. How can neuroscientists keep an ethical perspective without limiting the development of their field?

That is definitely a problem. I call this the paradox of control. On the one hand, we have increased possibilities to control on the environment and on ourselves via let's say smart systems, but because of these increased possibilities we begin to lose control of what (not) to do exactly. We become more powerful in a variety of ways in relation to ourselves and how we can impact our environment. But as Spiderman says: "With Great power comes great responsibility" (actually, it's a very old saying going back to the bible). I think this is very important. And I think that any responsible training should give you the skills for critical reflection and also the capacity to communicate with society in a responsible way. Which is something more than just giving your opinion. As an expert, you have the responsibility to share your knowledge on what is possible both positive and negative in such a way that people can come to their own conclusions.

Looking at your research, a topic you focus on is the legal implications associated with autonomous systems. Recently in Arizona a self-driving car killed a woman who crossed the street in front of it, although there was a human agent who was ready to take charge of the car in case of an emergency. What is your view of this incident and the legal implications surrounding it and autonomous systems in general?

Well, I wrote a paper in 2005 about robotics and the problems with autonomy. I explicitly say problems because I don't think there is one interpretation of autonomy that covers the whole field. Now this case specifically is terrible and fascinating from a philosophical perspective. First of all, we have the question of who is responsible for the outcome, the human or self-driving car. At the moment, the law regarding self-driving cars is such that the human driver is in control thus ultimately responsible, which is psychologically impossible. if you're in a car that is self-driving and works well, maybe you pay attention for 10 minutes and keep your hands on the wheel but after 20 or 30 minutes of the car driving without any problems, any sane human being would begin to do something else. So psychologically of course people are no longer paying attention. It's a very weird construction that is inserted purely for legal and financial reasons. Although I am not a legal expert, I could imagine that some people would try to argue on legal grounds that although they are attributed responsibility, the situation they are placed in undermines that responsibility. I think that the human responsibility in self-driving cars is a legal artefact that isn't based on solid psychological grounds. So, when you study AI, in many cases if not almost all, you need to take the psychology of the human agents that collaborate with the AI into account to understand the effects. If you ignore that it will be at your peril. Fortunately, here at Nijmegen we work as the AI department together with psychology in the department of social sciences. Which is very strange internationally speaking but I think it is one of the strengths of our program because it makes us a very cognitively oriented AI. Which means that all the human robot and human computer interaction studies are really well informed about the psychologically and even neuroscientifically (im)possible, which is also good for assessing the societal impact.

The second question here is what does it mean for a system to have full autonomy? I am not so sure whether this is actually possible. But here we get into philosophical deep water. There is this possibility to think about artificial agents as ultimately being constructed by natural systems. I've worked with genetic algorithms and artificial evolution, and you could say these things evolve on their own but I know from practice that this is based on your fitness function, the parameter settings, the environment settings, the sensory inputs and outputs that you provide them with and then, steered by your fitness function, it will develop in a certain direction. Now although this may be surprising and you may not be able to predict which way it will go, ultimately under the hood there is human intelligence, and this applies to machine learning as well. At some point, you put these things together and then you let them develop on their own but your still in control of the training data in relation to the actual learning algorithms. You are setting up the system and then you see where they go to semi-autonomously. In that sense, I don't think we have created systems such as biological systems that have a will of their own. The moment you decide a study and choose a certain topic your parents might say "no, go into law you will earn more money" but your response is "no, this what I want to do". I don't think we have artificial systems that have the same sense of agency that biological systems do and our lack of understanding in that field is still very deep. So, in that sense I don't think there is any artificial system with full autonomy in the sense that we use that word when we ask you all to vote or decide on your study. I always give the example of a refrigerator. We can make smart refrigerators that can interact with your agenda and see that your mother is coming for dinner so they cool the cakes you bought for her a little bit less so they will be at room temperature, they can also see that your birthday will be tomorrow, and that the members of your football team will all come, so the beer starts getting colder, and they can use so much data to manage so many different things that you probably don't really understand because it is so independent, so autonomous. But this is very different from a refrigerator that refuses to keep cooling and decides it wants to start barbequeing instead because that seems to be more fun to the refrigerator itself. That is a different kind of autonomy. We can create true complexity, a real independence from us where we can no longer keep up with what a system is doing because it is too fast. But a totally different type of autonomy is self-determination, choosing goals for your own benefit. This is also very relevant to the idea of killer robots, I don't think that killer robots will kill out of their own desire. We will still be setting their goals to achieve. There is no ultimate ends selection in these artificial systems. Of course, ultimately, we should be able to understand how this works in biological systems and then to implement it in artificial systems, but at the moment we simply lack a proper understanding of will and autonomy in a deep sense.

Considering your expertise in artificial intelligence do you think that if artificial systems achieve the capability of recursive self-improvement that they will become self-aware?

Until somebody explains to me exactly how from smart systems we get self-determination, I don't quite see how that's going to

happen. This is sometimes expressed as the orthogonality thesis. So, you have one dimension that is intelligence and we are pretty good at making progress along that dimension, our systems really are becoming smarter. There is another dimension that you can call will, or self-determination. Our best chess computers can beat masters as if they don't exist but if you put them in blunder mode they will happily lose all their games. They do not care. They still don't know the difference between winning or losing. They don't know they exist, and they don't want what is good for themselves and they don't know what is good for themselves. You can make self-destructive robots easily, it is just not a problem for them. And this leads into a possible third dimension, which is self-experience or awareness. There is no will or awareness in artificial systems, there is just very high but totally isolated intelligence that makes these systems really different from biological creatures. And that means that for all outcomes of intelligent systems behaviour, it's ultimately humans that remain responsible. Now this could change of course, and I believe as a scientific materialist that our will and our understanding should be explainable, but I notice in AI that we are understanding the basic principles of intelligence quite well but we seriously lack understanding of free will and self-awareness. Now ultimately, I believe we should be able to understand all three dimensions but for the next 10-20 years I don't see it coming for two of the three dimensions. I may be wrong and maybe there is a very smart person developing this, but I don't believe that we will increase intelligence and suddenly we will get the other one for free. You might get emergence but not suddenly in qualitatively different fields unless you are extremely lucky.

A very timely ethical topic is the issue of Cambridge Analytica and manipulation of Brexit and the US election. As a researcher do you find the violation of research ethics committed by Aleksandr Kogan a big issue?

If the Stasi or the KGB would have had access to this technology in the 60s it would have been a huge spying program in order to suppress all sort of politically undesired behaviours. Now we gave away this power not to a governmental institute but to an economic company that knows how to sell their product and some people used this for political manipulation. It is remarkable how slow we have been at understanding that the social media community is actually a mass surveillance machine with capacities much larger and much more penetrating than any other spy organization had before. You can call it a breach of academic integrity that you misuse data that you collected on the basis of a scientific research project for non-research applications, that's true. But I think that would be missing the real problem and that is that the data that is being collected in its current massive scale enables manipulation, threatens freedom of action and through that also freedom of thought. And this, in turn, can and does already undermine democracy on an enormous scale. That it was a researcher who used the data for something other than what they originally promised, that's bad, but va bene. I don't think is the biggest issue, it's the possibility to do this in the first place. As I understand it, Obama and others were already trying to do something along those lines, using micro-targeting to give more specific information in order to influence people, but now we're applying this approach at increased scales and levels of intensity.

Following on this topic, there are now neuromarketing companies integrating fMRI data into marketing campaigns. Is a line being crossed from being clever marketers to brain-washing the public?

Of course, this is why this subject is theoretically very relevant. People have been influencing one another since forever. If you read Frans de Waal's Chimpanzee Politics, who worked with chimps and bonobos you'll see all kinds of behavioural strategies that are being pursued not for their pragmatic effect on the environment but for the ability to influence others. Then with arrival of mass media, the ability to print books in the 15th century and later the arrival of newspapers, radio, television and internet you get more opportunities. It's just that now because we can make it so personal, you can really micro-target, you can really address this manipulation at a personal level and in ways that might bypass the awareness that you are getting restricted information that normally you have. Traditionally, people usually read a certain type of newspaper that features information they agree with it but the traditional demographic of a newspaper was always so large that there was always something that you disagreed with. If you walk on the street the advertisements are targeted at everyone in general and some of these you will find disagreeable and in a way that is what saves you. You will get stimuli that are outside of your bubble. These days especially with prolonged existence on the internet, it is increasingly difficult to escape your bubble because that's what they create for you. So, I don't see this as a difference in the principle of manipulation but it's the level of pervasiveness that starts making a principled difference. Here it's more of the same that at some point starts making a qualitative difference because there is no way to escape. Those kinds of old-fashioned non-fitting stimuli were still part of the information you acquired and this will begin to disappear and we don't know how this will affect autonomous decision making commercially or politically, except that it doesn't look good. And then if you add information about the brain in order to further increase effective presentation of information the concerns become even more serious. I do sometimes feel we're overestimating the contribution of neuroscience a little bit because behaviourally many of these effects are well known. It is good to understand the underlying neuronal mechanisms from a scientific perspective, but we might be disappointed in how much practical difference a deeper neuronal insight provides us with. In that sense, I believe neuromarketing might be a little bit of a hype, and although you might get some ideas of different forms of presentation based on your causal model of neuronal understanding, most of this will have been tested in practice. It would be different if you used brain stimulation. But then we're getting into yet another area of neurotechnology. Perhaps next time?

UNIVERSITY OF AMSTERDAM

IIS

abc amsterdam brain & cognition

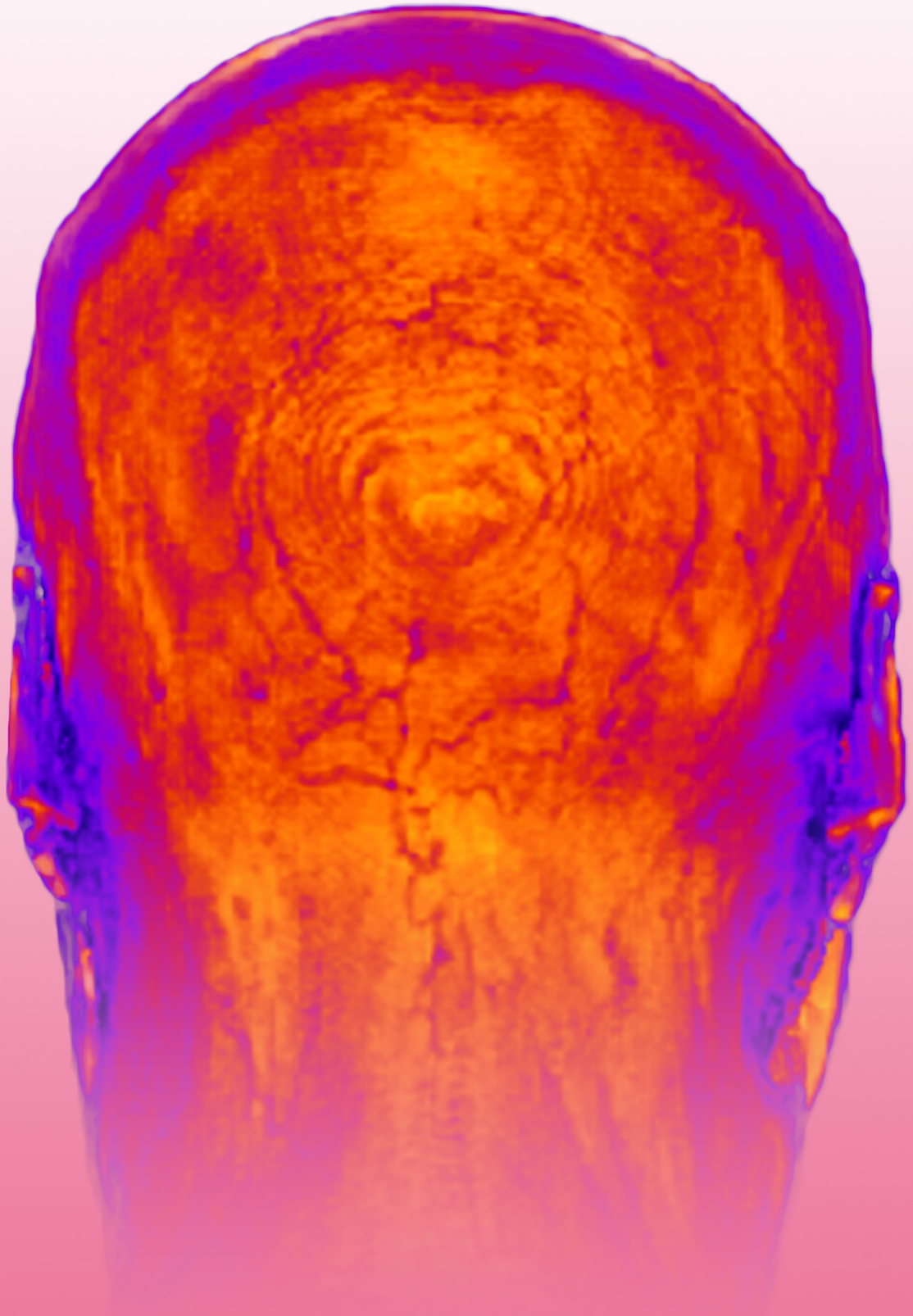

Website
student.uva.nl/bcs/content/az/abc-journal/abc-journal.html

Facebook page
facebook.com/ABCJournal